Heat Transfer Lectures
Fundamentals & Applications

UNIVERSITY OF TECHNOLOGY

Mechanical Engineering department

3rd power plant division

BOILING

Dr. Sattar Aljabair

Objectives

- Differentiate between evaporation and boiling, and gain familiarity with different types of boiling
- Develop a good understanding of the boiling curve, and the different boiling regimes corresponding to different regions of the boiling curve
- Calculate the heat flux and its critical value associated with nucleate boiling, and examine the methods of boiling heat transfer enhancement

BOILING HEAT TRANSFER

- **Evaporation** occurs at the *liquid–vapor interface* when the vapor pressure is less than the saturation pressure of the liquid at a given temperature.
- **Boiling** occurs at the *solid–liquid interface* when a liquid is brought into contact with a surface maintained at a temperature sufficiently above the saturation temperature of the liquid.

FIGURE 10–1
A liquid-to-vapor phase change process is called *evaporation* if it originates at a liquid–vapor interface and *boiling* if it occurs at a solid–liquid interface.

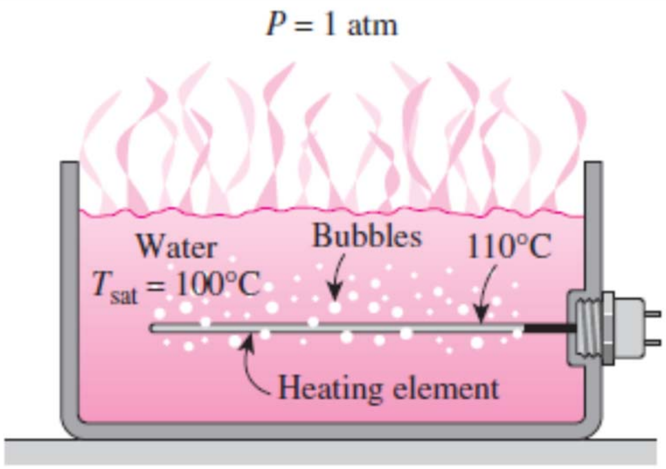

FIGURE 10–2
Boiling occurs when a liquid is brought into contact with a surface at a temperature above the saturation temperature of the liquid.

Boiling heat flux from a solid surface to the fluid

$$\dot{q}_{\text{boiling}} = h(T_s - T_{\text{sat}}) = h\Delta T_{\text{excess}} \qquad (\text{W/m}^2)$$

$$\Delta T_{\text{excess}} = T_s - T_{\text{sat}}$$ *excess temperature*

Classification of boiling

- Boiling is called **pool boiling** in the absence of bulk fluid flow.
- Any motion of the fluid is due to natural convection currents and the motion of the bubbles under the influence of buoyancy.
- Boiling is called **flow boiling** in the presence of bulk fluid flow.
- In flow boiling, the fluid is forced to move in a heated pipe or over a surface by external means such as a pump.

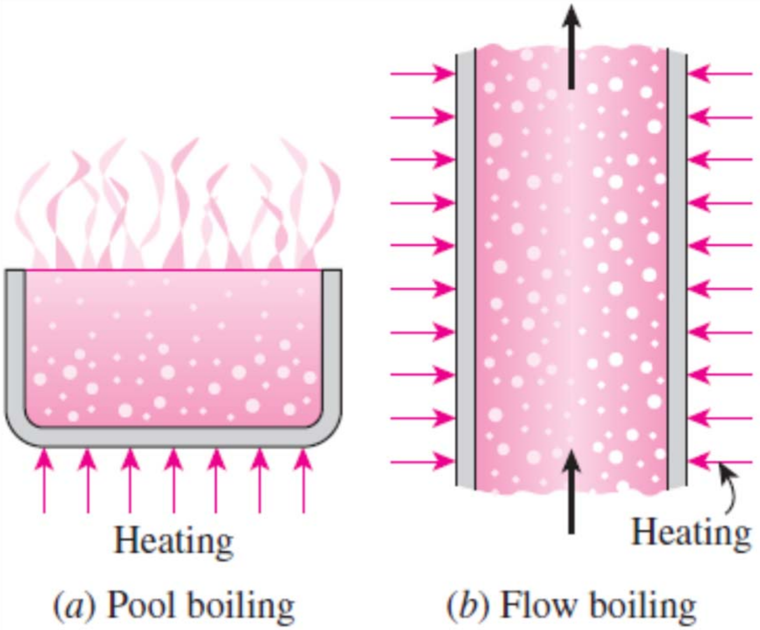

(*a*) Pool boiling (*b*) Flow boiling

FIGURE 10–3

Classification of boiling on the basis of the presence of bulk fluid motion.

Subcooled Boiling

- When the temperature of the main body of the liquid is below the saturation temperature.

Saturated Boiling

- When the temperature of the liquid is equal to the saturation temperature.

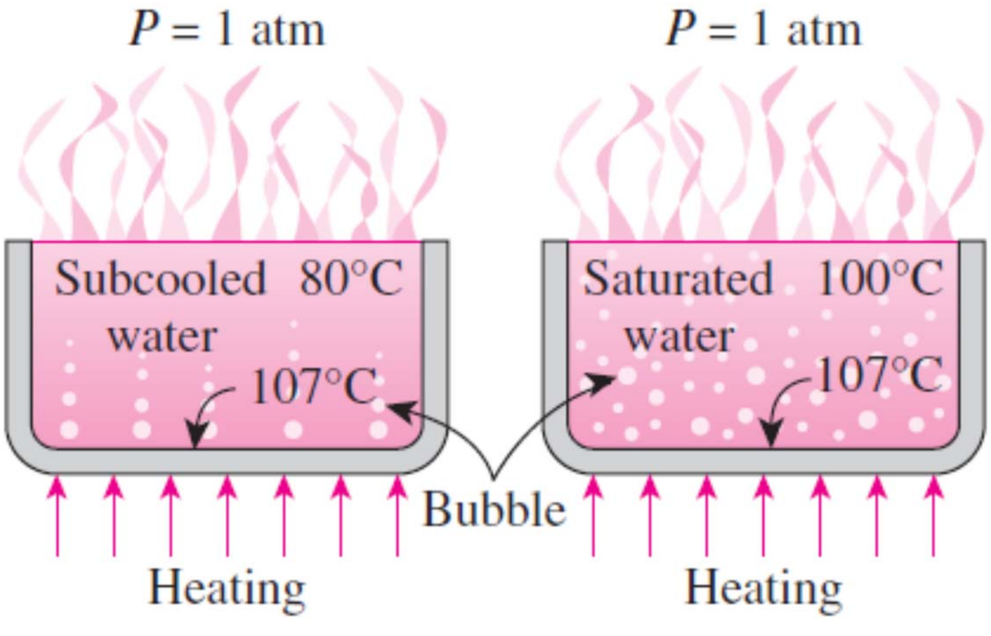

(*a*) Subcooled boiling (*b*) Saturated boiling

FIGURE 10–4
Classification of boiling on the basis of the presence of bulk liquid temperature.

POOL BOILING

In pool boiling, the fluid is not forced to flow by a mover such as a pump.

Any motion of the fluid is due to natural convection currents and the motion of the bubbles under the influence of buoyancy.

Boiling Regimes and the Boiling Curve

$$\dot{q}_{\text{boiling}} = h(T_s - T_{\text{sat}}) = h\Delta T_{\text{excess}}$$

Boiling takes different forms, depending on the $\Delta T_{excess} = T_s - T_{sat}$

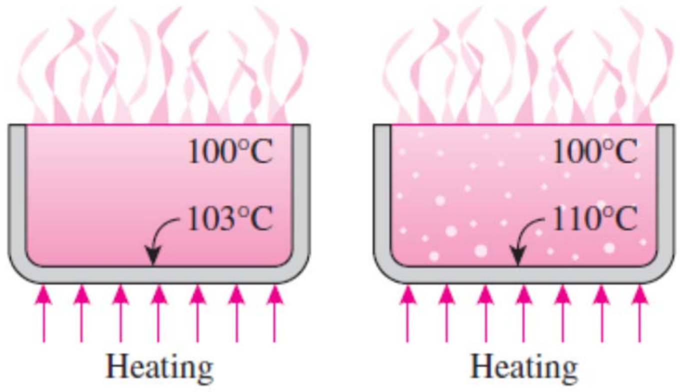

(*a*) Natural convection boiling

(*b*) Nucleate boiling

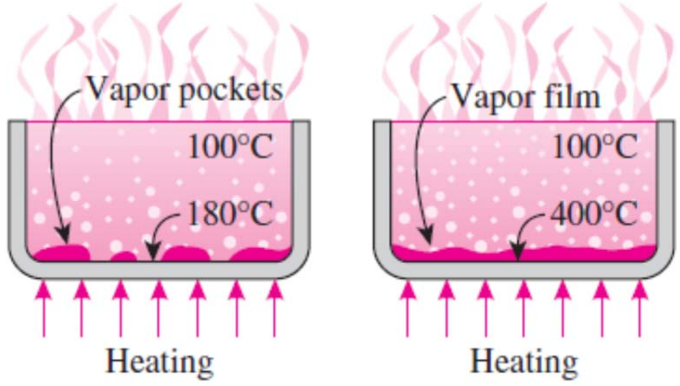

(*c*) Transition boiling

(*d*) Film boiling

FIGURE 10–5

Different boiling regimes in pool boiling.

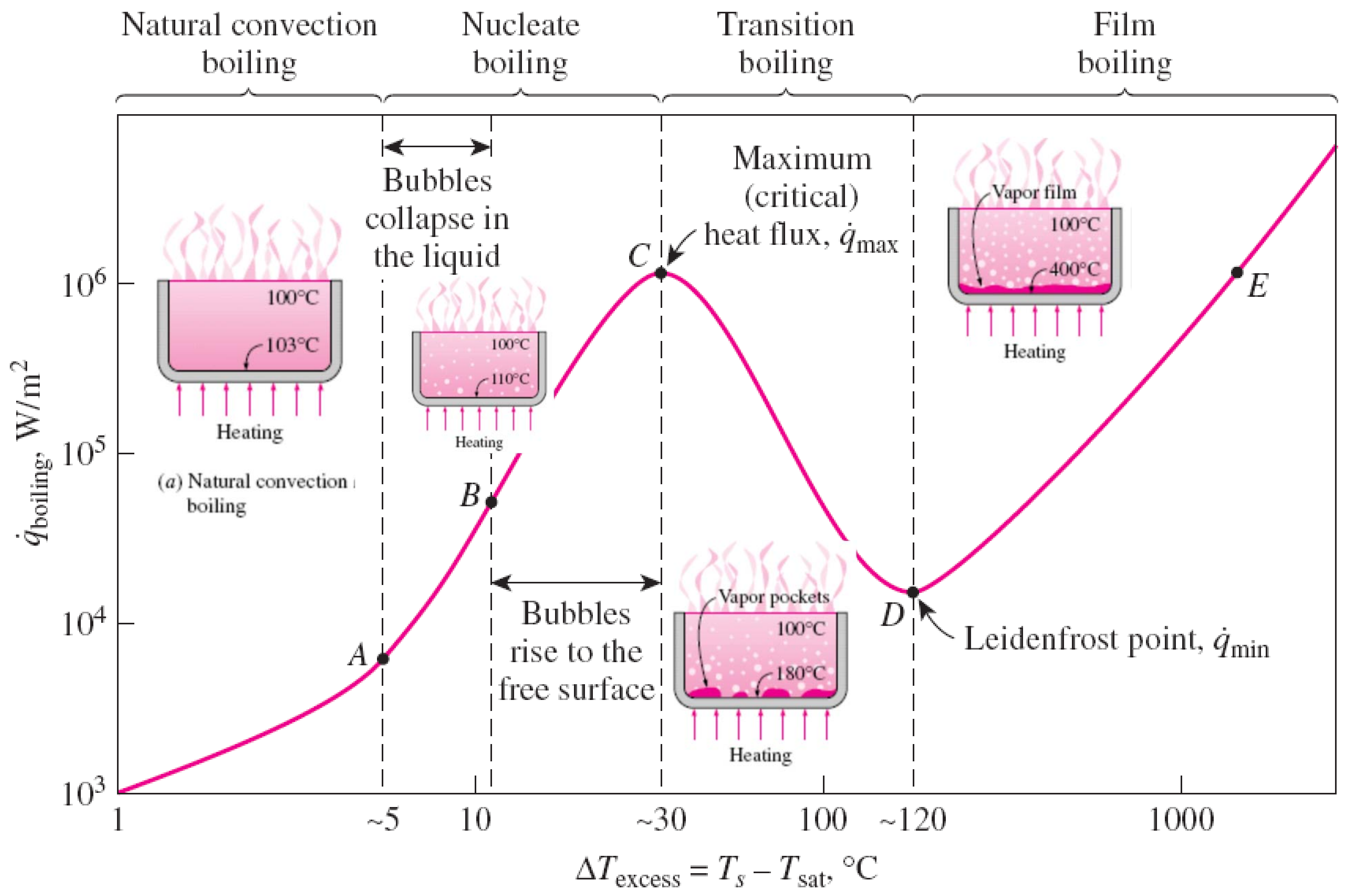

FIGURE 10–6

Typical boiling curve for water at 1 atm pressure.

Natural Convection Boiling (to Point *A* on the Boiling Curve)

- Bubbles do not form on the heating surface until the liquid is heated a few degrees above the saturation temperature (about 2 to 6°C for water)
- The liquid is slightly *superheated* in this case (*metastable* state).
- The fluid motion in this mode of boiling is governed by natural convection currents.
- Heat transfer from the heating surface to the fluid is by natural convection.
- For the conditions of Fig. 10–6, natural convection boiling ends at an excess temperature of about 5°C.

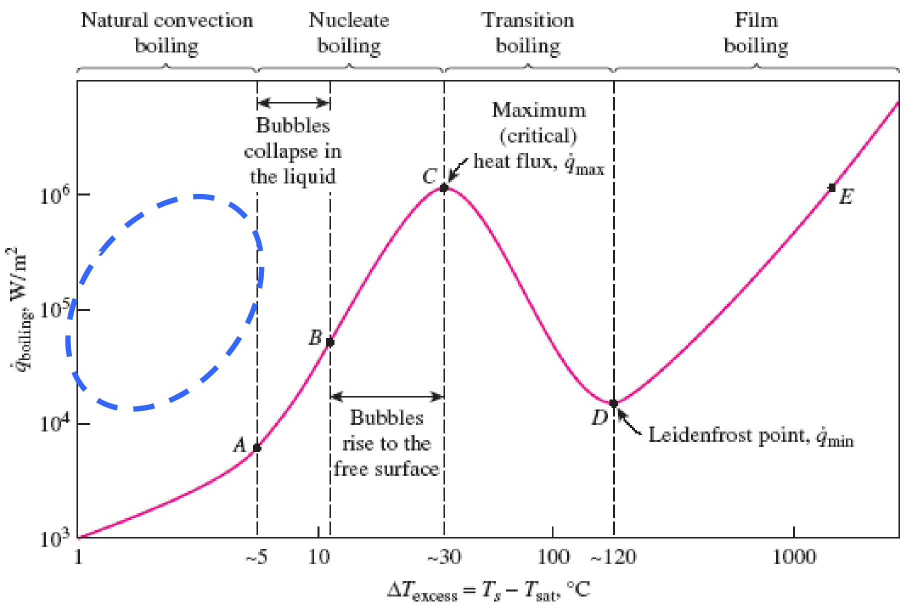

Nucleate Boiling (between Points A and C)

- The bubbles form at an increasing rate at an increasing number of nucleation sites as we move along the boiling curve toward point *C*.

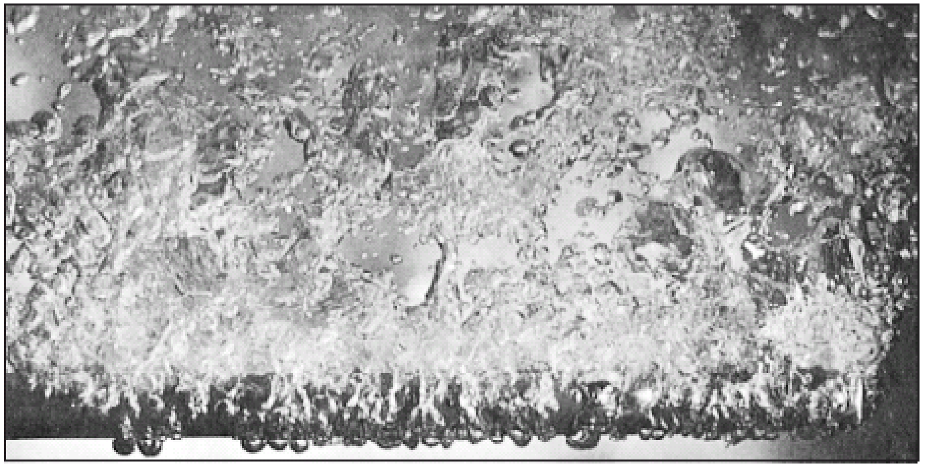

- **Region *A–B*** — *isolated bubbles.*

$$(5°\text{C} \le \Delta T_{\text{excess}} \le 10°\text{C})$$

- **Region *B–C*** — numerous *continuous columns of vapor* in the liquid.

$$(10°\text{C} \le \Delta T_{\text{excess}} \le 30°\text{C})$$

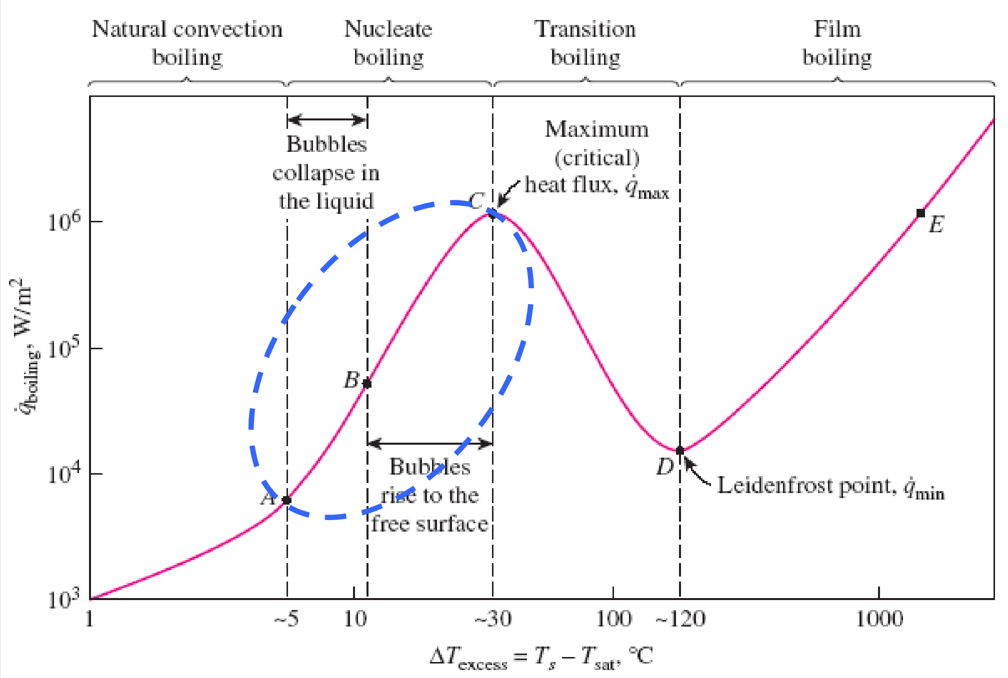

Point *A* is referred to as the ***onset of nucleate boiling (ONB)***.

- In region *A–B* the stirring and agitation caused by the entrainment of the liquid to the heater surface is primarily responsible for the increased heat transfer coefficient.
- In region *A–B* the large heat fluxes obtainable in this region are caused by the combined effect of liquid entrainment and evaporation.
- For the entire nucleate boiling range, the heat transfer coefficient ranges from about 2000 to 30,000 W/m²·K.

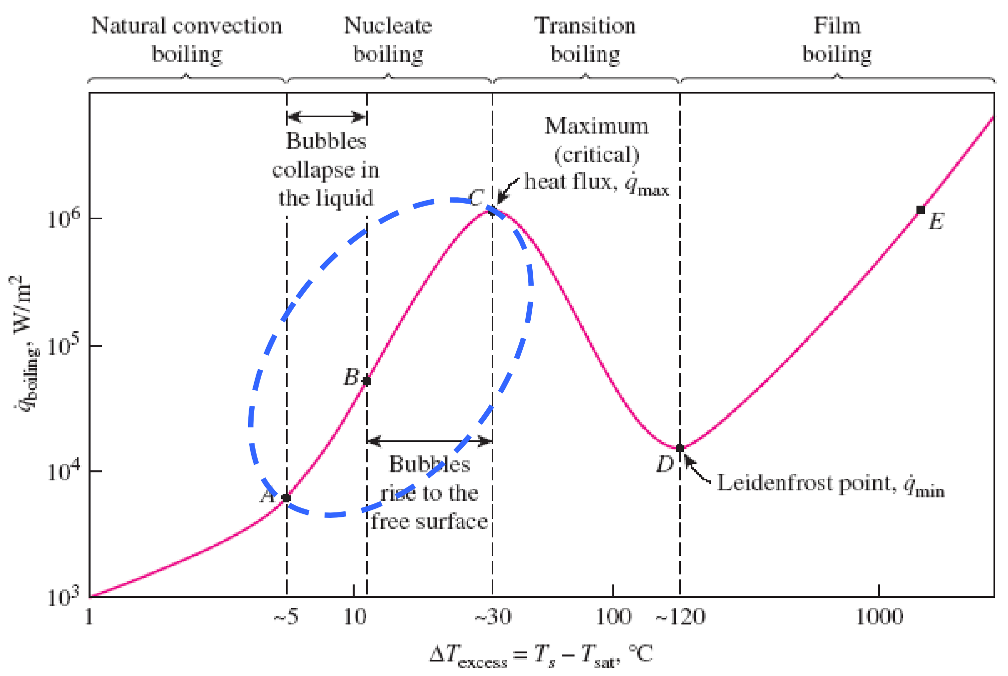

- After point *B* the heat flux increases at a lower rate with increasing ΔT_{excess}, and reaches a maximum at point *C*.
- The heat flux at this point is called the **critical** (or **maximum**) **heat flux**, and is of prime engineering importance.

Transition Boiling (between Points C and D)

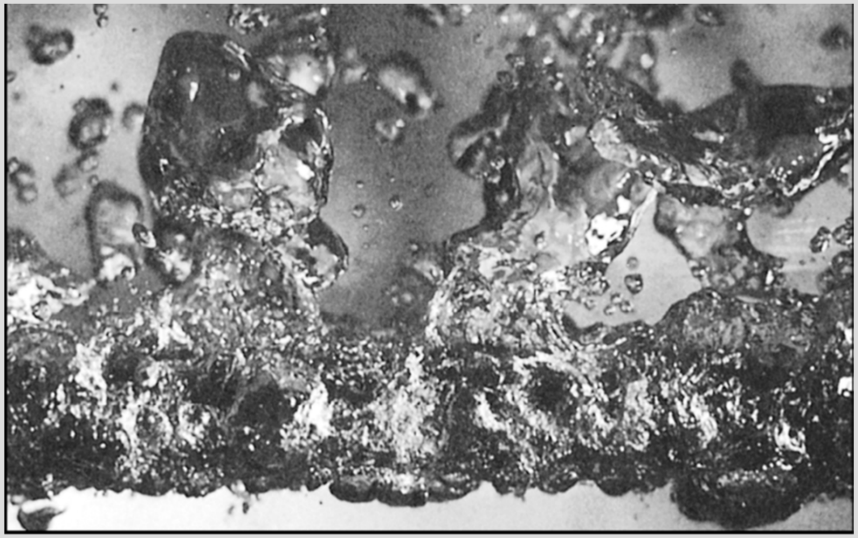

- When ΔT_{excess} is increased past point *C*, the heat flux decreases.
- This is because a large fraction of the heater surface is covered by a vapor film, which acts as an insulation.
- In the transition boiling regime, both nucleate and film boiling partially occur.
- Operation in the transition boiling regime, which is also called the ***unstable film boiling regime***, is avoided in practice.
- For water, transition boiling occurs over the excess temperature range from about 30°C to about 120°C.

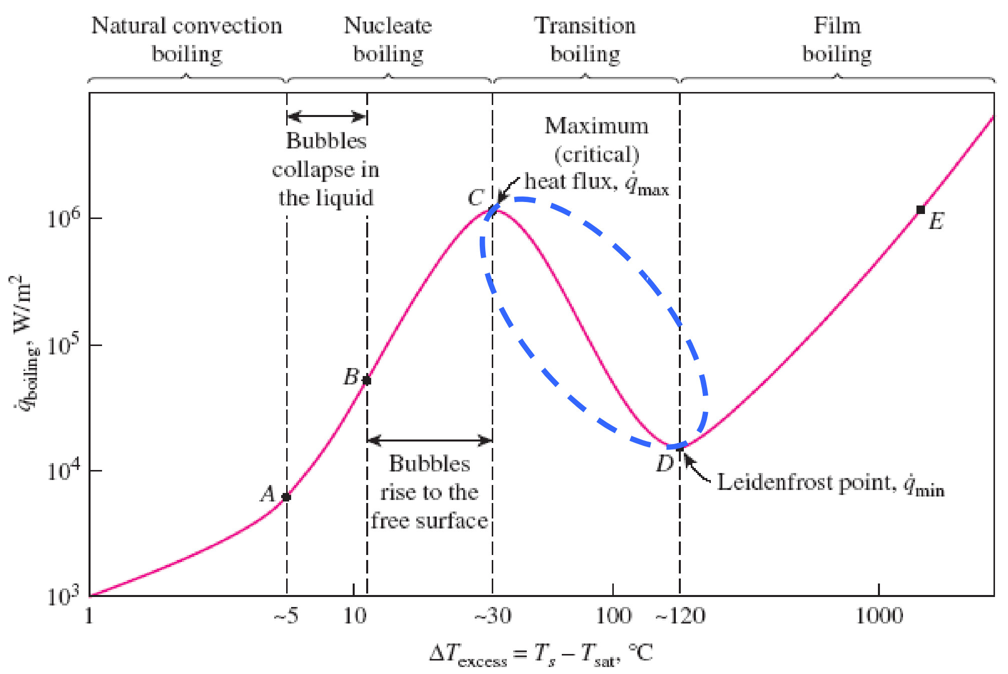

Film Boiling (beyond Point *D*

- Beyond point *D* the heater surface is completely covered by a continuous stable vapor film.
- Point *D*, where the heat flux reaches a minimum is called the **Leidenfrost point**.
- The presence of a vapor film between the heater surface and the liquid is responsible for the low heat transfer rates in the film boiling region.
- The heat transfer rate increases with increasing excess temperature due to radiation to the liquid.

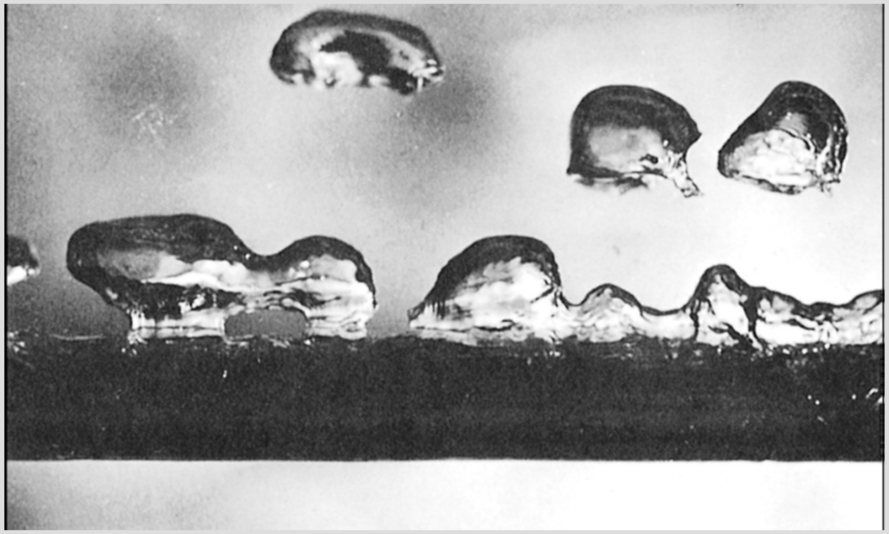

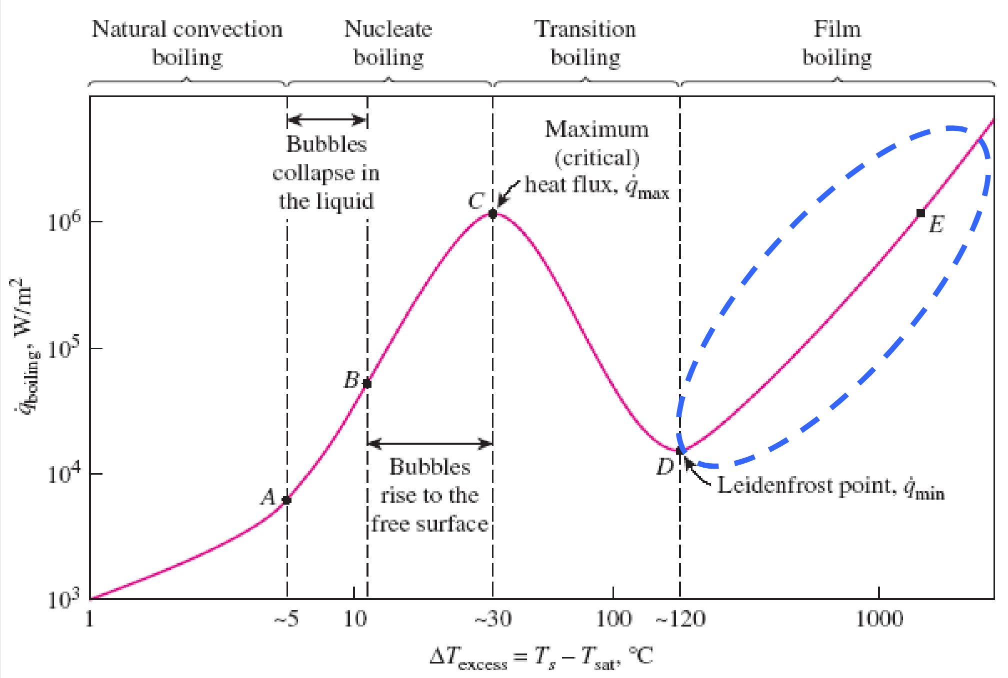

Burnout Phenomenon

- A typical boiling process does not follow the boiling curve beyond point *C.*
- When the power applied to the heated surface exceeded the value at point *C* even slightly, the surface temperature increased suddenly to point *E*.
- When the power is reduced gradually starting from point *E* the cooling curve follows Fig. 10–8 with a sudden drop in excess temperature when point *D* is reached.

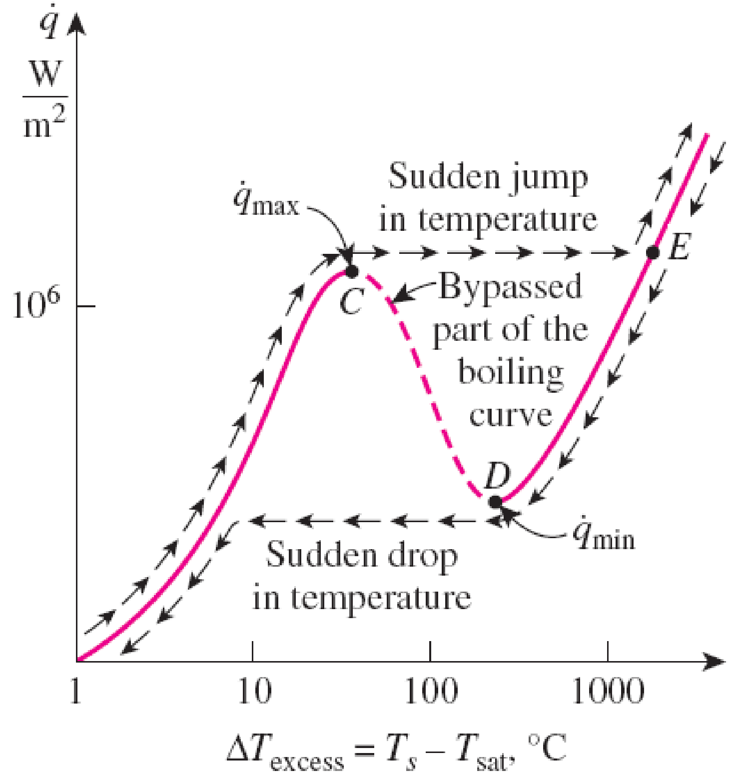

FIGURE 10–8

The actual boiling curve obtained with heated platinum wire in water as the heat flux is increased and then decreased.

Any attempt to increase the heat flux beyond q_{max} will cause the operation point on the boiling curve to jump suddenly from point *C* to point *E*.

However, surface temperature that corresponds to point *E* is beyond the melting point of most heater materials, and *burnout* occurs.

Therefore, point *C* on the boiling curve is also called the **burnout point**, and the heat flux at this point the **burnout heat flux.**

Most boiling heat transfer equipment in practice operate slightly below q_{max} to avoid any disastrous burnout.

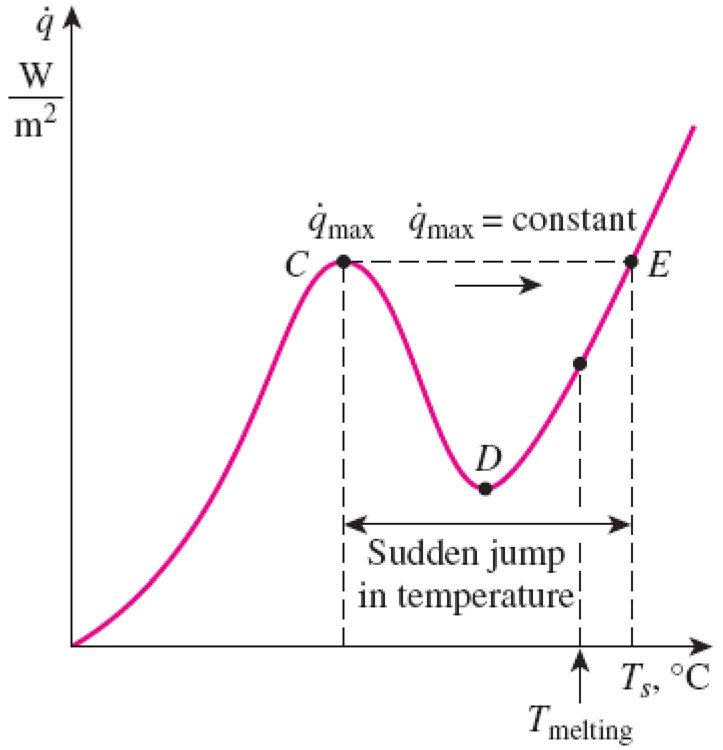

FIGURE 10–9
An attempt to increase the boiling heat flux beyond the critical value often causes the temperature of the heating element to jump suddenly to a value that is above the melting point, resulting in *burnout.*

Heat Transfer Correlations in Pool Boiling

- Boiling regimes differ considerably in their character.
- Different heat transfer relations need to be used for different boiling regimes.
- In the *natural convection boiling* regime heat transfer rates can be accurately determined using natural convection relations.

Nucleate Boiling

- No general theoretical relations for heat transfer in the nucleate boiling regime is available.
- Experimental based correlations are used.
- The rate of heat transfer strongly depends on the nature of nucleation and the type and the condition of the heated surface.

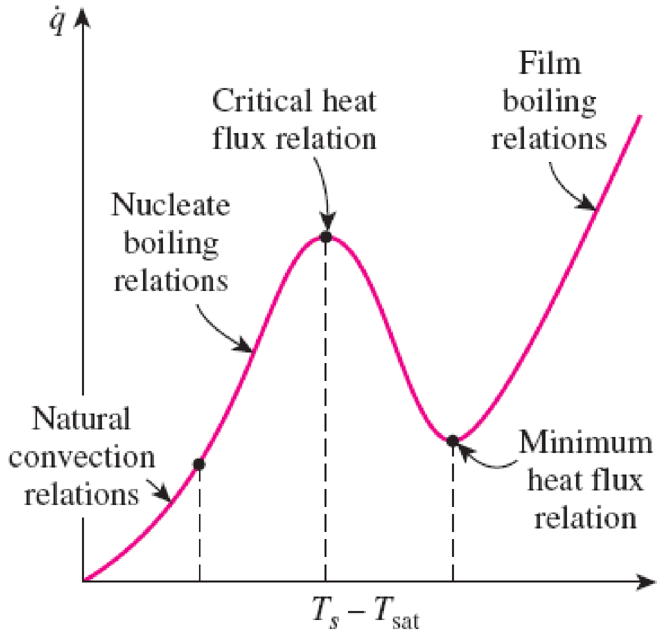

FIGURE 10–10
Different relations are used to determine the heat flux in different boiling regimes.

- For nucleate boiling a widely used correlation proposed in 1952 by Rohsenow:

$$\dot{q}_{\text{nucleate}} = \mu_l \, h_{fg} \left[\frac{g(\rho_l - \rho_v)}{\sigma} \right]^{1/2} \left[\frac{c_{pl}(T_s - T_{\text{sat}})}{C_{sf} \, h_{fg} \, \text{Pr}_l^n} \right]^3$$

$\dot{q}_{\text{nucleate}}$ = nucleate boiling heat flux, W/m^2
μ_l = viscosity of the liquid, kg/m·s
h_{fg} = enthalpy of vaporization, J/kg
g = gravitational acceleration, m/s^2
ρ_l = density of the liquid, kg/m^3
ρ_v = density of the vapor, kg/m^3
σ = surface tension of liquid–vapor interface, N/m
c_{pl} = specific heat of the liquid, J/kg·°C
T_s = surface temperature of the heater, °C
T_{sat} = saturation temperature of the fluid, °C
C_{sf} = experimental constant that depends on surface–fluid combination
Pr_l = Prandtl number of the liquid
n = experimental constant that depends on the fluid

$$\dot{q} = \left(\frac{\text{kg}}{\text{m} \cdot \text{s}} \right) \left(\frac{\text{J}}{\text{kg}} \right) \times \left(\frac{\frac{\text{m}}{\text{s}^2} \frac{\text{kg}}{\text{m}^3}}{\frac{\text{N}}{\text{m}}} \right)^{1/2} \left(\frac{\frac{\text{J}}{\text{kg} \cdot {}^\circ\text{C}} \, {}^\circ\text{C}}{\frac{\text{J}}{\text{kg}}} \right)^3$$

$$= \frac{\text{W}}{\text{m}} \left(\frac{1}{\text{m}^2} \right)^{1/2} (1)^3$$

$$= \text{W/m}^2$$

FIGURE 10–11

Equation 10–2 gives the boiling heat flux in W/m^2 when the quantities are expressed in the units specified in their descriptions.

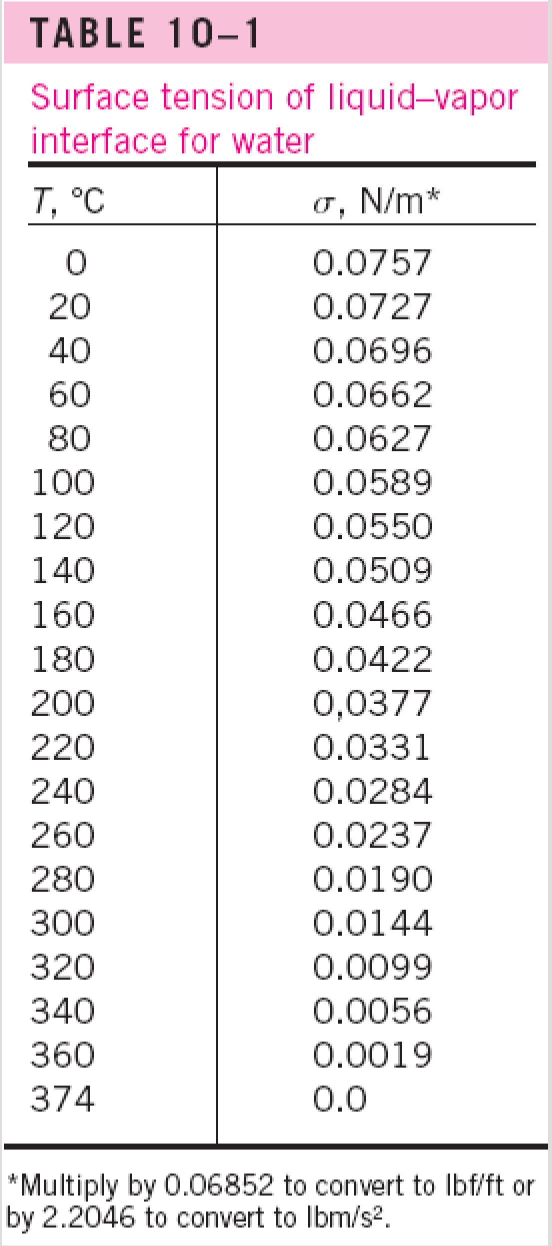

TABLE 10–1

Surface tension of liquid–vapor interface for water

T, °C	σ, N/m*
0	0.0757
20	0.0727
40	0.0696
60	0.0662
80	0.0627
100	0.0589
120	0.0550
140	0.0509
160	0.0466
180	0.0422
200	0,0377
220	0.0331
240	0.0284
260	0.0237
280	0.0190
300	0.0144
320	0.0099
340	0.0056
360	0.0019
374	0.0

*Multiply by 0.06852 to convert to lbf/ft or by 2.2046 to convert to lbm/s^2.

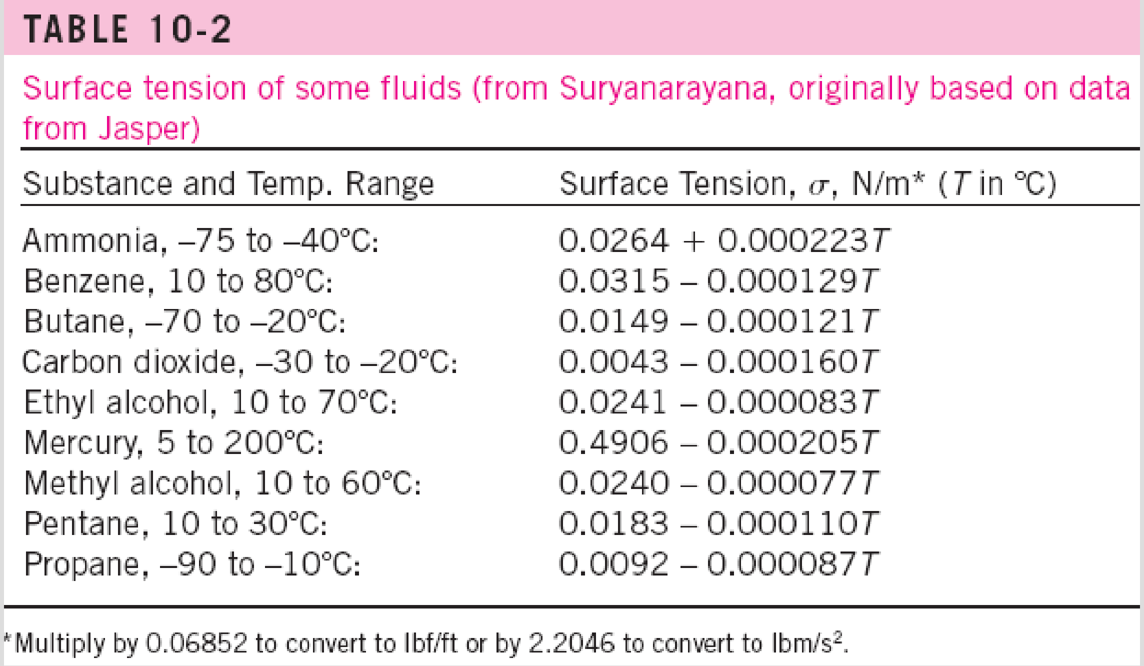

TABLE 10-2

Surface tension of some fluids (from Suryanarayana, originally based on data from Jasper)

Substance and Temp. Range	Surface Tension, σ, N/m* (T in °C)
Ammonia, –75 to –40°C:	$0.0264 + 0.000223T$
Benzene, 10 to 80°C:	$0.0315 - 0.000129T$
Butane, –70 to –20°C:	$0.0149 - 0.000121T$
Carbon dioxide, –30 to –20°C:	$0.0043 - 0.000160T$
Ethyl alcohol, 10 to 70°C:	$0.0241 - 0.000083T$
Mercury, 5 to 200°C:	$0.4906 - 0.000205T$
Methyl alcohol, 10 to 60°C:	$0.0240 - 0.000077T$
Pentane, 10 to 30°C:	$0.0183 - 0.000110T$
Propane, –90 to –10°C:	$0.0092 - 0.000087T$

*Multiply by 0.06852 to convert to lbf/ft or by 2.2046 to convert to lbm/s^2.

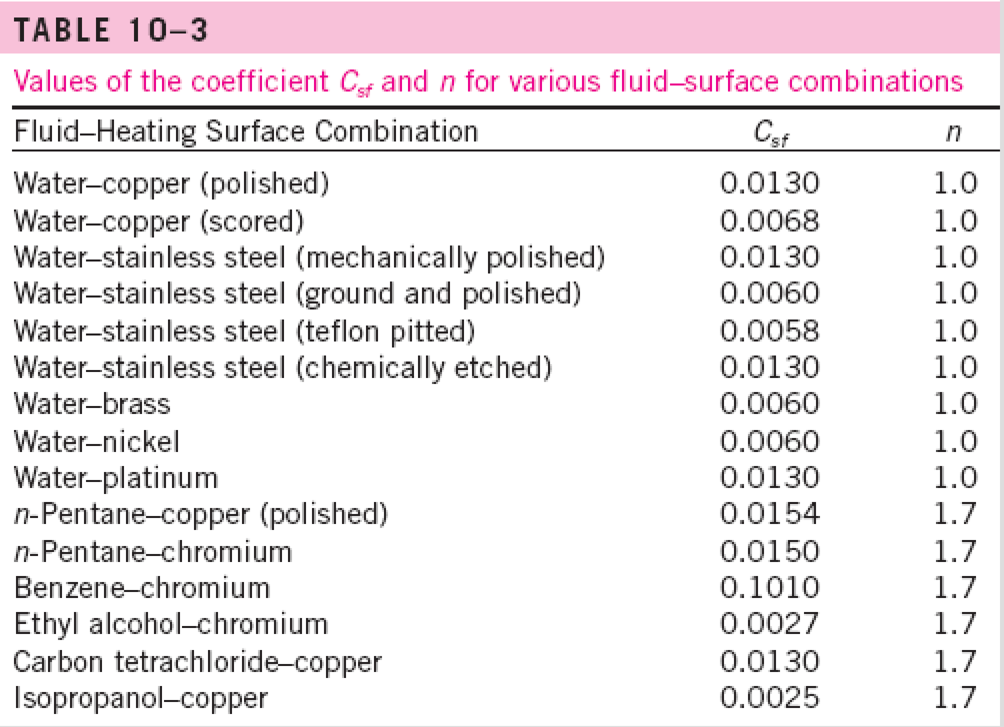

TABLE 10–3

Values of the coefficient C_{sf} and n for various fluid–surface combinations

Fluid–Heating Surface Combination	C_{sf}	n
Water–copper (polished)	0.0130	1.0
Water–copper (scored)	0.0068	1.0
Water–stainless steel (mechanically polished)	0.0130	1.0
Water–stainless steel (ground and polished)	0.0060	1.0
Water–stainless steel (teflon pitted)	0.0058	1.0
Water–stainless steel (chemically etched)	0.0130	1.0
Water–brass	0.0060	1.0
Water–nickel	0.0060	1.0
Water–platinum	0.0130	1.0
n-Pentane–copper (polished)	0.0154	1.7
n-Pentane–chromium	0.0150	1.7
Benzene–chromium	0.1010	1.7
Ethyl alcohol–chromium	0.0027	1.7
Carbon tetrachloride–copper	0.0130	1.7
Isopropanol–copper	0.0025	1.7

Peak Heat Flux

- The *maximum* (or *critical*) *heat flux* (CHF) in nucleate pool boiling:

$$\dot{q}_{\max} = C_{cr}\, h_{fg}[\sigma g \rho^2_v (\rho_l - \rho_v)]^{1/4}$$

C_{cr} is a constant whose value depends on the heater geometry, but generally is about 0.15.

- The CHF is independent of the fluid–heating surface combination, as well as the viscosity, thermal conductivity, and the specific heat of the liquid.
- The CHF increases with pressure up to about one-third of the critical pressure, and then starts to decrease and becomes zero at the critical pressure.
- The CHF is proportional to h_{fg}, and large maximum heat fluxes can be obtained using fluids with a large enthalpy of vaporization, such as water.

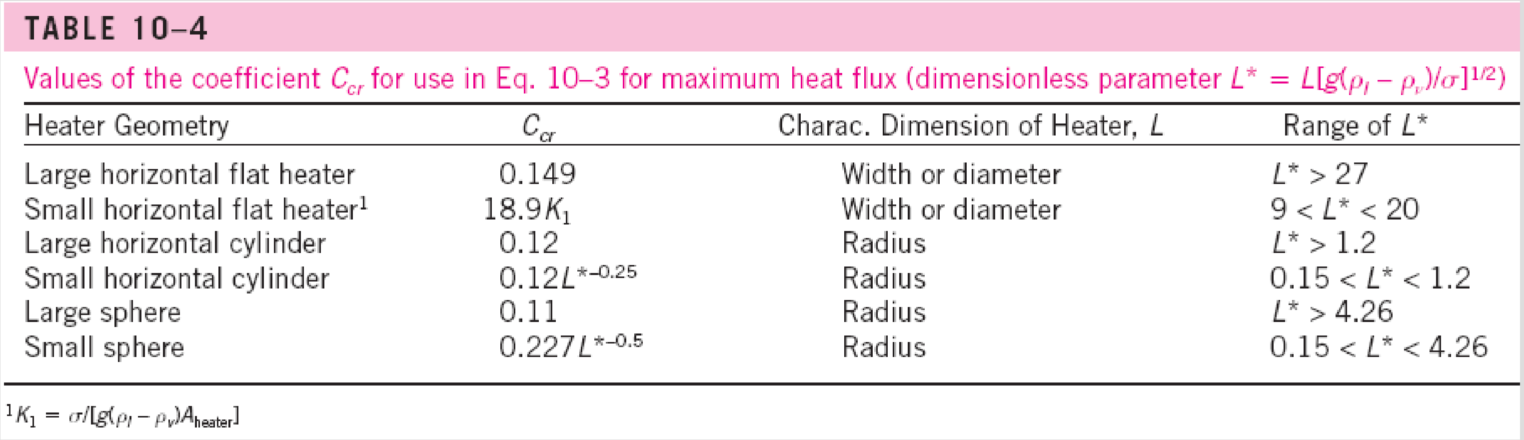

TABLE 10–4

Values of the coefficient C_{cr} for use in Eq. 10–3 for maximum heat flux (dimensionless parameter $L^* = L[g(\rho_l - \rho_v)/\sigma]^{1/2}$)

Heater Geometry	C_{cr}	Charac. Dimension of Heater, L	Range of L^*
Large horizontal flat heater	0.149	Width or diameter	$L^* > 27$
Small horizontal flat heater[1]	$18.9K_1$	Width or diameter	$9 < L^* < 20$
Large horizontal cylinder	0.12	Radius	$L^* > 1.2$
Small horizontal cylinder	$0.12L^{*-0.25}$	Radius	$0.15 < L^* < 1.2$
Large sphere	0.11	Radius	$L^* > 4.26$
Small sphere	$0.227L^{*-0.5}$	Radius	$0.15 < L^* < 4.26$

[1] $K_1 = \sigma/[g(\rho_l - \rho_v)A_{\text{heater}}]$

Minimum Heat Flux

- Minimum heat flux, which occurs at the Leidenfrost point, is of practical interest since it represents the lower limit for the heat flux in the film boiling regime.
- Zuber derived the following expression for the minimum heat flux for a *large horizontal plate*

$$\dot{q}_{\min} = 0.09\rho_v h_{fg}\left[\frac{\sigma g(\rho_l - \rho_v)}{(\rho_l + \rho_v)^2}\right]^{1/4}$$

- This relation above can be in error by 50% or more.

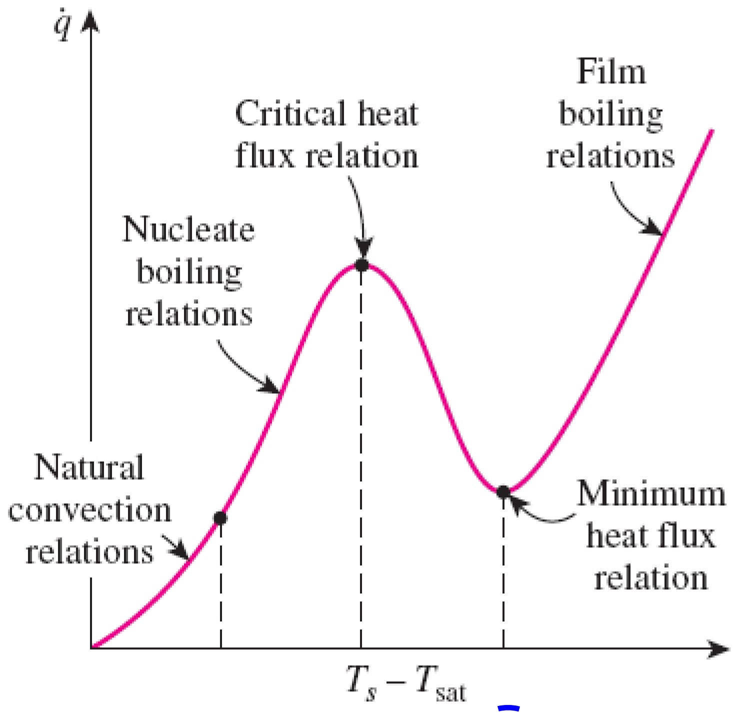

FIGURE 10–10
Different relations are used to determine the heat flux in different boiling regimes.

Transition boiling regime

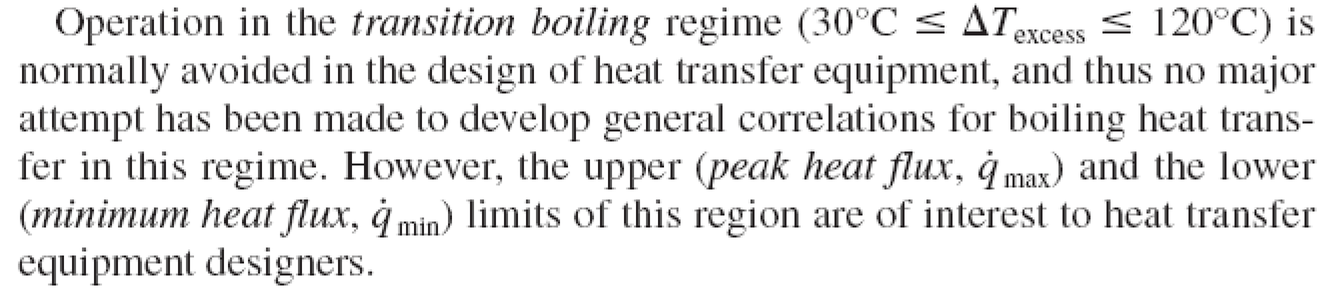
Operation in the *transition boiling* regime (30°C $\leq \Delta T_{\text{excess}} \leq$ 120°C) is normally avoided in the design of heat transfer equipment, and thus no major attempt has been made to develop general correlations for boiling heat transfer in this regime. However, the upper (*peak heat flux*, $\dot{q}_{\max}$) and the lower (*minimum heat flux*, $\dot{q}_{\min}$) limits of this region are of interest to heat transfer equipment designers.

Film Boiling

The heat flux for film boiling on a *horizontal cylinder* or *sphere* of diameter *D* is given by

$$\dot{q}_{\text{film}} = C_{\text{film}} \left[\frac{g k_v^3 \; \rho_v (\rho_l - \rho_v)[h_{fg} + 0.4 c_{pv} (T_s - T_{\text{sat}})]}{\mu_v D (T_s - T_{\text{sat}})} \right]^{1/4} (T_s - T_{\text{sat}})$$

$$C_{\text{film}} = \begin{Bmatrix} 0.62 \text{ for horizontal cylinders} \\ 0.67 \text{ for spheres} \end{Bmatrix}$$

- At high surface temperatures (typically above 300°C), heat transfer across the vapor film by *radiation* becomes significant and needs to be considered.

$$\dot{q}_{\text{rad}} = \varepsilon \sigma \left(T_s^4 - T_{\text{sat}}^4\right)$$

For $\dot{q}_{\text{rad}} < \dot{q}_{\text{film}}$,

$$\dot{q}_{\text{total}} = \dot{q}_{\text{film}} + \frac{3}{4} \dot{q}_{\text{rad}}$$

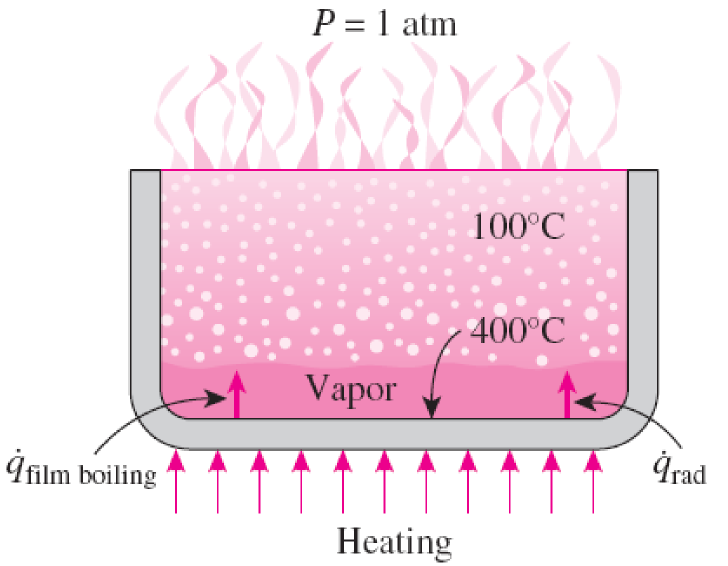

FIGURE 10–12

At high heater surface temperatures, radiation heat transfer becomes significant during film boiling.

Enhancement of Heat Transfer in Pool Boiling

- The rate of heat transfer in the nucleate boiling regime strongly depends on the number of active nucleation sites on the surface, and the rate of bubble formation at each site.
- Therefore, modification that enhances *nucleation* on the heating surface will also enhance *heat transfer* in nucleate boiling.
- *Irregularities* on the heating surface, including roughness and dirt, serve as additional nucleation sites during boiling.
- The effect of surface roughness is observed to decay with time.

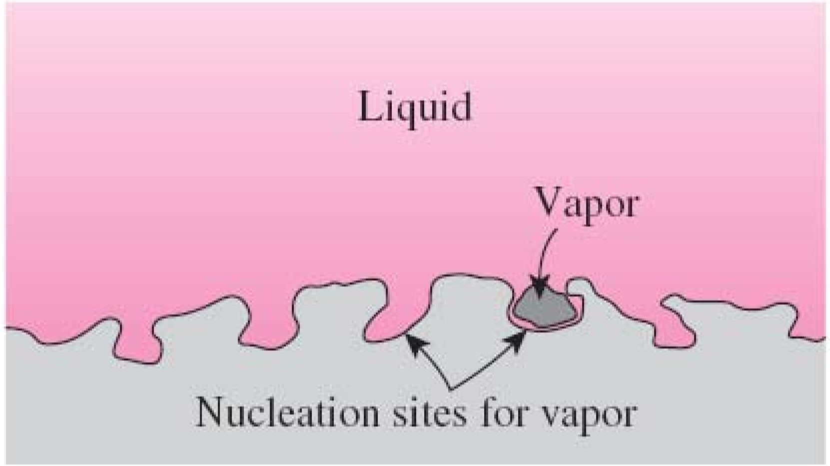

FIGURE 10–13
The cavities on a rough surface act as nucleation sites and enhance boiling heat transfer.

- Surfaces that provide enhanced heat transfer in nucleate boiling *permanently* are being manufactured and are available in the market.
- Heat transfer can be enhanced by a factor of up to 10 during nucleate boiling, and the critical heat flux by a factor of 3.
- The use of finned surfaces is also known to enhance nucleate boiling heat transfer and the maximum heat flux.
- Boiling heat transfer can also be enhanced by other techniques such as *mechanical agitation* and *surface vibration*.
- These techniques are not practical, however, because of the complications involved.

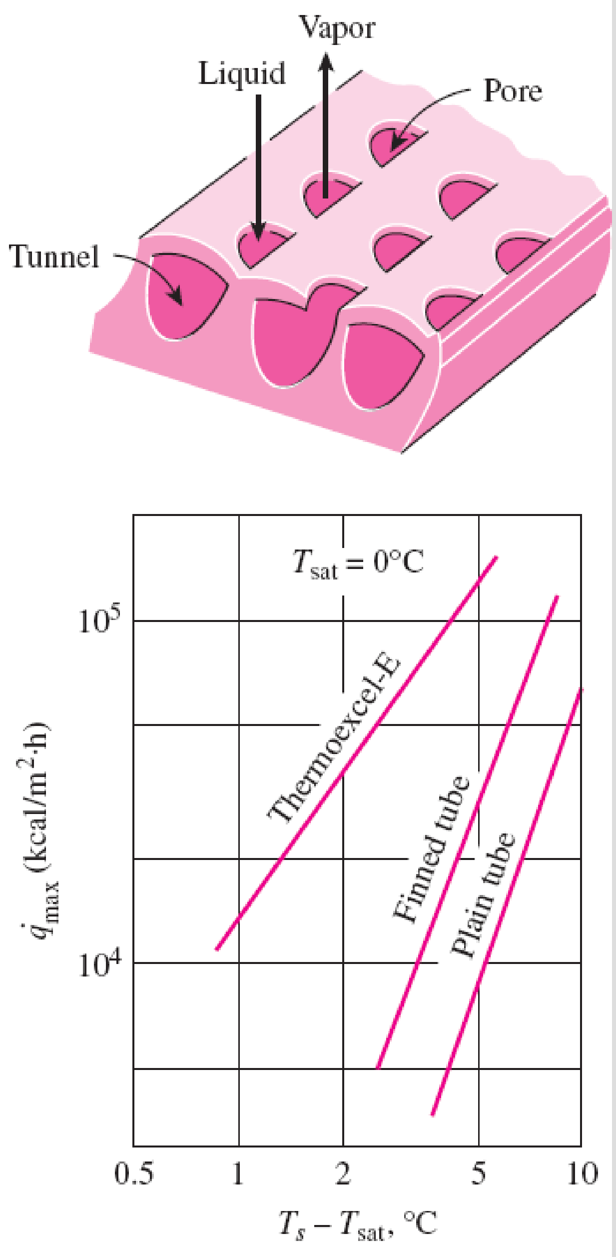

FIGURE 10–14
The enhancement of boiling heat transfer in Freon-12 by a mechanically roughened surface, thermoexcel-E.

FLOW BOILING

- In **flow boiling**, the fluid is forced to move by an external source such as a pump as it undergoes a phase-change process.
- It exhibits the combined effects of convection and pool boiling.
- *External flow boiling* over a plate or cylinder is similar to pool boiling, but the added motion increases both the nucleate boiling heat flux and the maximum heat flux considerably.
- The higher the velocity, the higher the nucleate boiling heat flux and the critical heat flux.
- *Internal flow boiling*, commonly referred to as *two-phase flow*, is much more complicated in nature because there is no free surface for the vapor to escape, and thus both the liquid and the vapor are forced to flow together.

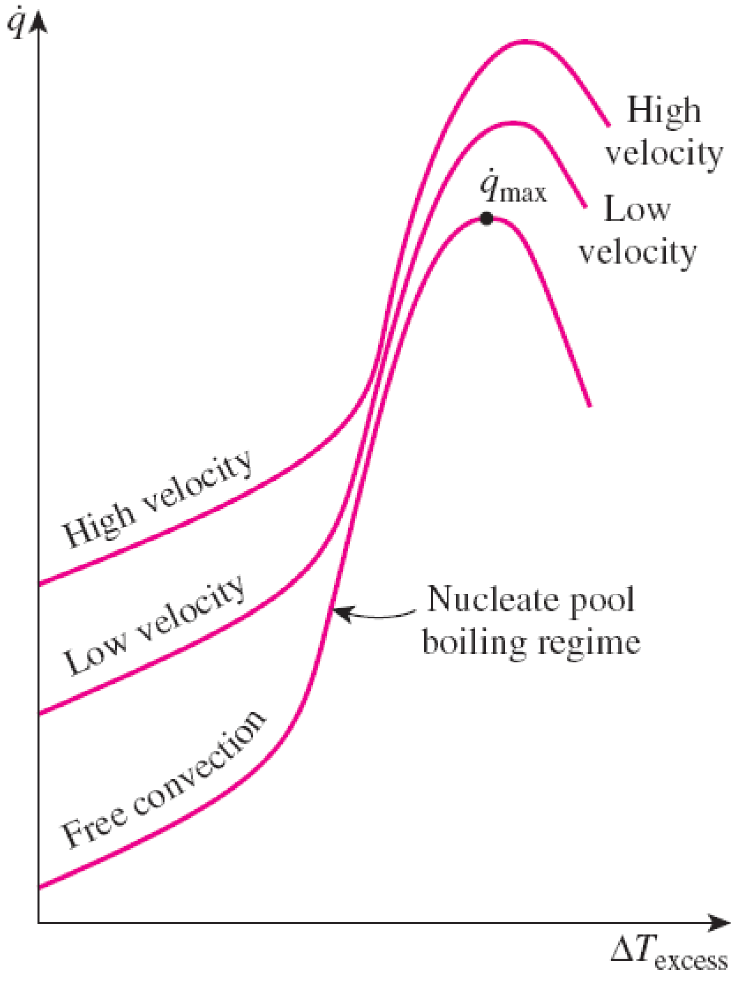

FIGURE 10–18
The effect of forced convection on external flow boiling for different flow velocities.

- The two-phase flow in a tube exhibits different flow boiling regimes, depending on the relative amounts of the liquid and the vapor phases.
- Note that the tube contains a liquid before the bubbly flow regime and a vapor after the mist-flow regime.
- Heat transfer in those two cases can be determined using the appropriate relations for single-phase convection heat transfer.

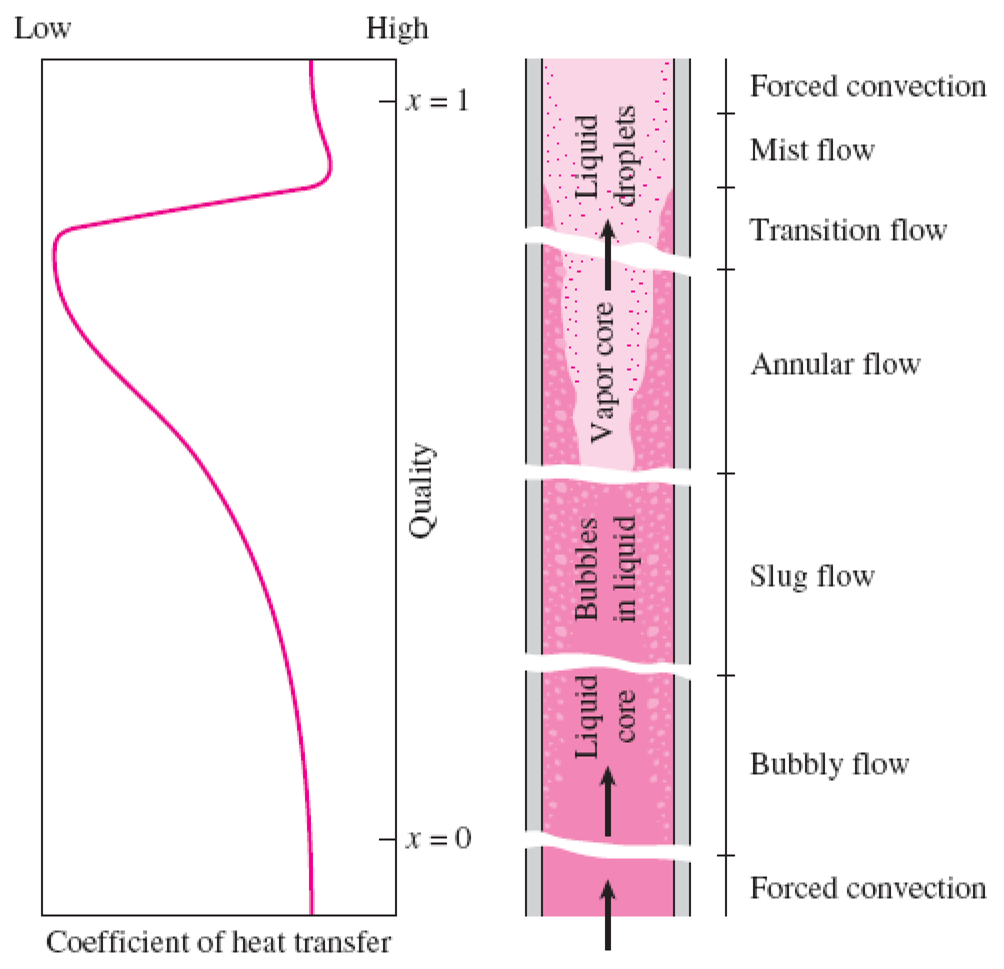

FIGURE 10–19
Different flow regimes encountered in flow boiling in a tube under forced convection.

- Liquid single-phase flow
  - ✓ In the inlet region the liquid is subcooled and heat transfer to the liquid is by *forced convection* (assuming no subcooled boiling).
- Bubbly flow
  - ✓ Individual bubbles
  - ✓ Low mass qualities
- Slug flow
  - ✓ Bubbles coalesce into slugs of vapor.
  - ✓ Moderate mass qualities
- Annular flow
  - ✓ Core of the flow consists of vapor only, and liquid adjacent to the walls.
  - ✓ Very high heat transfer coefficients
- Mist flow
  - ✓ A sharp decrease in the heat transfer coefficient
- Vapor single-phase flow
  - ✓ The liquid phase is completely evaporated and vapor is superheated.

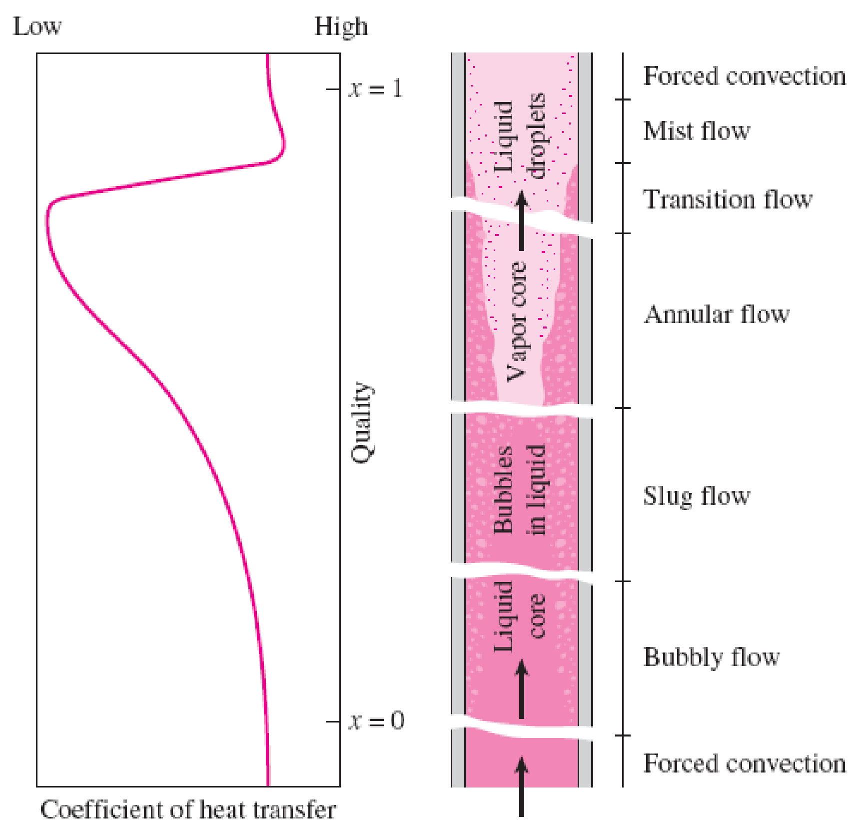

Heat Transfer Lectures
Fundamentals & Applications

UNIVERSITY OF TECHNOLOGY

Mechanical Engineering department

3rd power plant division

CONDENSATION

Dr. Sattar Aljabair

CONDENSATION HEAT TRANSFER

Condensation occurs when the temperature of a vapor is reduced *below* its saturation temperature.

Film condensation

- The condensate wets the surface and forms a liquid film.
- The surface is blanketed by a liquid film which serves as a *resistance* to heat transfer.

Dropwise condensation

- The condensed vapor forms droplets on the surface.
- The droplets slide down when they reach a certain size.
- No liquid film to resist heat transfer.
- As a result, heat transfer rates that are more than 10 times larger than with film condensation can be achieved.

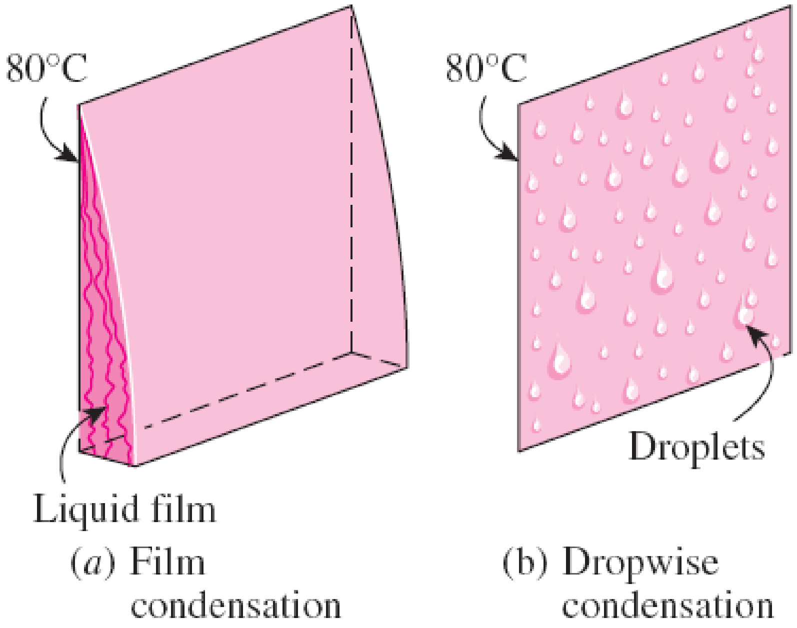

(*a*) Film condensation

(b) Dropwise condensation

FIGURE 10–20

When a vapor is exposed to a surface at a temperature below T_{sat}, condensation in the form of a liquid film or individual droplets occurs on the surface.

FILM CONDENSATION

- Liquid film starts forming at the top of the plate and flows downward under the influence of gravity.
- δ *increases* in the flow direction x
- Heat in the amount h_{fg} is released during condensation and is *transferred* through the film to the plate surface.
- T_s must be below the saturation temperature for condensation.
- The *temperature* of the condensate is T_{sat} at the interface and decreases gradually to T_s at the wall.

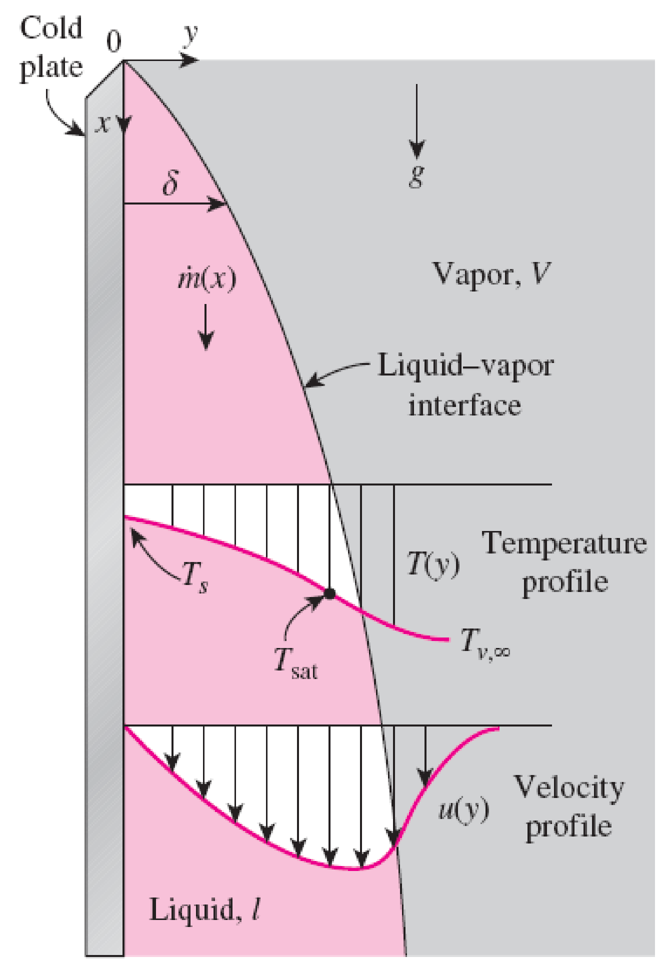

FIGURE 10–21
Film condensation on a vertical plate.

$$\mathrm{Re} = \frac{D_h \rho_l V_l}{\mu_l} = \frac{4 A_c \rho_l V_l}{p \mu_l} = \frac{4 \rho_l V_l \delta}{\mu_l} = \frac{4 \dot{m}}{p \mu_l}$$

$D_h = 4A_c/p = 4\delta$ = hydraulic diameter of the condensate flow, m
p = wetted perimeter of the condensate, m
$A_c = -p\delta$ = wetted perimeter × film thickness, m^2, cross-sectional area of the condensate flow at the lowest part of the flow
ρ_l = density of the liquid, kg/m^3
μ_l = viscosity of the liquid, kg/m·s
V_l = average velocity of the condensate at the lowest part of the flow, m/s
$\dot{m} = \rho_1 V_1 A_c$ = mass flow rate of the condensate at the lowest part, kg/s

Heat transfer in condensation depends on whether the condensate flow is *laminar* or *turbulent*. The criterion for the flow regime is provided by the Reynolds number.

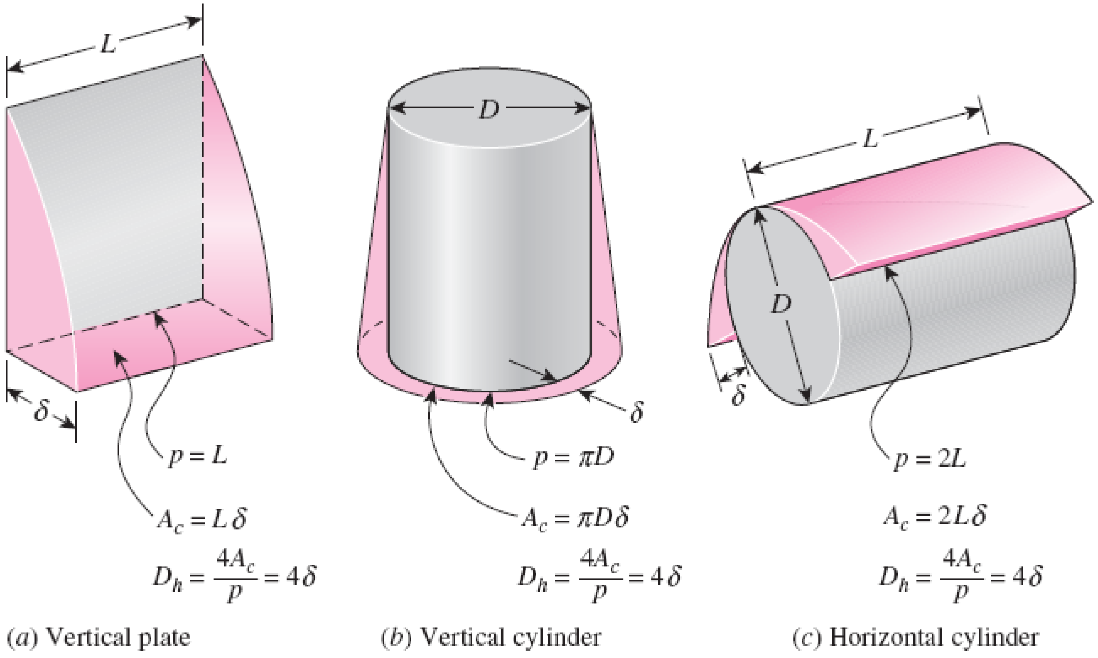

(*a*) Vertical plate (*b*) Vertical cylinder (*c*) Horizontal cylinder

FIGURE 10–22

The wetted perimeter p, the condensate cross-sectional area A_c, and the hydraulic diameter D_h for some common geometries.

When the final state is subcooled liquid instead of saturated liquid:

$$h^*_{fg} = h_{fg} + 0.68c_{pl}(T_{\text{sat}} - T_s)$$

Modified latent heat of vaporization

For vapor that enters the condenser as **superheated vapor** at a temperature T_v instead of as saturated vapor:

$$h^*_{fg} = h_{fg} + 0.68c_{pl}(T_{\text{sat}} - T_s) + c_{pv}(T_v - T_{\text{sat}})$$

$$\dot{Q}_{\text{conden}} = hA_s(T_{\text{sat}} - T_s) = \dot{m}h^*_{fg}$$

Rate of heat transfer

$$\text{Re} = \frac{4\dot{Q}_{\text{conden}}}{p\mu_l h^*_{fg}} = \frac{4A_s h(T_{\text{sat}} - T_s)}{p\mu_l h^*_{fg}}$$

This relation is convenient to use to determine the Reynolds number when the condensation heat transfer coefficient or the rate of heat transfer is known.

$$T_f = (T_{\text{sat}} + T_s)/2$$

The properties of the liquid should be evaluated at the *film temperature*

The h_{fg} should be evaluated at T_{sat}

Flow Regimes

- The dimensionless parameter controlling the transition between regimes is the Reynolds number defined as:

$$\mathrm{Re} = \frac{D_h \rho_l V_l}{\mu_l} = \frac{4 A_c \rho_l V_l}{p \mu_l} = \frac{4 \rho_l V_l \delta}{\mu_l} = \frac{4 \dot{m}}{p \mu_l}$$

- Three prime flow regimes:
  - ✓ Re < 30 ─ Laminar (wave-free)
  - ✓ 30 < Re < 1800 ─ Laminar (wavy)
  - ✓ Re > 1800 ─ Turbulent
- The Reynolds number increases in the flow direction.

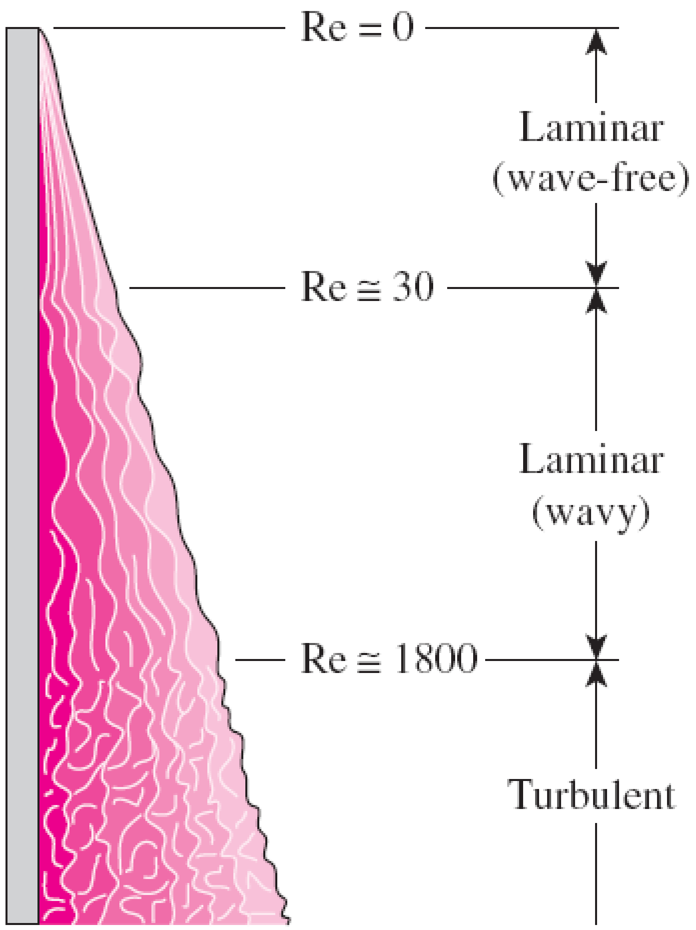

FIGURE 10–23
Flow regimes during film condensation on a vertical plate.

Heat Transfer Correlations for Film Condensation

1 Vertical Plates

Assumptions:

1. Both the plate and the vapor are maintained at *constant temperatures* of T_s and T_{sat}, respectively, and the temperature across the liquid film varies *linearly.*

2. Heat transfer across the liquid film is by pure *conduction*.

3. The velocity of the vapor is low (or zero) so that it exerts *no drag* on the condensate (no viscous shear on the liquid–vapor interface).

4. The flow of the condensate is *laminar* (Re<30) and the properties of the liquid are constant.

5. The acceleration of the condensate layer is negligible.

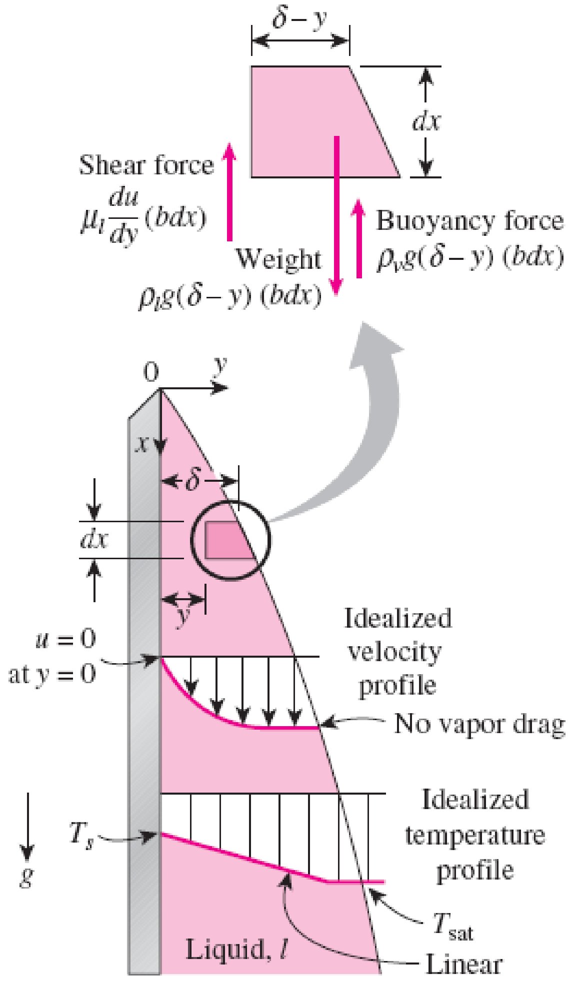

FIGURE 10–24
The volume element of condensate on a vertical plate considered in Nusselt's analysis.

Then Newton's second law of motion for the volume element shown in Fig. 10–24 in the vertical x-direction can be written as

$$\sum F_x = ma_x = 0$$

since the acceleration of the fluid is zero. Noting that the only force acting downward is the weight of the liquid element, and the forces acting upward are the viscous shear (or fluid friction) force at the left and the buoyancy force, the force balance on the volume element becomes

$$F_{\text{downward}\downarrow} = F_{\text{upward}\uparrow}$$

$$\text{Weight} = \text{Viscous shear force} + \text{Buoyancy force}$$

$$\rho_l g(\delta - y)(bdx) = \mu_l \frac{du}{dy}(bdx) + \rho_v\, g(\delta - y)(bdx)$$

Canceling the plate width b and solving for du/dy gives

$$\frac{du}{dy} = \frac{g(\rho_l - \rho_v)g(\rho - y)}{\mu_l}$$

Integrating from $y = 0$ where $u = 0$ (because of the no-slip boundary condition) to $y = y$ where $u = u(y)$ gives

$$u(y) = \frac{g(\rho_l - \rho_v)g}{\mu_l}\left(y\delta - \frac{y^2}{2}\right) \tag{10–12}$$

The mass flow rate of the condensate at a location x, where the boundary layer thickness is δ, is determined from

$$\dot{m}(x) = \int_A \rho_l u(y)dA = \int_{y=0}^{\delta} \rho_l u(y)bdy \tag{10–13}$$

Substituting the $u(y)$ relation from Equation 10–12 into Eq. 10–13 gives

$$\dot{m}\,(x) = \frac{gb\rho_l(\rho_l - \rho_v)\delta^3}{3\mu_l} \tag{10–14}$$

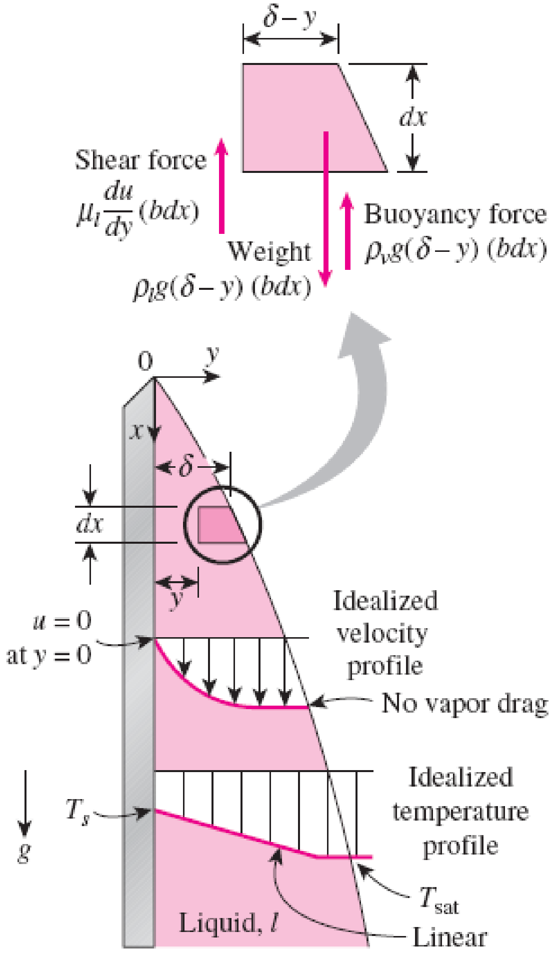

FIGURE 10–24

The volume element of condensate on a vertical plate considered in Nusselt's analysis.

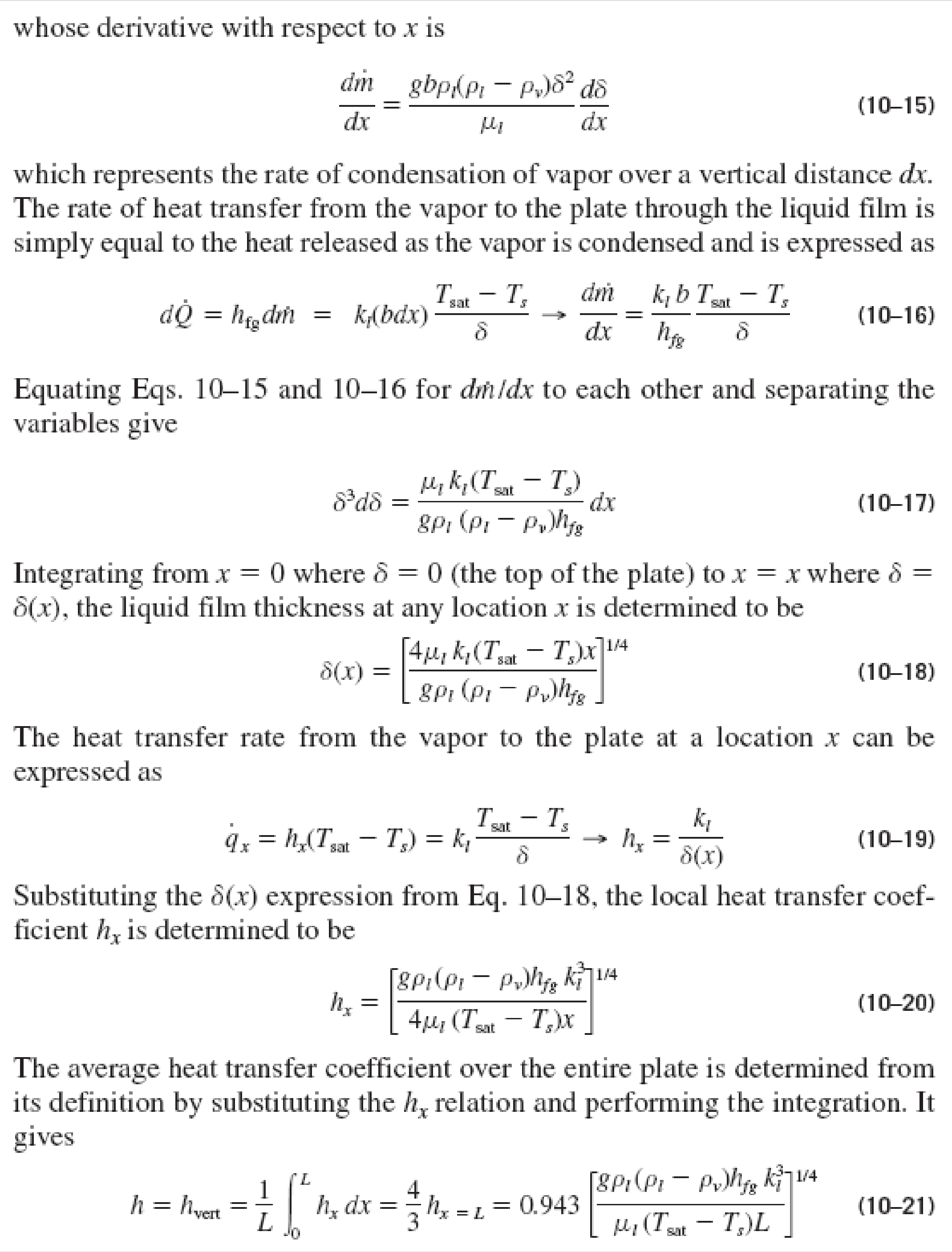

whose derivative with respect to x is

$$\frac{d\dot{m}}{dx} = \frac{gb\rho_l(\rho_l - \rho_v)\delta^2}{\mu_l}\frac{d\delta}{dx} \tag{10–15}$$

which represents the rate of condensation of vapor over a vertical distance dx. The rate of heat transfer from the vapor to the plate through the liquid film is simply equal to the heat released as the vapor is condensed and is expressed as

$$d\dot{Q} = h_{fg}d\dot{m} \quad = \quad k_l(bdx)\frac{T_{sat} - T_s}{\delta} \rightarrow \frac{d\dot{m}}{dx} = \frac{k_l\,b}{h_{fg}}\frac{T_{sat} - T_s}{\delta} \tag{10–16}$$

Equating Eqs. 10–15 and 10–16 for $d\dot{m}/dx$ to each other and separating the variables give

$$\delta^3 d\delta = \frac{\mu_l\,k_l(T_{sat} - T_s)}{g\rho_l\,(\rho_l - \rho_v)h_{fg}}\,dx \tag{10–17}$$

Integrating from $x = 0$ where $\delta = 0$ (the top of the plate) to $x = x$ where $\delta = \delta(x)$, the liquid film thickness at any location x is determined to be

$$\delta(x) = \left[\frac{4\mu_l\,k_l(T_{sat} - T_s)x}{g\rho_l\,(\rho_l - \rho_v)h_{fg}}\right]^{1/4} \tag{10–18}$$

The heat transfer rate from the vapor to the plate at a location x can be expressed as

$$\dot{q}_x = h_x(T_{sat} - T_s) = k_l\frac{T_{sat} - T_s}{\delta} \rightarrow h_x = \frac{k_l}{\delta(x)} \tag{10–19}$$

Substituting the $\delta(x)$ expression from Eq. 10–18, the local heat transfer coefficient h_x is determined to be

$$h_x = \left[\frac{g\rho_l(\rho_l - \rho_v)h_{fg}\,k_l^3}{4\mu_l\,(T_{sat} - T_s)x}\right]^{1/4} \tag{10–20}$$

The average heat transfer coefficient over the entire plate is determined from its definition by substituting the h_x relation and performing the integration. It gives

$$h = h_{vert} = \frac{1}{L}\int_0^L h_x\,dx = \frac{4}{3}h_{x=L} = 0.943\left[\frac{g\rho_l(\rho_l - \rho_v)h_{fg}\,k_l^3}{\mu_l\,(T_{sat} - T_s)L}\right]^{1/4} \tag{10–21}$$

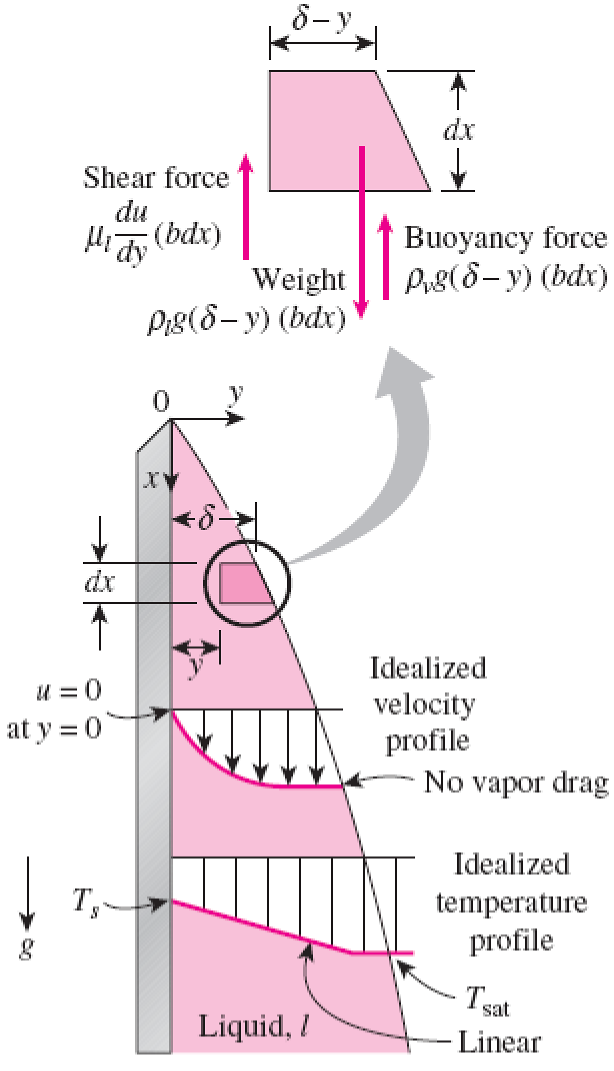

FIGURE 10–24

The volume element of condensate on a vertical plate considered in Nusselt's analysis.

The *average heat transfer coefficient* for laminar film condensation over a vertical flat plate of height *L* is

$$h_{\text{vert}} = 0.943\left[\frac{g\rho_l(\rho_l - \rho_v)h^*_{fg}\,k_l^3}{\mu_l\,(T_{\text{sat}} - T_s)L}\right]^{1/4} \qquad (\text{W/m}^2\cdot\text{K}), \qquad 0 < \text{Re} < 30 \qquad \text{(10-22)}$$

g = gravitational acceleration, m/s²
ρ_l, ρ_v = densities of the liquid and vapor, respectively, kg/m³
μ_l = viscosity of the liquid, kg/m·s
$h^*_{fg} = h_{fg} + 0.68c_{pl}(T_{\text{sat}} - T_s)$ = modified latent heat of vaporization, J/kg
k_l = thermal conductivity of the liquid, W/m·K
L = height of the vertical plate, m
T_s = surface temperature of the plate, °C
T_{sat} = saturation temperature of the condensing fluid, °C

$$\text{Re} \cong \frac{4g\rho_l(\rho_l - \rho_v)\delta^3}{3\mu_l^2} = \frac{4g\rho_l^2}{3\mu_l^2}\left(\frac{k_l}{h_{x=L}}\right)^3 = \frac{4g}{3\nu_l^2}\left(\frac{k_l}{3h_{\text{vert}}/4}\right)^3$$

$$h_{\text{vert}} \cong 1.47k_l\,\text{Re}^{-1/3}\left(\frac{g}{\nu_l^2}\right)^{1/3}, \qquad \begin{array}{l} 0 < \text{Re} < 30 \\ \rho_v \ll \rho_l \end{array}$$

$$T_f = (T_{\text{sat}} + T_s)/2$$

All properties of the liquid are to be evaluated at the film temperature. The h_{fg} and ρ_v are to be evaluated at the saturation temperature T_{sat}.

$$h_{\text{vert}} = \left(\frac{\dfrac{\text{m}}{\text{s}^2}\,\dfrac{\text{kg}}{\text{m}^3}\,\dfrac{\text{kg}}{\text{m}^3}\,\dfrac{\text{J}}{\text{kg}}\left(\dfrac{\text{W}}{\text{m}\cdot\text{K}}\right)^3}{\dfrac{\text{kg}}{\text{m}\cdot\text{s}}\cdot\text{K}\cdot\text{m}}\right)^{1/4}$$

$$= \left[\frac{\text{m}}{\text{s}}\,\frac{1}{\text{m}^6}\,\frac{\text{W}^3}{\text{m}^3\cdot\text{K}^3}\,\frac{\text{J}}{\text{K}}\right]$$

$$= \left(\frac{\text{W}^4}{\text{m}^8\cdot\text{K}^4}\right)^{1/4}$$

$$= \text{W/m}^2\cdot\text{K}$$

FIGURE 10–25
Equation 10–22 gives the condensation heat transfer coefficient in W/m²·K when the quantities are expressed in the units specified in their descriptions.

Wavy Laminar Flow on Vertical Plates

The average heat transfer coefficient in wavy laminar condensate flow for $\rho_v \ll \rho_l$ and $30 < \text{Re} < 1800$

$$h_{\text{vert, wavy}} = \frac{\text{Re}\, k_l}{1.08\,\text{Re}^{1.22} - 5.2}\left(\frac{g}{\nu_l^2}\right)^{1/3}, \qquad \begin{array}{l} 30 < \text{Re} < 1800 \\ \rho_v \ll \rho_l \end{array}$$

$$h_{\text{vert, wavy}} = 0.8\,\text{Re}^{0.11}\, h_{\text{vert (smooth)}}$$

A simpler alternative to the relation above

$$\text{Re}_{\text{vert, wavy}} = \left[4.81 + \frac{3.70\, L k_l (T_{\text{sat}} - T_s)}{\mu_l\, h_{fg}^*}\left(\frac{g}{\nu_l^2}\right)^{1/3}\right]^{0.820}, \qquad \rho_v \ll \rho_l$$

Turbulent Flow on Vertical Plates

Turbulent flow of condensate on *vertical plates:*

$$h_{\text{vert, turbulent}} = \frac{\text{Re}\, k_l}{8750 + 58\,\text{Pr}^{-0.5}\,(\text{Re}^{0.75} - 253)} \left(\frac{g}{\nu_l^2}\right)^{1/3}, \qquad \begin{matrix} \text{Re} > 1800 \\ \rho_v \ll \rho_l \end{matrix}$$

$$\rho_v \lll \rho_l$$

The physical properties of the condensate are again to be evaluated at the film temperature $T_f = (T_{\text{sat}} + T_s)/2$.

$$\text{Re}_{\text{vert, turbulent}} = \left[\frac{0.0690\, L k_l\, \text{Pr}^{0.5}\,(T_{\text{sat}} - T_s)}{\mu_l\, h_{fg}^*} \left(\frac{g}{\nu_l^2}\right)^{1/3} - 151\,\text{Pr}^{0.5} + 253\right]^{4/3}$$

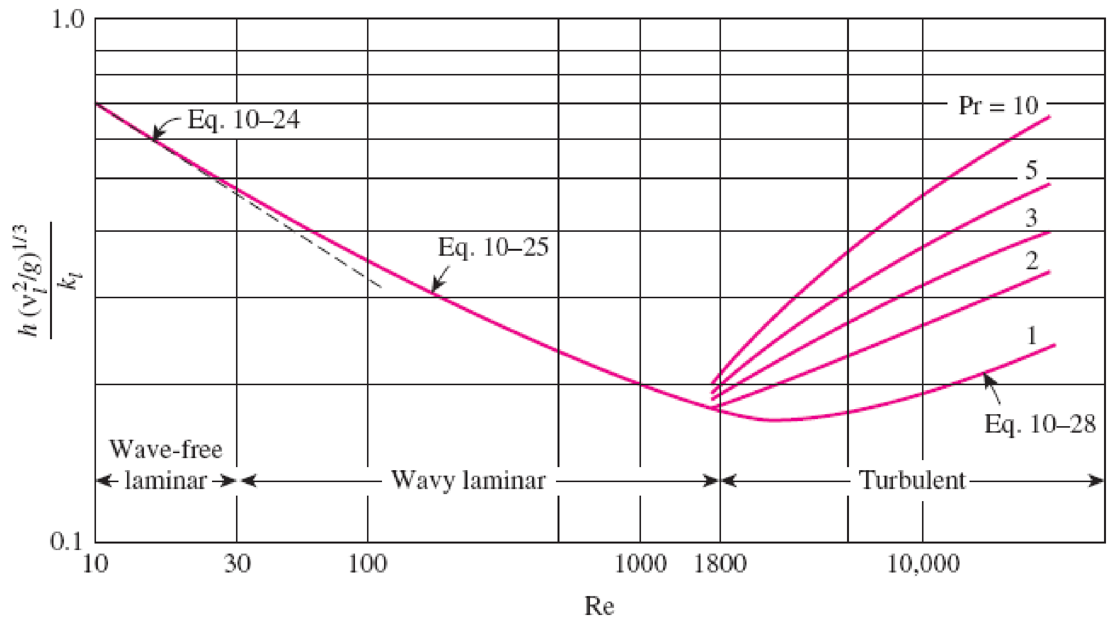

FIGURE 10–26
Nondimensionalized heat transfer coefficients for the wave-free laminar, wavy laminar, and turbulent flow of condensate on vertical plates.

2 Inclined Plates

Equation 10–22 was developed for vertical plates, but it can also be used for laminar film condensation on the upper surfaces of plates that are *inclined* by an angle θ from the *vertical,* by replacing *g* in that equation by $g \cos\theta$.

$$h_{\text{inclined}} = h_{\text{vert}} (\cos \theta)^{1/4} \qquad \text{(laminar)}$$

$$h_{\text{vert}} = 0.943 \left[\frac{g \rho_l (\rho_l - \rho_v) h^*_{fg} k_l^3}{\mu_l (T_{\text{sat}} - T_s) L} \right]^{1/4} \qquad (\text{W/m}^2 \cdot \text{K}), \qquad 0 < \text{Re} < 30$$

(10-22)

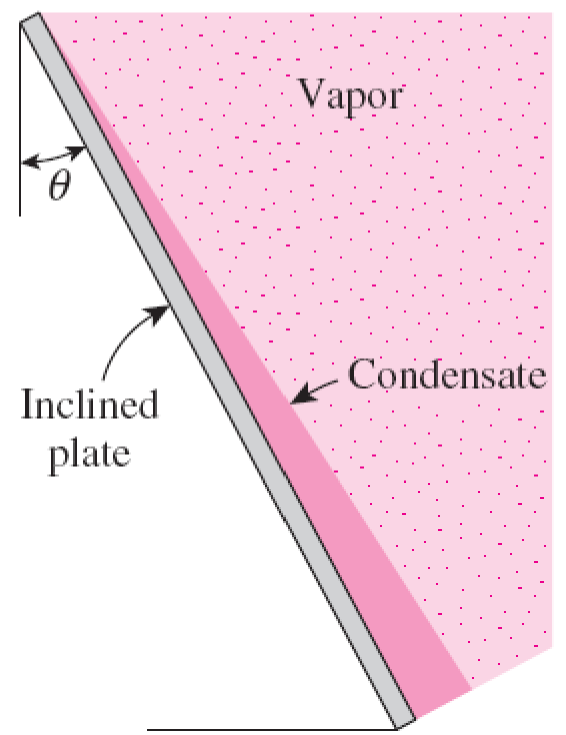

FIGURE 10–27
Film condensation on an inclined plate.

3 Vertical Tubes

Equation 10–22 for vertical plates can also be used to calculate the average heat transfer coefficient for laminar film condensation on the outer surfaces of vertical tubes provided that the tube diameter is large relative to the thickness of the liquid film.

4 Horizontal Tubes and Spheres

The average heat transfer coefficient for film condensation on the outer surfaces of a *horizontal tube* is

$$h_{\text{horiz}} = 0.729\left[\frac{g\rho_l(\rho_l-\rho_v)\,h^*_{fg}\,k_l^3}{\mu_l(T_{\text{sat}}-T_s)D}\right]^{1/4} \quad (\text{W/m}^2\cdot\text{K})$$

For a ***sphere***, replace the constant 0.729 by 0.815.

A comparison of the heat transfer coefficient relations for a vertical tube of height *L* and a horizontal tube of diameter *D* yields

$$\frac{h_{\text{vert}}}{h_{\text{horiz}}} = 1.29\left(\frac{D}{L}\right)^{1/4}$$

Setting $h_{\text{vert}} = h_{\text{horiz}}$ gives $L = 1.29^4D = 2.77D$

For a tube whose length is 2.77 times its diameter, the average heat transfer coefficient for laminar film condensation will be the *same* whether the tube is positioned horizontally or vertically.

For *L* > 2.77*D*, the heat transfer coefficient is higher in the horizontal position.

Considering that the length of a tube in any practical application is several times its diameter, it is common practice to place the tubes in a condenser *horizontally* to maximize the condensation heat transfer coefficient on the outer surfaces of the tubes.

5 Horizontal Tube Banks

FIGURE 10–28

Film condensation on a vertical tier of horizontal tubes.

The average thickness of the liquid film at the lower tubes is much larger as a result of condensate falling on top of them from the tubes directly above.

Therefore, the average heat transfer coefficient at the lower tubes in such arrangements is smaller.

Assuming the condensate from the tubes above to the ones below drain smoothly, the average film condensation heat transfer coefficient for all tubes in a vertical tier can be expressed as

$$h_{\text{horiz}, N\text{ tubes}} = 0.729 \left[\frac{g\rho_l(\rho_l-\rho_v)\,h^*_{fg}\,k_l^3}{\mu_l(T_{\text{sat}}-T_s)\,ND}\right]^{1/4} = \frac{1}{N^{1/4}}\,h_{\text{horiz, 1 tube}}$$

$$h_{\text{horiz}} = 0.729 \left[\frac{g\rho_l(\rho_l-\rho_v)\,h^*_{fg}\,k_l^3}{\mu_l(T_{\text{sat}}-T_s)D}\right]^{1/4} \quad (\text{W/m}^2\cdot\text{K})$$

This relation does not account for the increase in heat transfer due to the ripple formation and turbulence caused during drainage, and thus generally yields conservative results.

Effect of Vapor Velocity

In the analysis above we assumed the vapor velocity to be small and thus the vapor drag exerted on the liquid film to be negligible, which is usually the case.

However, when the vapor velocity is high, the vapor will “pull” the liquid at the interface along since the vapor velocity at the interface must drop to the value of the liquid velocity.

If the vapor flows downward (i.e., in the same direction as the liquid), this additional force will increase the average velocity of the liquid and thus decrease the film thickness.

This, in turn, will decrease the thermal resistance of the liquid film and thus increase heat transfer.

Upward vapor flow has the opposite effects: the vapor exerts a force on the liquid in the opposite direction to flow, thickens the liquid film, and thus decreases heat transfer.

The Presence of Noncondensable Gases in Condensers

Experimental studies show that the presence of noncondensable gases in the vapor has a detrimental effect on condensation heat transfer.

Even small amounts of a noncondensable gas in the vapor cause significant drops in heat transfer coefficient during condensation.

It is common practice to periodically vent out the noncondensable gases that accumulate in the condensers to ensure proper operation.

Heat transfer in the presence of a noncondensable gas strongly depends on the nature of the vapor flow and the flow velocity.

A *high flow velocity* is more likely to remove the stagnant noncondensable gas from the vicinity of the surface, and thus *improve* heat transfer.

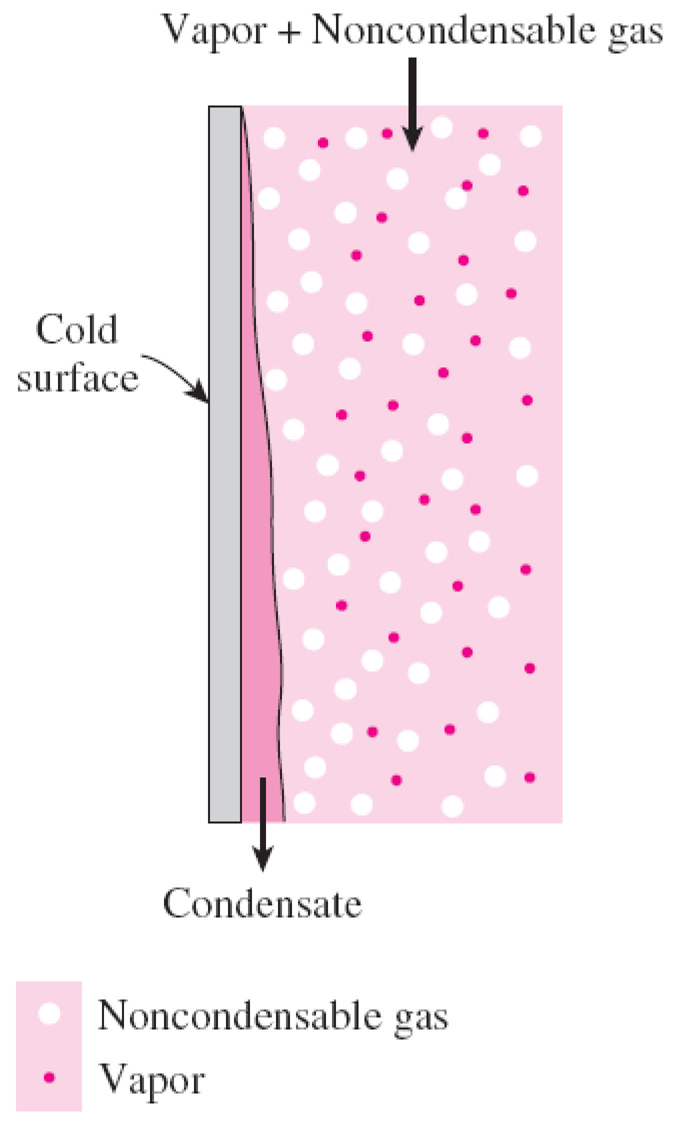

FIGURE 10–29
The presence of a noncondensable gas in a vapor prevents the vapor molecules from reaching the cold surface easily, and thus impedes condensation heat transfer.

FILM CONDENSATION INSIDE HORIZONTAL TUBES

Most condensation processes encountered in refrigeration and air-conditioning applications involve condensation on the *inner surfaces* of horizontal or vertical tubes.

Heat transfer analysis of condensation inside tubes is complicated by the fact that it is strongly influenced by the vapor velocity and the rate of liquid accumulation on the walls of the tubes.

For *low vapor velocities:*

$$h_{\text{internal}} = 0.555\left[\frac{g\rho_l(\rho_l - \rho_v)\,k_l^3}{\mu_l\,(T_{\text{sat}} - T_s)D}\left(h_{fg} + \frac{3}{8}\,c_{pl}(T_{\text{sat}} - T_s)\right)\right]^{1/4}$$

$$\text{Re}_{\text{vapor}} = \left(\frac{\rho_v V_v D}{\mu_v}\right)_{\text{inlet}} < 35{,}000$$

The Reynolds number of the vapor is to be evaluated at the tube *inlet* conditions using the internal tube diameter as the characteristic length.

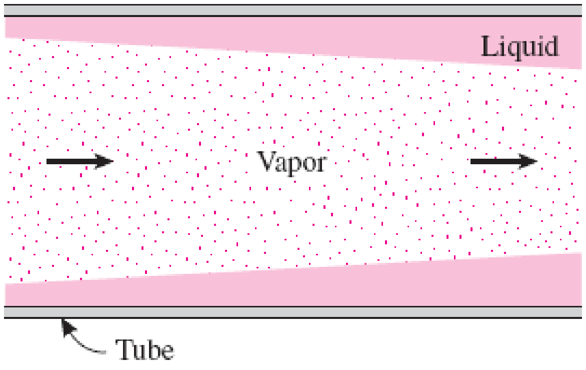

(*a*) High vapor velocities

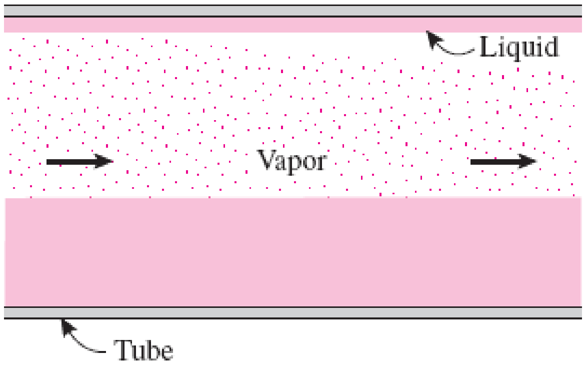

(*b*) Low vapor velocities

FIGURE 10–34
Condensate flow in a horizontal tube with high and low vapor velocities.

DROPWISE CONDENSATION

Dropwise condensation, characterized by countless droplets of varying diameters on the condensing surface instead of a continuous liquid film and extremely large heat transfer coefficients can be achieved with this mechanism.

The small droplets that form at the nucleation sites on the surface grow as a result of continued condensation, coalesce into large droplets, and slide down when they reach a certain size, clearing the surface and exposing it to vapor. There is no liquid film in this case to resist heat transfer.

As a result, with dropwise condensation, heat transfer coefficients can be achieved that are more than 10 times larger than those associated with film condensation.

The challenge in dropwise condensation is not to achieve it, but rather, to *sustain* it for prolonged periods of time.

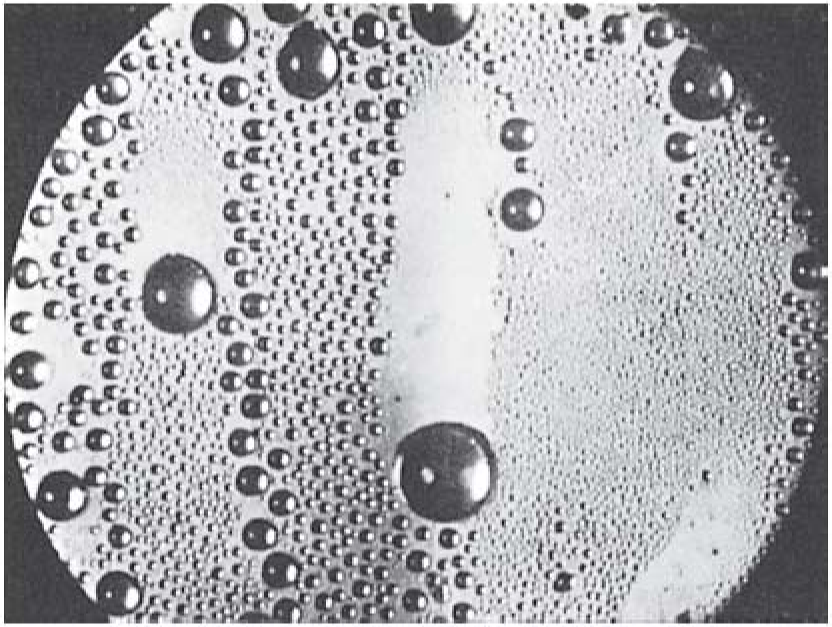

FIGURE 10–35

Dropwise condensation of steam on a vertical surface.

Dropwise condensation of steam on copper surfaces:

$$h_{\text{dropwise}} = \begin{cases} 51{,}104 + 2044T_{\text{sat}}, & 22^\circ\text{C} < T_{\text{sat}}, 100^\circ\text{C} \\ 255{,}310 & T_{\text{sat}} > 100^\circ\text{C} \end{cases}$$

Heat Transfer Lectures
Fundamentals & Applications

UNIVERSITY OF TECHNOLOGY

Mechanical Engineering department 3rd power plant division

HEAT EXCHANGERS

Dr. Sattar Aljabair

Objectives

- Recognize numerous types of heat exchangers, and classify them
- Develop an awareness of fouling on surfaces, and determine the overall heat transfer coefficient for a heat exchanger
- Perform a general energy analysis on heat exchangers
- Obtain a relation for the logarithmic mean temperature difference for use in the LMTD method, and modify it for different types of heat exchangers using the correction factor
- Develop relations for effectiveness, and analyze heat exchangers when outlet temperatures are not known using the effectiveness-NTU method
- Know the primary considerations in the selection of heat exchangers.

TYPES OF HEAT EXCHANGERS

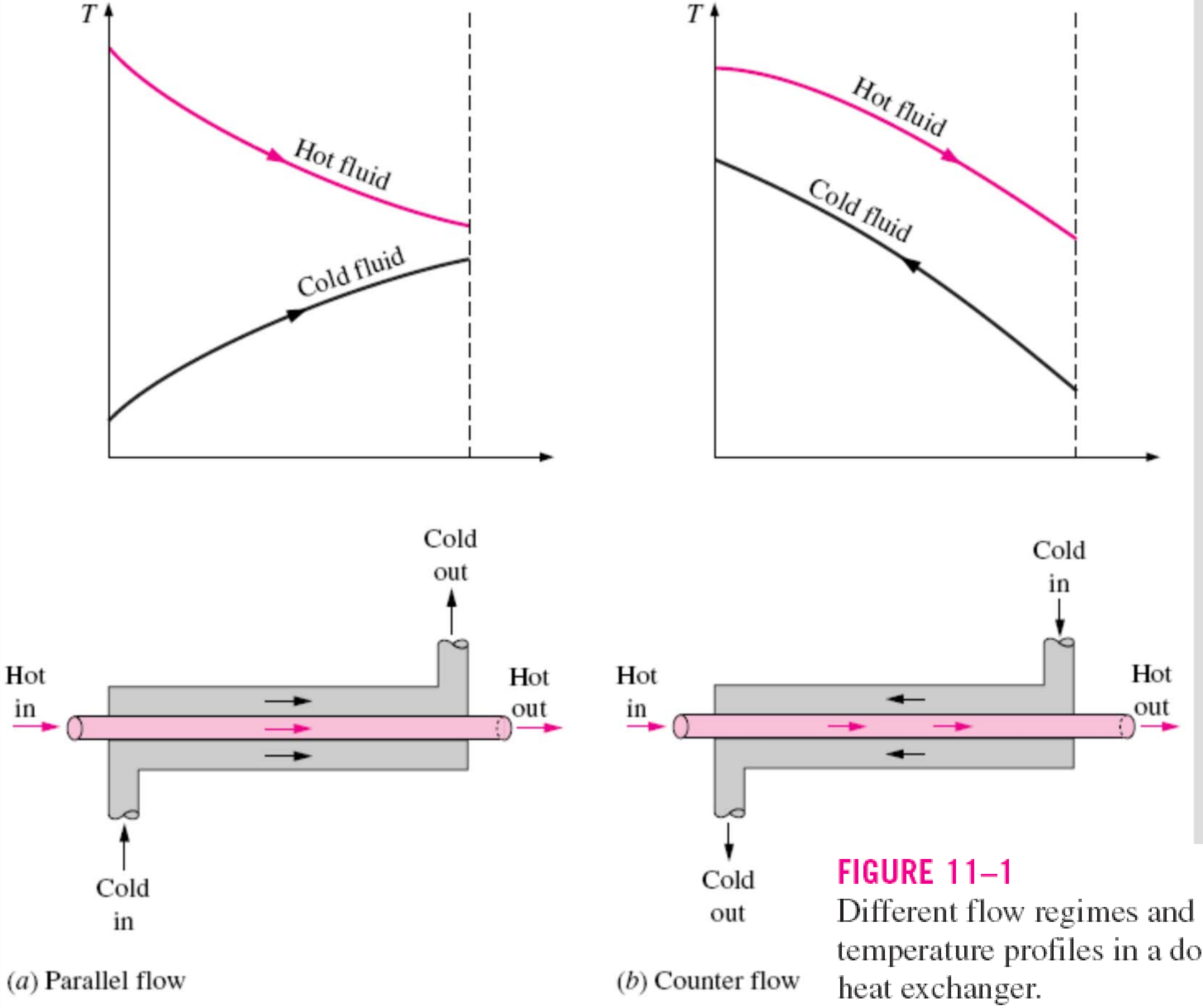

(*a*) Parallel flow

(*b*) Counter flow

FIGURE 11–1
Different flow regimes and associated temperature profiles in a double-pipe heat exchanger.

Compact heat exchanger: It has a large heat transfer surface area per unit volume (e.g., car radiator, human lung). A heat exchanger with the *area density* $\beta > 700\ m^2/m^3$ is classified as being compact.

Cross-flow: In compact heat exchangers, the two fluids usually move *perpendicular* to each other. The cross-flow is further classified as *unmixed* and *mixed flow.*

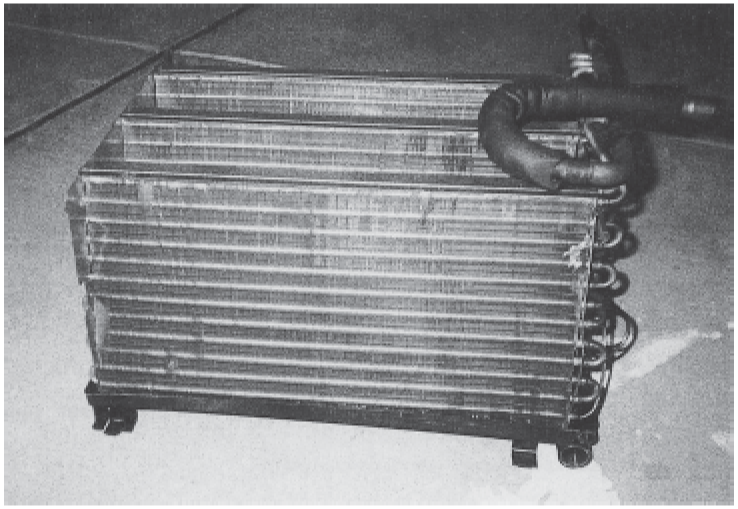

FIGURE 11–2

A gas-to-liquid compact heat exchanger for a residential air-conditioning system.

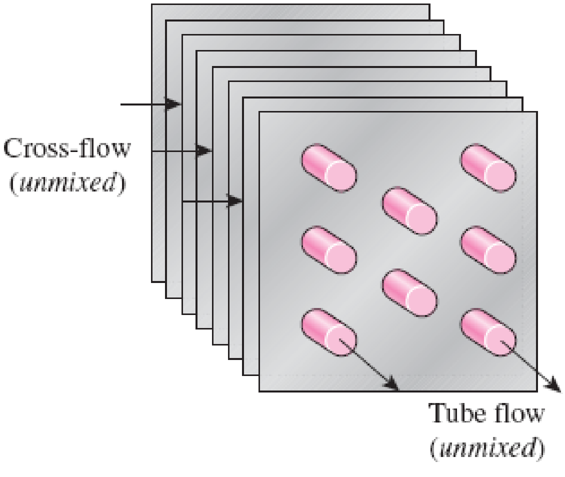

(*a*) Both fluids unmixed

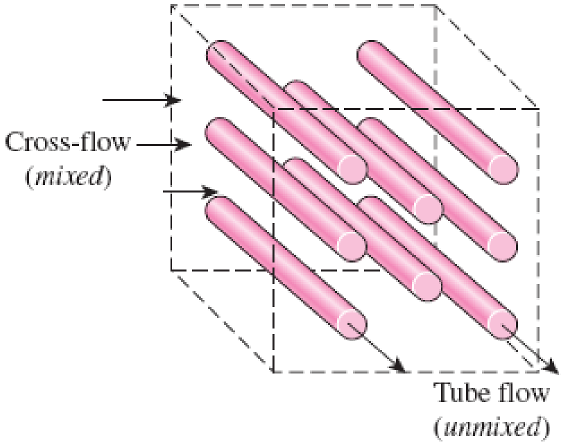

(*b*) One fluid mixed, one fluid unmixed

FIGURE 11–3

Different flow configurations in cross-flow heat exchangers.

Shell-and-tube heat exchanger: The most common type of heat exchanger in industrial applications.

They contain a large number of tubes (sometimes several hundred) packed in a shell with their axes parallel to that of the shell. Heat transfer takes place as one fluid flows inside the tubes while the other fluid flows outside the tubes through the shell.

Shell-and-tube heat exchangers are further classified according to the number of shell and tube passes involved.

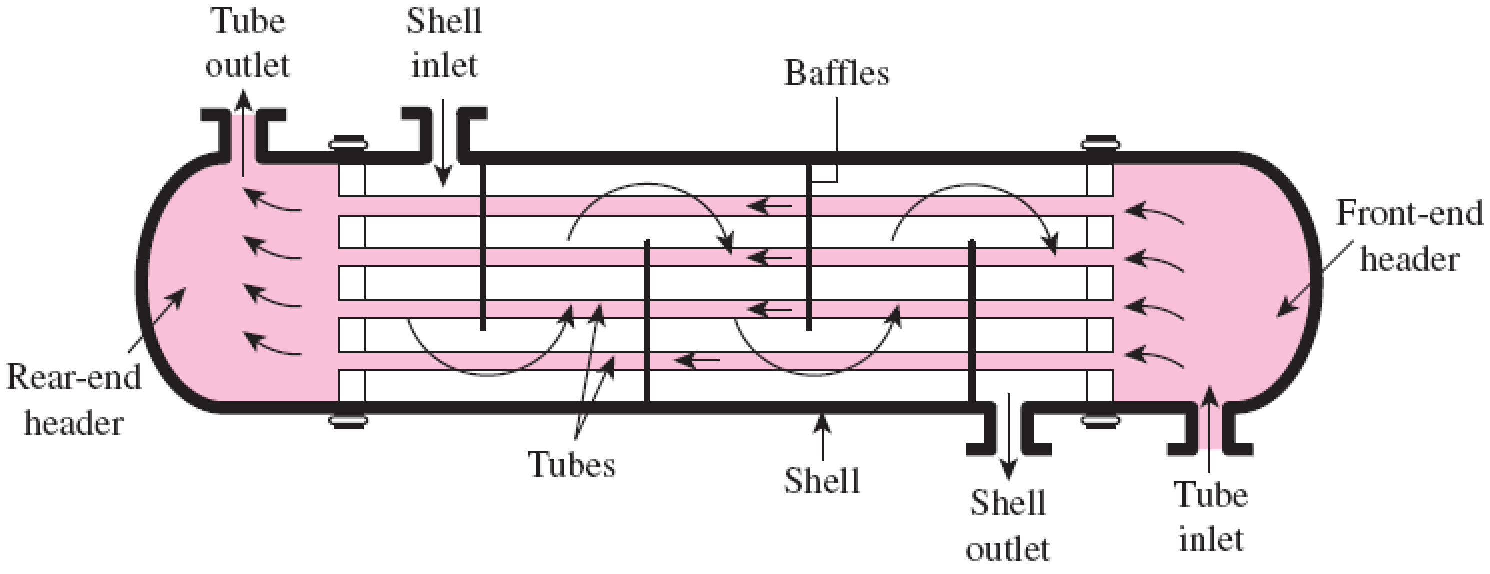

FIGURE 11–4

The schematic of a shell-and-tube heat exchanger (one-shell pass and one-tube pass).

Regenerative heat exchanger: Involves the alternate passage of the hot and cold fluid streams through the same flow area.

Dynamic-type regenerator: Involves a rotating drum and continuous flow of the hot and cold fluid through different portions of the drum so that any portion of the drum passes periodically through the hot stream, storing heat, and then through the cold stream, rejecting this stored heat.

Condenser: One of the fluids is cooled and condenses as it flows through the heat exchanger.

Boiler: One of the fluids absorbs heat and vaporizes.

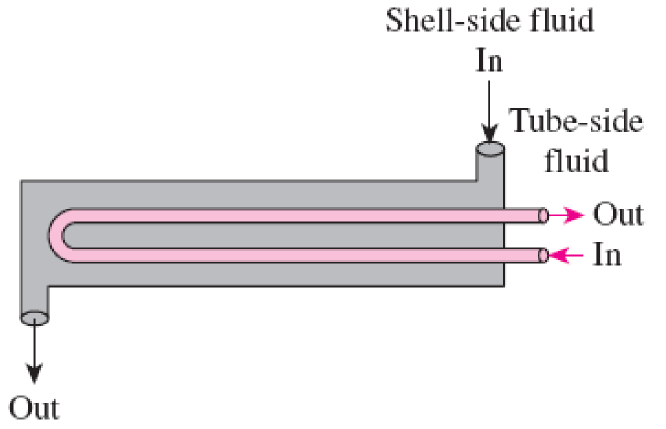

(*a*) One-shell pass and two-tube passes

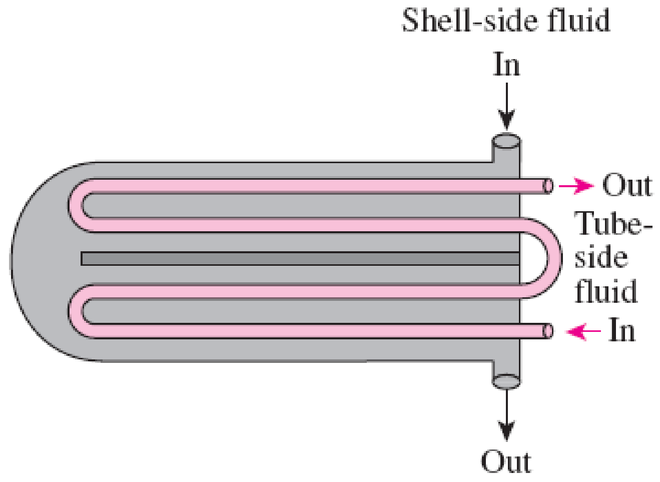

(*b*) Two-shell passes and four-tube passes

FIGURE 11–5
Multipass flow arrangements in shell-and-tube heat exchangers.

Plate and frame (or just plate) heat exchanger: Consists of a series of plates with corrugated flat flow passages. The hot and cold fluids flow in alternate passages, and thus each cold fluid stream is surrounded by two hot fluid streams, resulting in very effective heat transfer. Well suited for liquid-to-liquid applications.

A plate-and-frame liquid-to-liquid heat exchanger.

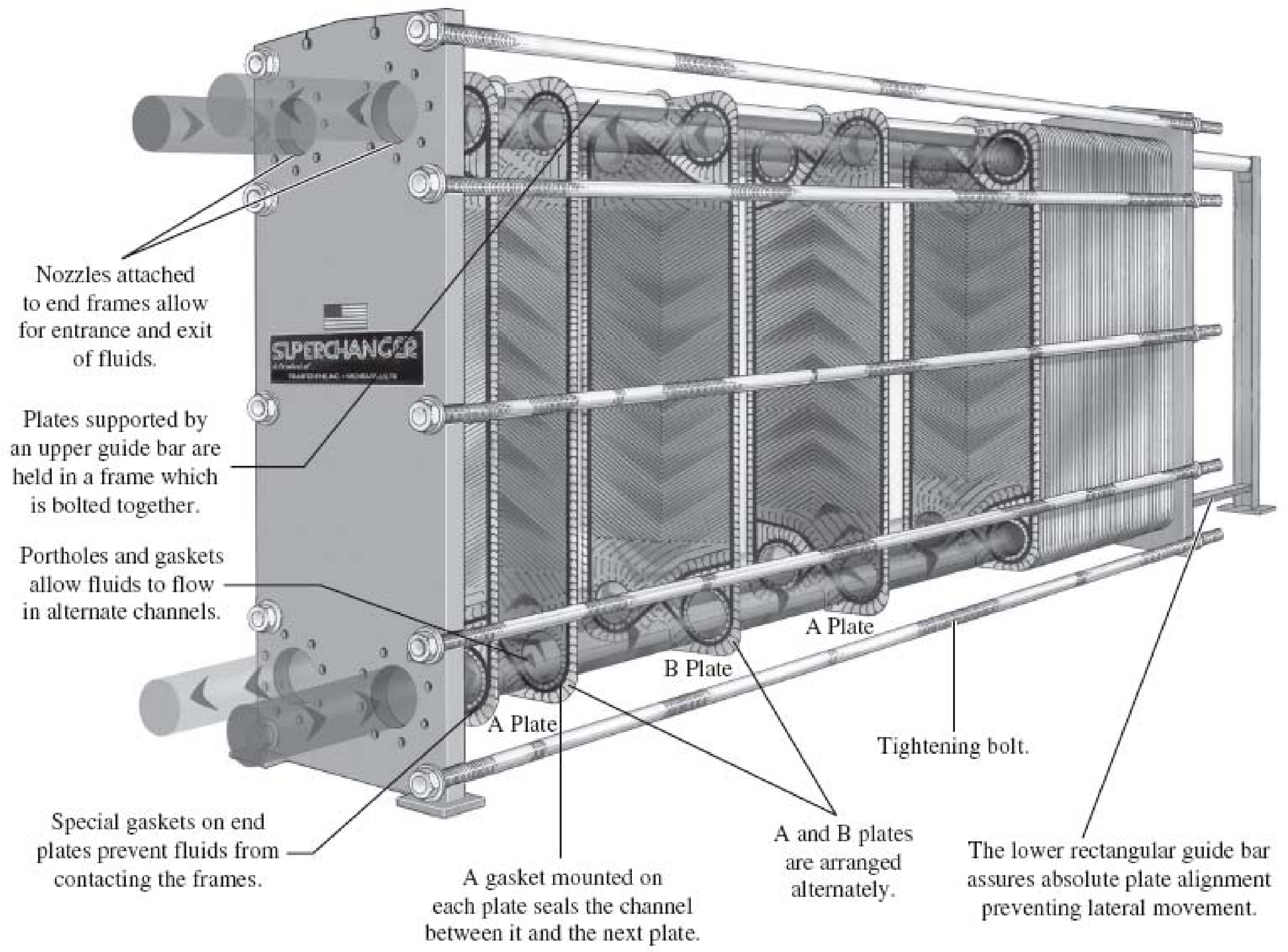

THE OVERALL HEAT TRANSFER COEFFICIENT

- A heat exchanger typically involves two flowing fluids separated by a solid wall.
- Heat is first transferred from the hot fluid to the wall by *convection*, through the wall by *conduction*, and from the wall to the cold fluid again by *convection.*
- Any radiation effects are usually included in the convection heat transfer coefficients.

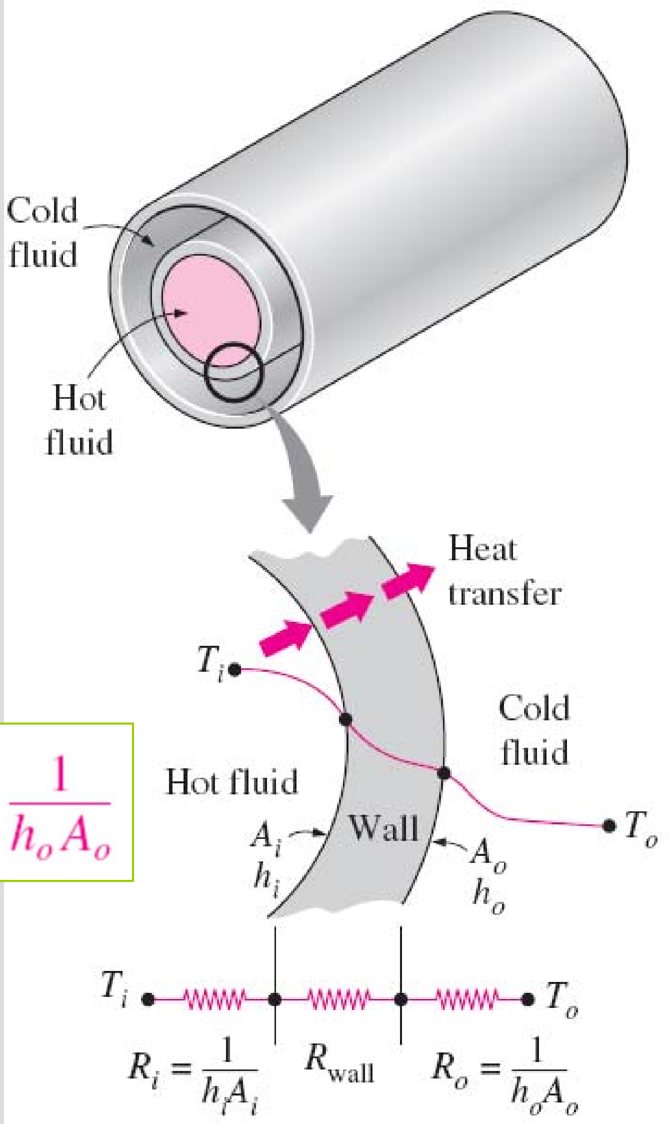

$$R_{\text{wall}} = \frac{\ln (D_o/D_i)}{2\pi kL}$$

$$R = R_{\text{total}} = R_i + R_{\text{wall}} + R_o = \frac{1}{h_i A_i} + \frac{\ln (D_o/D_i)}{2\pi kL} + \frac{1}{h_o A_o}$$

$$A_i = \pi D_i L \text{ and } A_o = \pi D_o L$$

Thermal resistance network associated with heat transfer in a double-pipe heat exchanger.

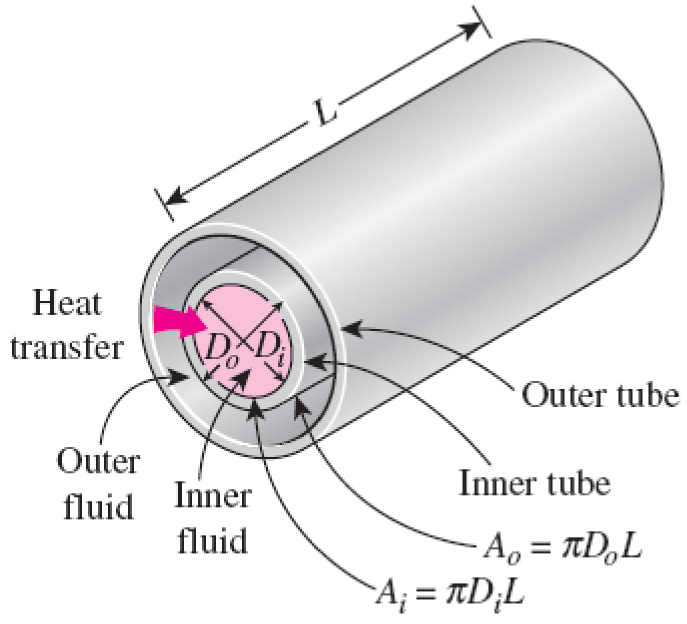

FIGURE 11–8

The two heat transfer surface areas associated with a double-pipe heat exchanger (for thin tubes, $D_i \approx D_o$ and thus $A_i \approx A_o$).

$$\dot{Q} = \frac{\Delta T}{R} = UA\Delta T = U_iA_i\Delta T = U_oA_o\Delta T$$

U the overall heat transfer coefficient, W/m$^2\cdot$°C

$$\frac{1}{UA_s} = \frac{1}{U_iA_i} = \frac{1}{U_oA_o} = R = \frac{1}{h_iA_i} + R_{\text{wall}} + \frac{1}{h_oA_o}$$

$$U_iA_i = U_oA_o, \text{ but } U_i \neq U_o \text{ unless } A_i = A_o$$

When $R_{\text{wall}} \approx 0$ $A_i \approx A_o \approx A_s$

$$\frac{1}{U} \approx \frac{1}{h_i} + \frac{1}{h_o} \qquad U \approx U_i \approx U_o$$

The overall heat transfer coefficient U is dominated by the *smaller* convection coefficient. When one of the convection coefficients is *much smaller* than the other (say, $h_i \ll h_o$), we have $1/h_i \gg 1/h_o$, and thus $U \approx h_i$. This situation arises frequently when one of the fluids is a gas and the other is a liquid. In such cases, fins are commonly used on the gas side to enhance the product UA and thus the heat transfer on that side.

The overall heat transfer coefficient ranges from about 10 W/m$^2\cdot$°C for gas-to-gas heat exchangers to about 10,000 W/m$^2\cdot$°C for heat exchangers that involve phase changes.

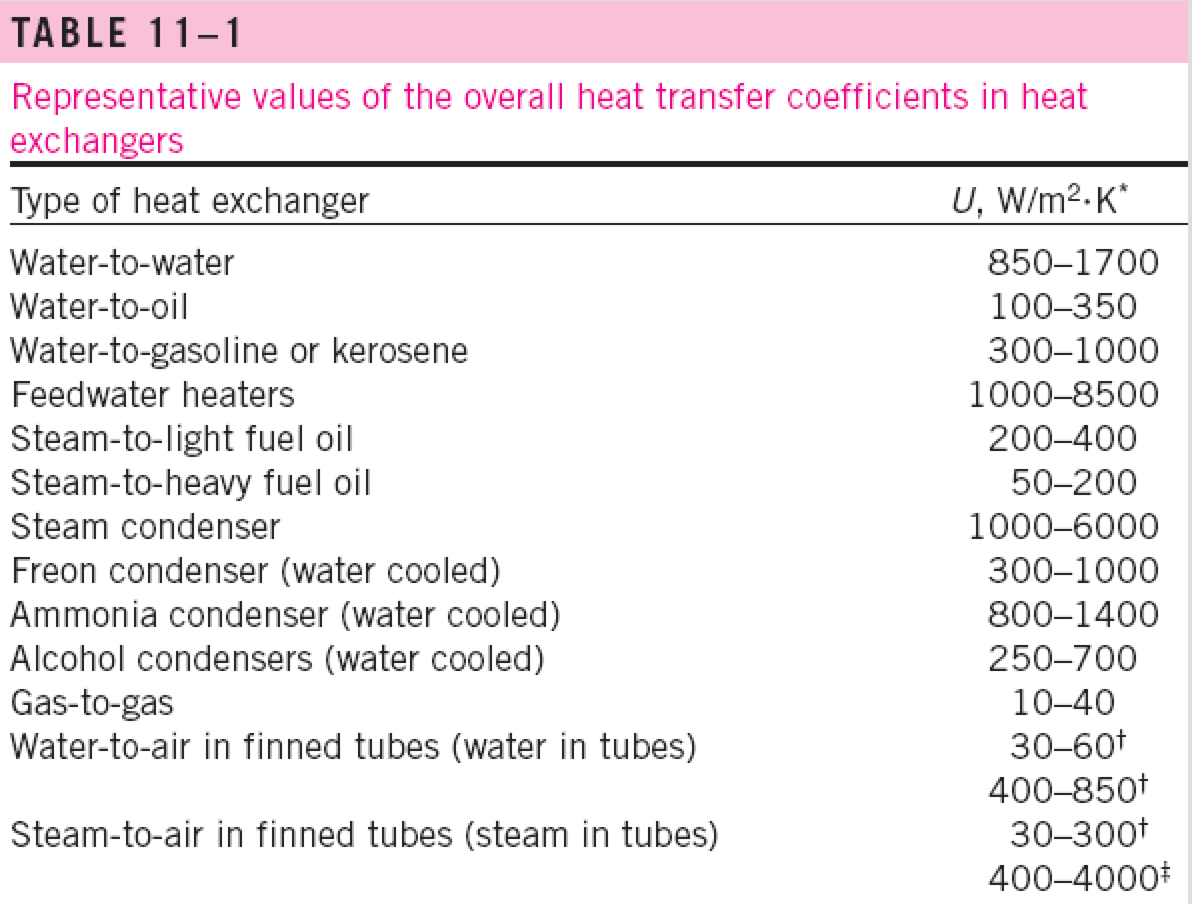

TABLE 11–1

Representative values of the overall heat transfer coefficients in heat exchangers

Type of heat exchanger	U, W/m$^2\cdot$K*
Water-to-water	850–1700
Water-to-oil	100–350
Water-to-gasoline or kerosene	300–1000
Feedwater heaters	1000–8500
Steam-to-light fuel oil	200–400
Steam-to-heavy fuel oil	50–200
Steam condenser	1000–6000
Freon condenser (water cooled)	300–1000
Ammonia condenser (water cooled)	800–1400
Alcohol condensers (water cooled)	250–700
Gas-to-gas	10–40
Water-to-air in finned tubes (water in tubes)	30–60† 400–850†
Steam-to-air in finned tubes (steam in tubes)	30–300† 400–4000‡

When the tube is *finned* on one side to enhance heat transfer, the total heat transfer surface area on the finned side is

$$A_s = A_{\text{total}} = A_{\text{fin}} + A_{\text{unfinned}}$$

For short fins of high thermal conductivity, we can use this total area in the convection resistance relation **$R_{\text{conv}} = 1/hA_s$**

$$A_s = A_{\text{unfinned}} + \eta_{\text{fin}} A_{\text{fin}}$$

To account for fin efficiency

Fouling Factor

The performance of heat exchangers usually deteriorates with time as a result of accumulation of *deposits* on heat transfer surfaces. The layer of deposits represents *additional resistance* to heat transfer. This is represented by a **fouling factor R_f**.

$$\frac{1}{UA_s} = \frac{1}{U_iA_i} = \frac{1}{U_oA_o} = R = \frac{1}{h_iA_i} + \frac{R_{f,i}}{A_i} + \frac{\ln(D_o/D_i)}{2\pi kL} + \frac{R_{f,o}}{A_o} + \frac{1}{h_oA_o}$$

The fouling factor increases with the *operating temperature* *and* the length of service and decreases with the *velocity* of the fluids.

FIGURE 11–9

Precipitation fouling of ash particles on superheater tubes.

TABLE 11–2

Representative fouling factors (thermal resistance due to folling for a unit surface area)

Fluid	R_f, m²·K/W
Distilled water, sea-water, river water, boiler feedwater:	
Below 50°C	0.0001
Above 50°C	0.0002
Fuel oil	0.0009
Steam (oil-free)	0.0001
Refrigerants (liquid)	0.0002
Refrigerants (vapor)	0.0004
Alcohol vapors	0.0001
Air	0.0004

ANALYSIS OF HEAT EXCHANGERS

An engineer often finds himself or herself in a position

1. to *select a heat exchanger* that will achieve a *specified temperature change* in a fluid stream of known mass flow rate - **the *log mean temperature difference* (or LMTD) method**.
2. to *predict the outlet temperatures* of the hot and cold fluid streams in a *specified heat exchanger* - **the *effectiveness–NTU* method**.

The rate of heat transfer in heat exchanger (HE is insulated):

$$\dot{Q} = \dot{m}_c c_{pc}(T_{c,\,\text{out}} - T_{c,\,\text{in}})$$

$$\dot{Q} = \dot{m}_h c_{ph}(T_{h,\,\text{in}} - T_{h,\,\text{out}})$$

$\dot{m}_c, \dot{m}_h$ = mass flow rates

c_{pc}, c_{ph} = specific heats

$T_{c,\,\text{out}}, T_{h,\,\text{out}}$ = outlet temperatures

$T_{c,\,\text{in}}, T_{h,\,\text{in}}$ = inlet temperatures

$$C_h = \dot{m}_h c_{ph} \qquad \text{and} \qquad C_c = \dot{m}_c c_{pc}$$

heat capacity rate

$$\dot{Q} = C_c(T_{c,\,\text{out}} - T_{c,\,\text{in}}) \qquad \dot{Q} = C_h(T_{h,\,\text{in}} - T_{h,\,\text{out}})$$

Two fluid streams that have the same capacity rates experience the same temperature change in a well-insulated heat exchanger.

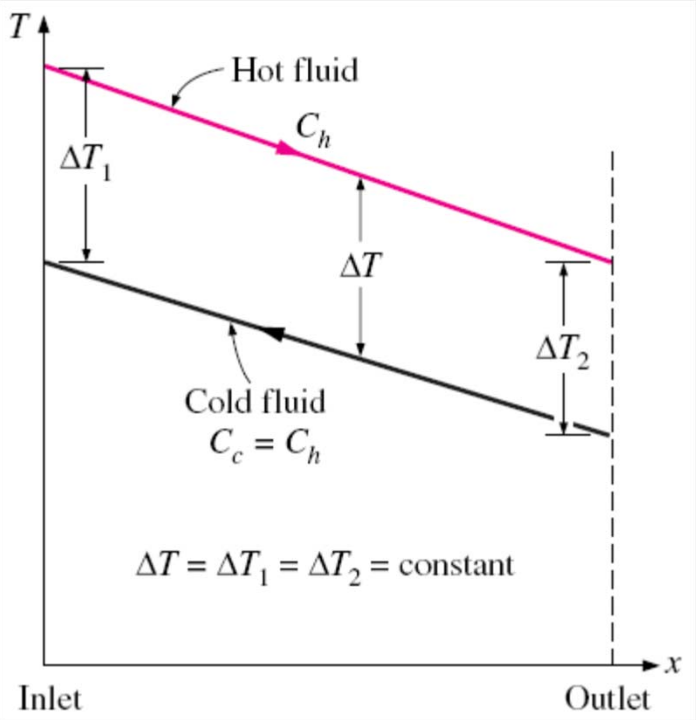

$\dot{m}$ is the rate of evaporation or condensation of the fluid $\dot{Q} = \dot{m} h_{fg}$

h_{fg} is the enthalpy of vaporization of the fluid at the specified temperature or pressure.

The heat capacity rate of a fluid during a phase-change process must approach infinity since the temperature change is practically zero.

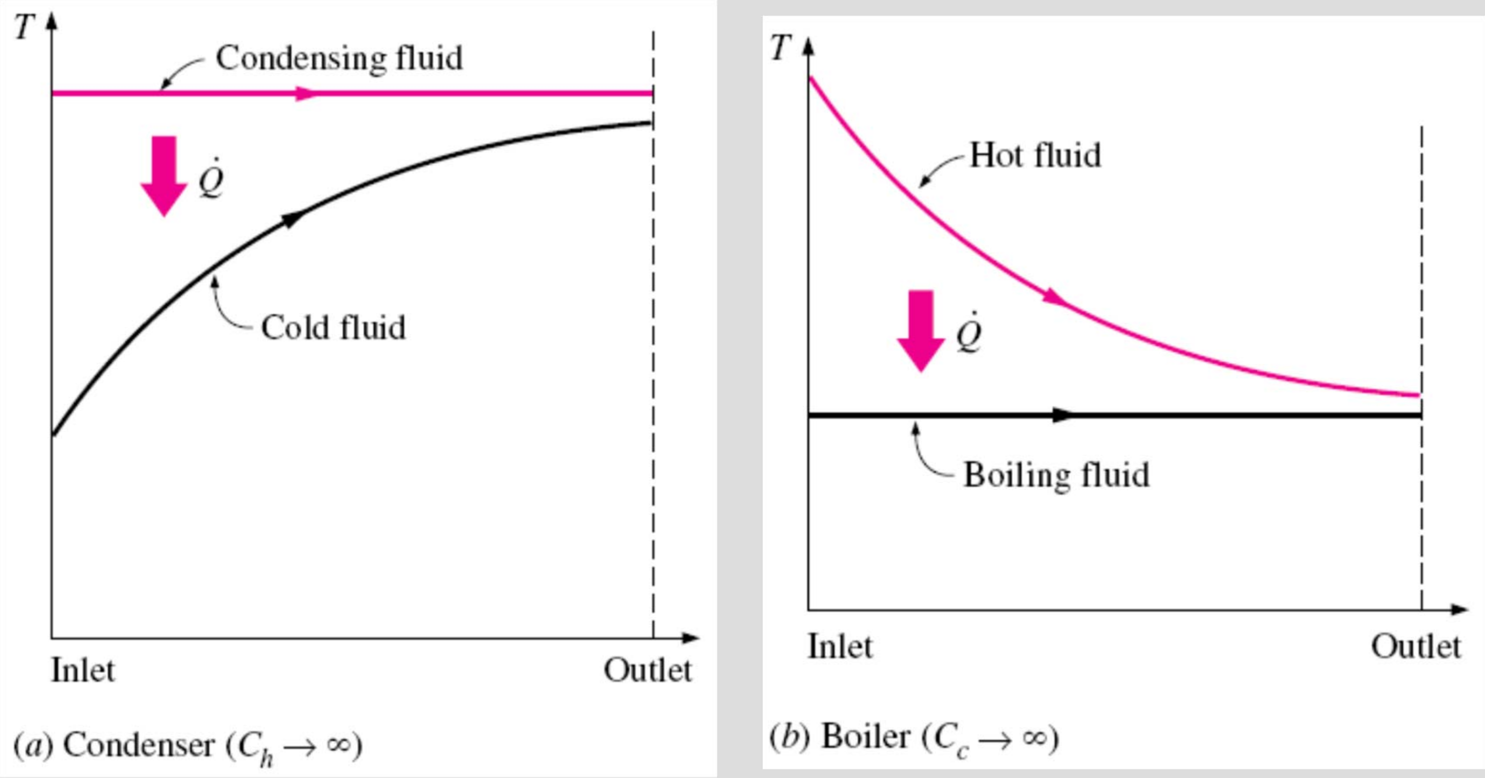

(*a*) Condenser ($C_h \to \infty$)

(*b*) Boiler ($C_c \to \infty$)

Variation of fluid temperatures in a heat exchanger when one of the fluids condenses or boils.

$\dot{Q} = UA_s \, \Delta T_m$ ΔT_m an appropriate mean (average) temperature difference between the two fluids

THE LOG MEAN TEMPERATURE DIFFERENCE METHOD

$$\delta\dot{Q} = -\dot{m}_h c_{ph}\, dT_h \qquad \delta\dot{Q} = \dot{m}_c c_{pc}\, dT_c$$

$$dT_h = -\frac{\delta\dot{Q}}{\dot{m}_h c_{ph}} \qquad dT_c = \frac{\delta\dot{Q}}{\dot{m}_c c_{pc}}$$

$$dT_h - dT_c = d(T_h - T_c) = -\delta\dot{Q}\left(\frac{1}{\dot{m}_h c_{ph}} + \frac{1}{\dot{m}_c c_{pc}}\right)$$

$$\delta\dot{Q} = U(T_h - T_c)\, dA_s$$

$$\frac{d(T_h - T_c)}{T_h - T_c} = -U\, dA_s\left(\frac{1}{\dot{m}_h c_{ph}} + \frac{1}{\dot{m}_c c_{pc}}\right)$$

$$\ln\frac{T_{h,\text{out}} - T_{c,\text{out}}}{T_{h,\text{in}} - T_{c,\text{in}}} = -UA_s\left(\frac{1}{\dot{m}_h c_{ph}} + \frac{1}{\dot{m}_c c_{pc}}\right)$$

$$\dot{Q} = UA_s\, \Delta T_{\text{lm}}$$

$$\Delta T_{\text{lm}} = \frac{\Delta T_1 - \Delta T_2}{\ln(\Delta T_1/\Delta T_2)}$$

log mean temperature difference

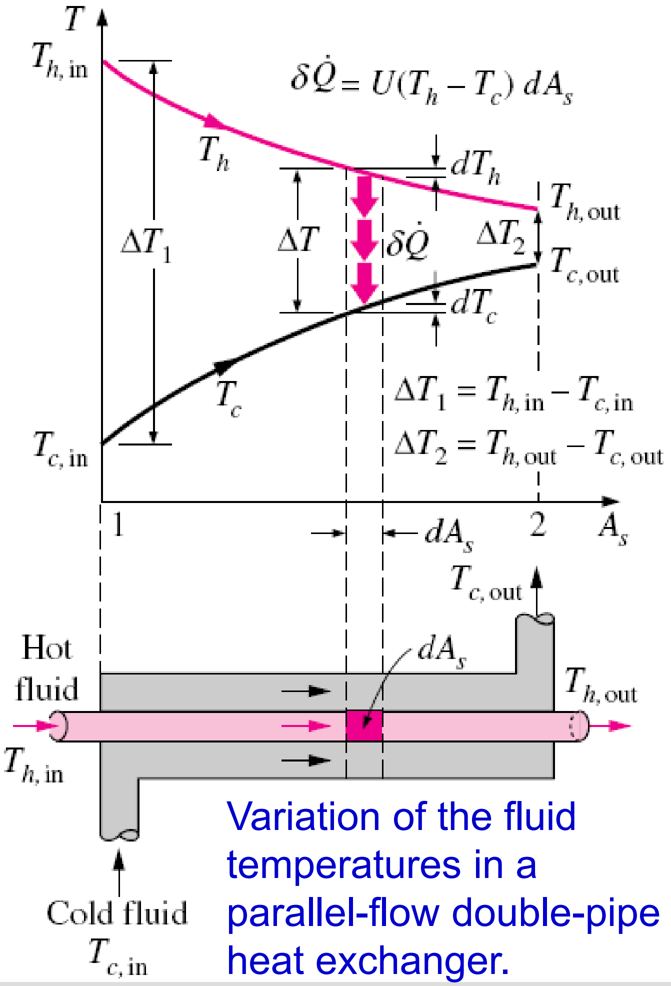

Variation of the fluid temperatures in a parallel-flow double-pipe heat exchanger.

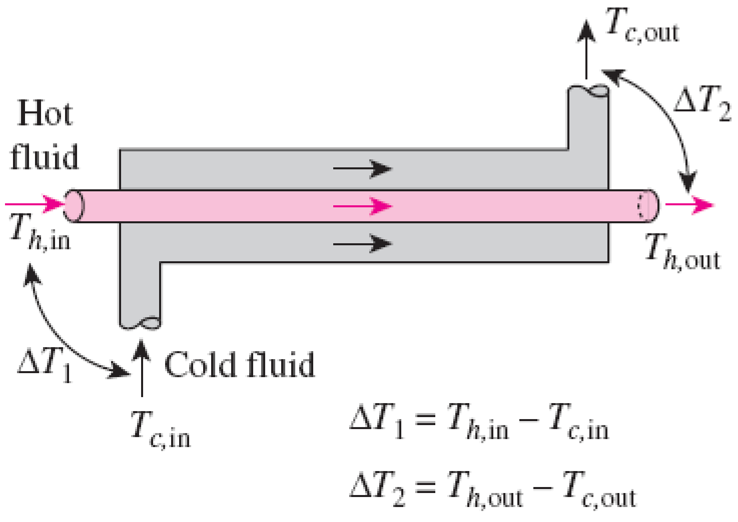

(*a*) Parallel-flow heat exchangers

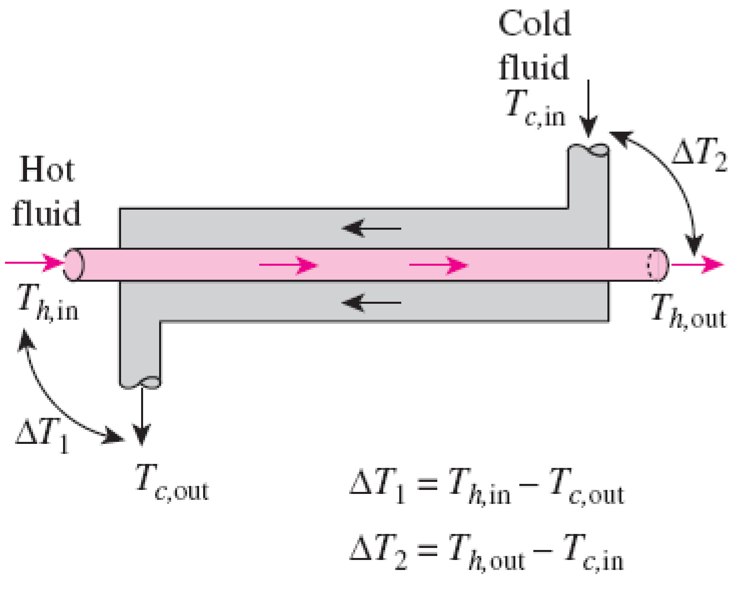

(*b*) Counter-flow heat exchangers

The arithmetic mean temperature difference

$$\Delta T_{\text{am}} = \tfrac{1}{2}(\Delta T_1 + \Delta T_2)$$

The logarithmic mean temperature difference ΔT_{lm} is an *exact* representation of the *average temperature difference* between the hot and cold fluids.

Note that ΔT_{lm} is always less than ΔT_{am}. Therefore, using ΔT_{am} in calculations instead of ΔT_{lm} will overestimate the rate of heat transfer in a heat exchanger between the two fluids.

When ΔT_1 differs from ΔT_2 by no more than 40 percent, the error in using the arithmetic mean temperature difference is less than 1 percent. But the error increases to undesirable levels when ΔT_1 differs from ΔT_2 by greater amounts.

FIGURE 11–15
The ΔT_1 and ΔT_2 expressions in parallel-flow and counter-flow heat exchangers.

Counter-Flow Heat Exchangers

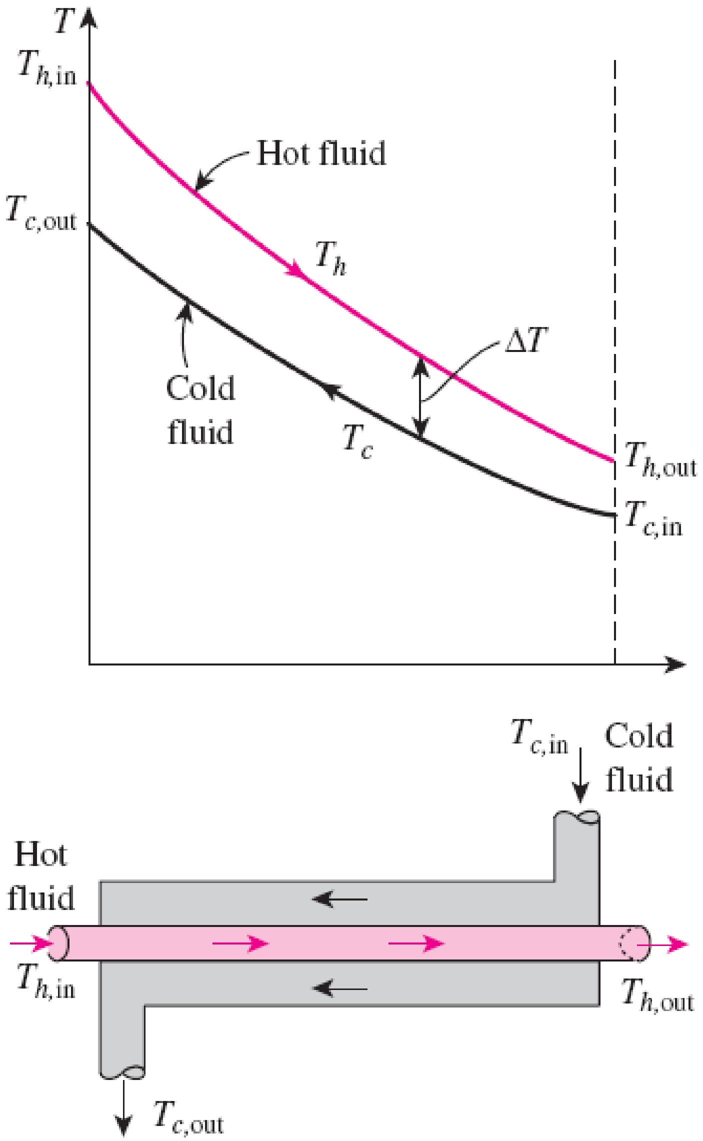

FIGURE 11–16

The variation of the fluid temperatures in a counter-flow double-pipe heat exchanger.

In the limiting case, the cold fluid will be heated to the inlet temperature of the hot fluid.

However, the outlet temperature of the cold fluid can *never* exceed the inlet temperature of the hot fluid.

For specified inlet and outlet temperatures, ΔT_{lm} a counter-flow heat exchanger is always greater than that for a parallel-flow heat exchanger.

That is, $\Delta T_{lm,\,CF} > \Delta T_{lm,\,PF}$, and thus a smaller surface area (and thus a smaller heat exchanger) is needed to achieve a specified heat transfer rate in a counter-flow heat exchanger.

When the *heat capacity rates* of the two fluids are *equal*

$$\Delta T_{lm} = \Delta T_1 = \Delta T_2$$

Multipass and Cross-Flow Heat Exchangers: Use of a Correction Factor

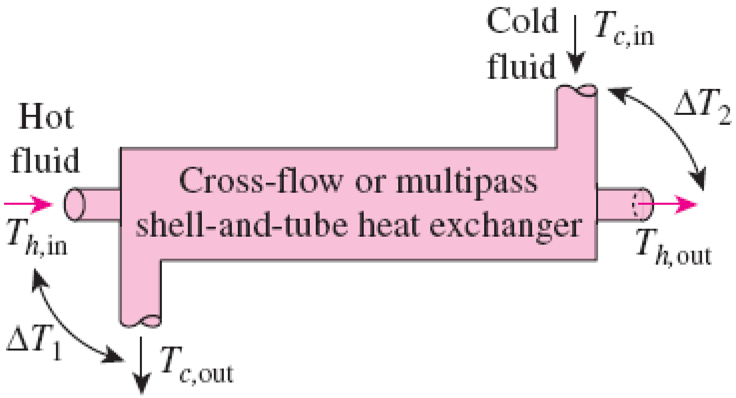

Heat transfer rate:

$$\dot{Q} = UA_s F \Delta T_{\text{lm,CF}}$$

where $$\Delta T_{\text{lm,CF}} = \frac{\Delta T_1 - \Delta T_2}{\ln(\Delta T_1/\Delta T_2)}$$

$$\Delta T_1 = T_{h,\text{in}} - T_{c,\text{out}}$$

$$\Delta T_2 = T_{h,\text{out}} - T_{c,\text{in}}$$

and $F = \ldots$ (Fig. 11–18)

FIGURE 11–17
The determination of the heat transfer rate for cross-flow and multipass shell-and-tube heat exchangers using the correction factor.

$$\Delta T_{\text{lm}} = F\,\Delta T_{\text{lm, CF}}$$

***F* correction factor** depends on the *geometry* of the heat exchanger and the inlet and outlet temperatures of the hot and cold fluid streams.

F for common cross-flow and shell-and-tube heat exchanger configurations is given in the figure versus two temperature ratios *P* and *R* defined as

$$P = \frac{t_2 - t_1}{T_1 - t_1}$$

$$R = \frac{T_1 - T_2}{t_2 - t_1} = \frac{(\dot{m}c_p)_{\text{tube side}}}{(\dot{m}c_p)_{\text{shell side}}}$$

1 and 2 *inlet* and *outlet*
T* and *t *shell*- and *tube-side* temperatures

***F* = 1 for a condenser or boiler**

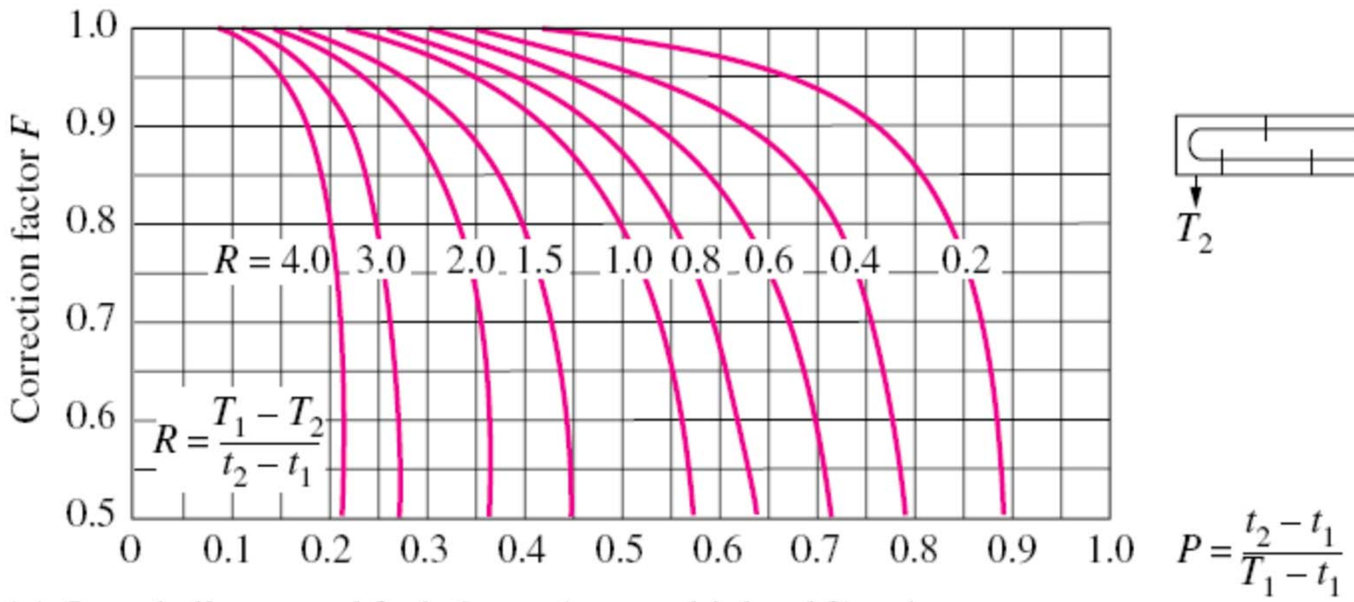

(*a*) One-shell pass and 2, 4, 6, etc. (any multiple of 2), tube passes

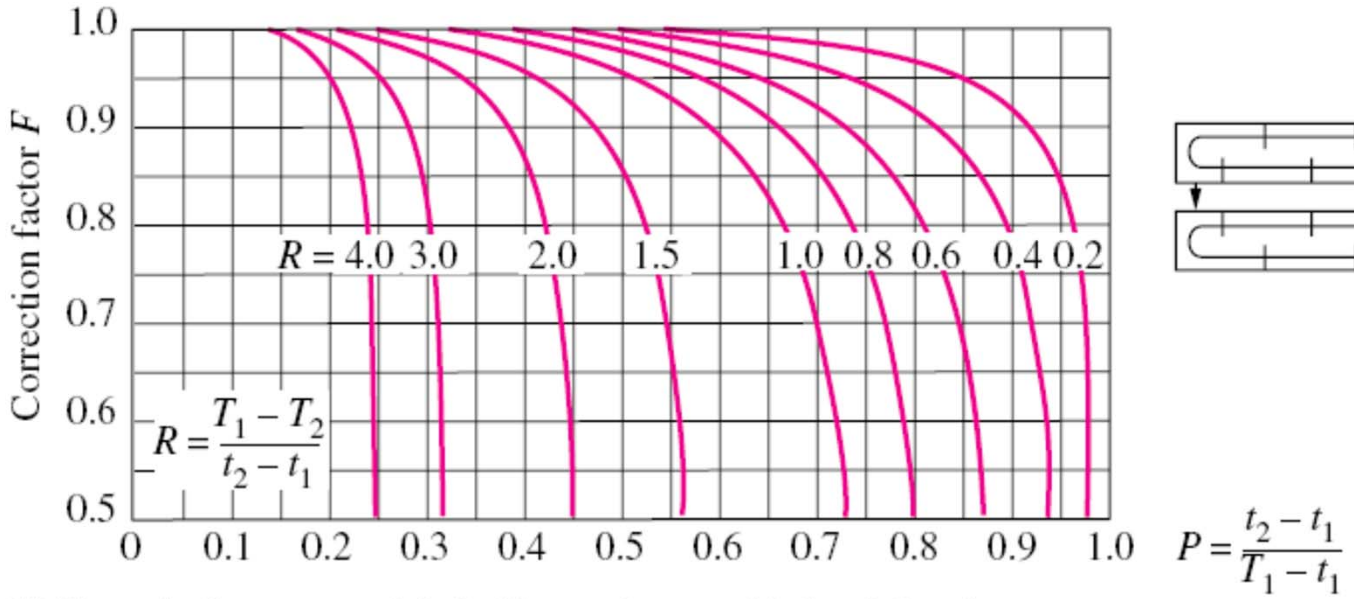

(*b*) Two-shell passes and 4, 8, 12, etc. (any multiple of 4), tube passes

Correction factor *F* charts for common shell-and-tube heat exchangers.

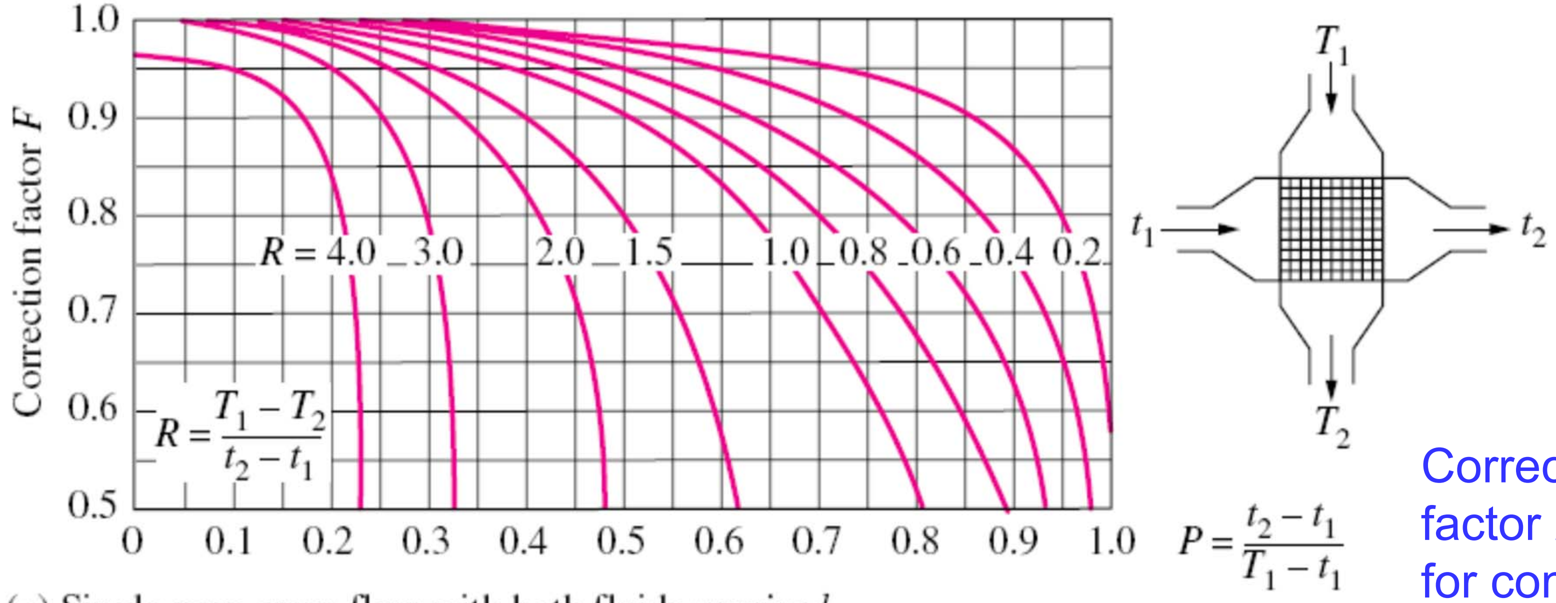

(c) Single-pass cross-flow with both fluids *unmixed*

Correction factor *F* charts for common cross-flow heat exchangers.

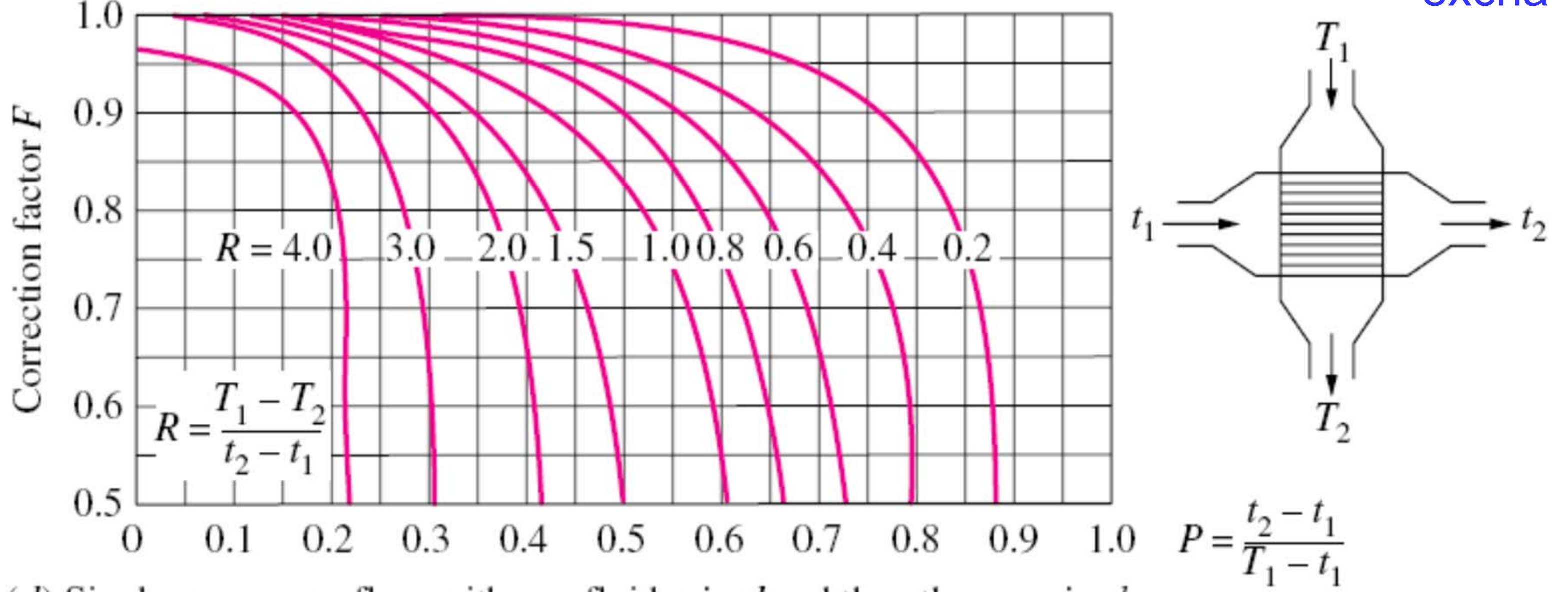

(d) Single-pass cross-flow with one fluid *mixed* and the other *unmixed*

The LMTD method is very suitable for determining the *size* of a heat exchanger to realize prescribed outlet temperatures when the mass flow rates and the inlet and outlet temperatures of the hot and cold fluids are specified.

With the LMTD method, the task is to ***select*** a heat exchanger that will meet the prescribed heat transfer requirements. The procedure to be followed by the selection process is:

1. Select the type of heat exchanger suitable for the application.
2. Determine any unknown inlet or outlet temperature and the heat transfer rate using an energy balance.
3. Calculate the log mean temperature difference ΔT_{lm} and the correction factor F, if necessary.
4. Obtain (select or calculate) the value of the overall heat transfer coefficient U.
5. Calculate the heat transfer surface area A_s .

The task is completed by selecting a heat exchanger that has a heat transfer surface area equal to or larger than A_s.

THE EFFECTIVENESS–NTU METHOD

A second kind of problem encountered in heat exchanger analysis is the determination of the *heat transfer rate* and the *outlet temperatures* of the hot and cold fluids for prescribed fluid mass flow rates and inlet temperatures when the *type* and *size* of the heat exchanger are specified.

Heat transfer effectiveness

$$\varepsilon = \frac{\dot{Q}}{\dot{Q}_{\max}} = \frac{\text{Actual heat transfer rate}}{\text{Maximum possible heat transfer rate}}$$

$$\dot{Q} = C_c(T_{c,\text{ out}} - T_{c,\text{ in}}) = C_h(T_{h,\text{ in}} - T_{h,\text{ out}})$$

$$C_c = \dot{m}_c c_{pc} \text{ and } C_h = \dot{m}_c c_{ph}$$

$$\Delta T_{\max} = T_{h,\text{ in}} - T_{c,\text{ in}}$$

$$\dot{Q}_{\max} = C_{\min}(T_{h,\text{ in}} - T_{c,\text{ in}})$$

the maximum possible heat transfer rate

$C_{\min}$ is the smaller of C_h and C_c

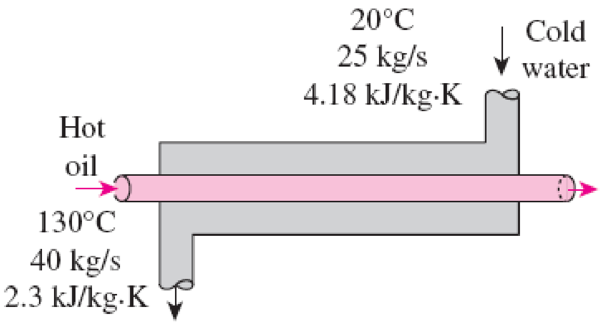

$$C_c = \dot{m}_c c_{pc} = 104.5 \text{ kW/K}$$

$$C_h = \dot{m}_c c_{ph} = 92 \text{ kW/K}$$

$$C_{\min} = 92 \text{ kW/K}$$

$$\Delta T_{\max} = T_{h,\text{in}} - T_{c,\text{in}} = 110°\text{C}$$

$$\dot{Q}_{\max} = C_{\min}\,\Delta T_{\max} = 10{,}120 \text{ kW}$$

FIGURE 11–23
The determination of the maximum rate of heat transfer in a heat exchanger.

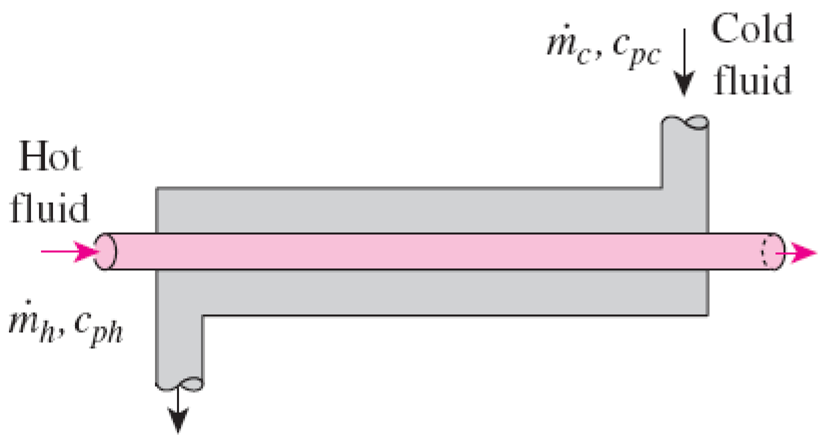

$$\dot{Q} = \dot{m}_h c_{ph} \Delta T_h$$
$$= \dot{m}_c c_{pc} \Delta T_c$$

If $\dot{m}_c c_{pc} = \dot{m}_h c_{ph}$

then $\Delta T_h = \Delta T_c$

FIGURE 11–25
The temperature rise of the cold fluid in a heat exchanger will be equal to the temperature drop of the hot fluid when the heat capacity rates of the hot and cold fluids are identical.

Actual heat transfer rate

$$\dot{Q} = \varepsilon \dot{Q}_{\max} = \varepsilon C_{\min}(T_{h,\text{ in}} - T_{c,\text{ in}})$$

if $C_c = C_{\min}$:

$$\varepsilon = \frac{\dot{Q}}{\dot{Q}_{\max}} = \frac{C_c(T_{c,\text{out}} - T_{c,\text{in}})}{C_c(T_{h,\text{in}} - T_{c,\text{in}})} = \frac{T_{c,\text{out}} - T_{c,\text{in}}}{T_{h,\text{in}} - T_{c,\text{in}}}$$

if $C_h = C_{\min}$:

$$\varepsilon = \frac{\dot{Q}}{\dot{Q}_{\max}} = \frac{C_h(T_{h,\text{in}} - T_{h,\text{out}})}{C_h(T_{h,\text{in}} - T_{c,\text{in}})} = \frac{T_{h,\text{out}} - T_{h,\text{out}}}{T_{h,\text{in}} - T_{c,\text{in}}}$$

The effectiveness of a heat exchanger depends on the *geometry* of the heat exchanger as well as the *flow arrangement.*

Therefore, different types of heat exchangers have different effectiveness relations.

We illustrate the development of the effectiveness e relation for the double-pipe *parallel-flow* heat exchanger.

$$\ln\frac{T_{h,\,\text{out}}-T_{c,\,\text{out}}}{T_{h,\,\text{in}}-T_{c,\,\text{in}}}=-\frac{UA_s}{C_c}\left(1+\frac{C_c}{C_h}\right)$$

$$T_{h,\,\text{out}}=T_{h,\,\text{in}}-\frac{C_c}{C_h}(T_{c,\,\text{out}}-T_{c,\,\text{in}})$$

$$\ln\frac{T_{h,\,\text{in}}-T_{c,\,\text{in}}+T_{c,\,\text{in}}-T_{c,\,\text{out}}-\frac{C_c}{C_h}(T_{c,\,\text{out}}-T_{c,\,\text{in}})}{T_{h,\,\text{in}}-T_{c,\,\text{in}}}=-\frac{UA_s}{C_c}\left(1+\frac{C_c}{C_h}\right)$$

$$\ln\left[1-\left(1+\frac{C_c}{C_h}\right)\frac{T_{c,\,\text{out}}-T_{c,\,\text{in}}}{T_{h,\,\text{in}}-T_{c,\,\text{in}}}\right]=-\frac{UA_s}{C_c}\left(1+\frac{C_c}{C_h}\right)$$

$$\varepsilon=\frac{\dot{Q}}{\dot{Q}_{\max}}=\frac{C_c(T_{c,\,\text{out}}-T_{c,\,\text{in}})}{C_{\min}(T_{h,\,\text{in}}-T_{c,\,\text{in}})}\longrightarrow\frac{T_{c,\,\text{out}}-T_{c,\,\text{in}}}{T_{h,\,\text{in}}-T_{c,\,\text{in}}}=\varepsilon\frac{C_{\min}}{C_c}$$

$$\varepsilon_{\text{parallel flow}}=\frac{1-\exp\left[-\frac{UA_s}{C_c}\left(1+\frac{C_c}{C_h}\right)\right]}{\left(1+\frac{C_c}{C_h}\right)\frac{C_{\min}}{C_c}}$$

$$\varepsilon_{\text{parallel flow}}=\frac{1-\exp\left[-\frac{UA_s}{C_{\min}}\left(1+\frac{C_{\min}}{C_{\max}}\right)\right]}{1+\frac{C_{\min}}{C_{\max}}}$$

Effectiveness relations of the heat exchangers typically involve the *dimensionless* group UA_s / C_{min}.

This quantity is called the **number of transfer units NTU**.

$$\text{NTU} = \frac{UA_s}{C_{\min}} = \frac{UA_s}{(\dot{m}c_p)_{\min}}$$

For specified values of U and C_{min}, the value of NTU *is a measure of the surface area* A_s. Thus, the larger the NTU, the larger the heat exchanger.

$$c = \frac{C_{\min}}{C_{\max}}$$ capacity ratio

The effectiveness of a heat exchanger is a function of the number of transfer units NTU and the capacity ratio *c*.

$$\varepsilon = \text{function}\,(UA_s/C_{\min}, C_{\min}/C_{\max}) = \text{function}\,(\text{NTU}, c)$$

TABLE 11–4

Effectiveness relations for heat exchangers: NTU $= UA_s/C_{\min}$ and $c = C_{\min}/C_{\max} = (\dot{m}c_p)_{\min}/(\dot{m}c_p)_{\max}$

Heat exchanger type	Effectiveness relation
1 *Double pipe:*	
Parallel-flow	$\varepsilon = \dfrac{1 - \exp[-\text{NTU}(1 + c)]}{1 + c}$
Counter-flow	$\varepsilon = \dfrac{1 - \exp[-\text{NTU}(1 - c)]}{1 - c\exp[-\text{NTU}(1 - c)]}$
2 *Shell-and-tube:* One-shell pass 2, 4,…tube passes	$\varepsilon = 2\left\{1 + c + \sqrt{1 + c^2}\,\dfrac{1 + \exp[-\text{NTU}\sqrt{1 + c^2}]}{1 - \exp[-\text{NTU}\sqrt{1 + c^2}]}\right\}^{-1}$
3 *Cross-flow (single-pass)* Both fluids unmixed	$\varepsilon = 1 - \exp\left\{\dfrac{\text{NTU}^{0.22}}{c}[\exp(-c\,\text{NTU}^{0.78}) - 1]\right\}$
$C_{\max}$ mixed, $C_{\min}$ unmixed	$\varepsilon = \dfrac{1}{c}(1 - \exp\{-c[1 - \exp(-\text{NTU})]\})$
$C_{\min}$ mixed, $C_{\max}$ unmixed	$\varepsilon = 1 - \exp\left\{-\dfrac{1}{c}[1 - \exp(-c\,\text{NTU})]\right\}$
4 *All heat exchangers with c = 0*	$\varepsilon = 1 - \exp(-\text{NTU})$

Effectiveness for heat exchangers.

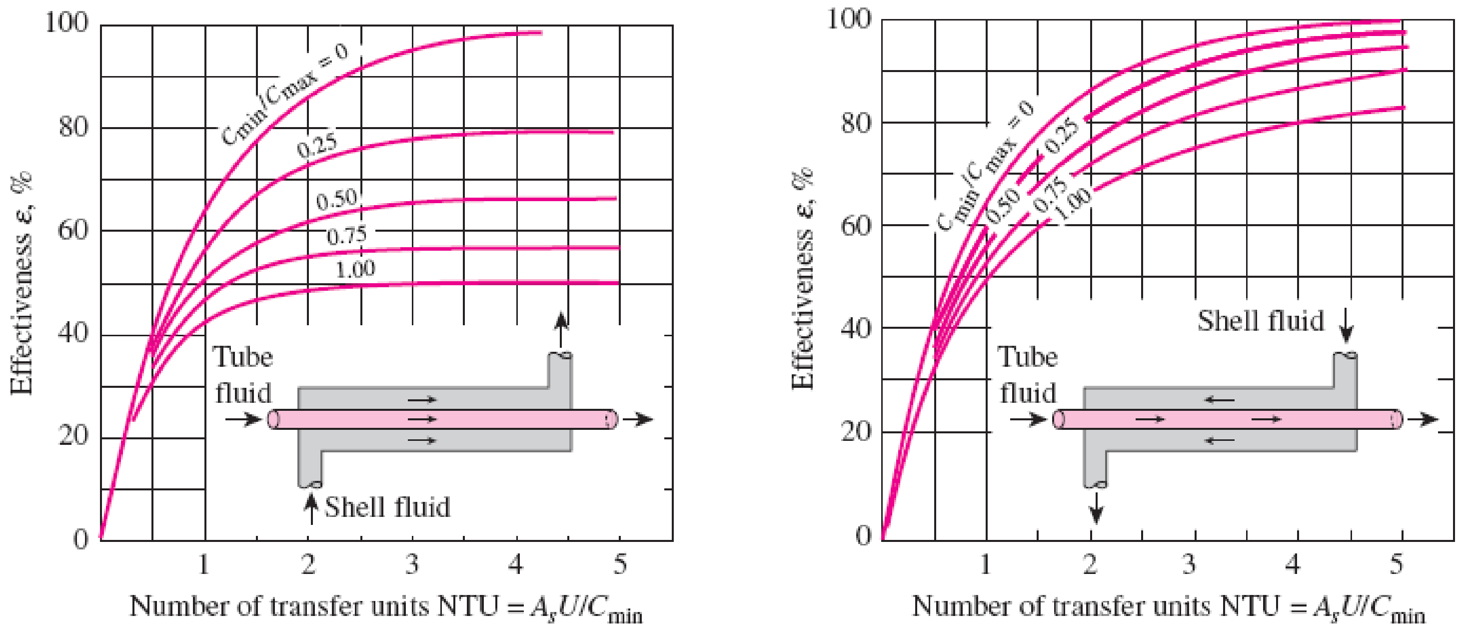

(*a*) Parallel-flow

(*b*) Counter-flow

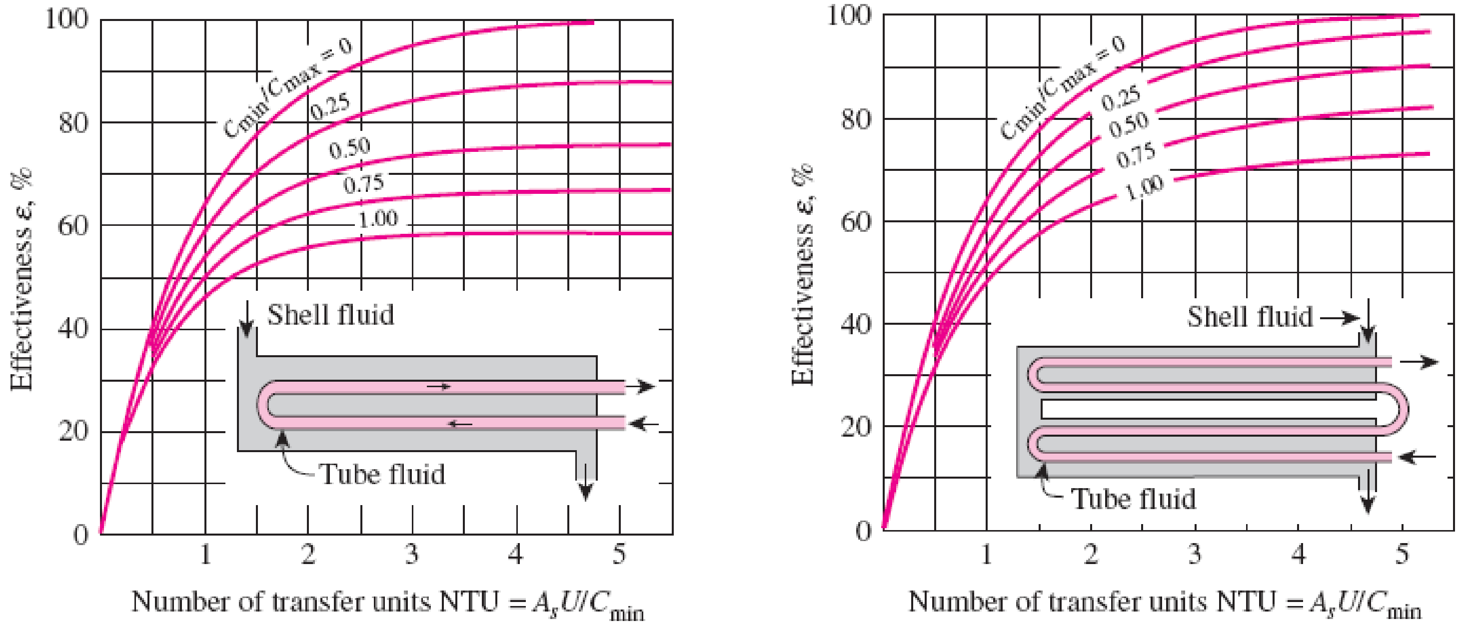

(*c*) One-shell pass and 2, 4, 6, … tube passes

(*d*) Two-shell passes and 4, 8, 12, … tube passes

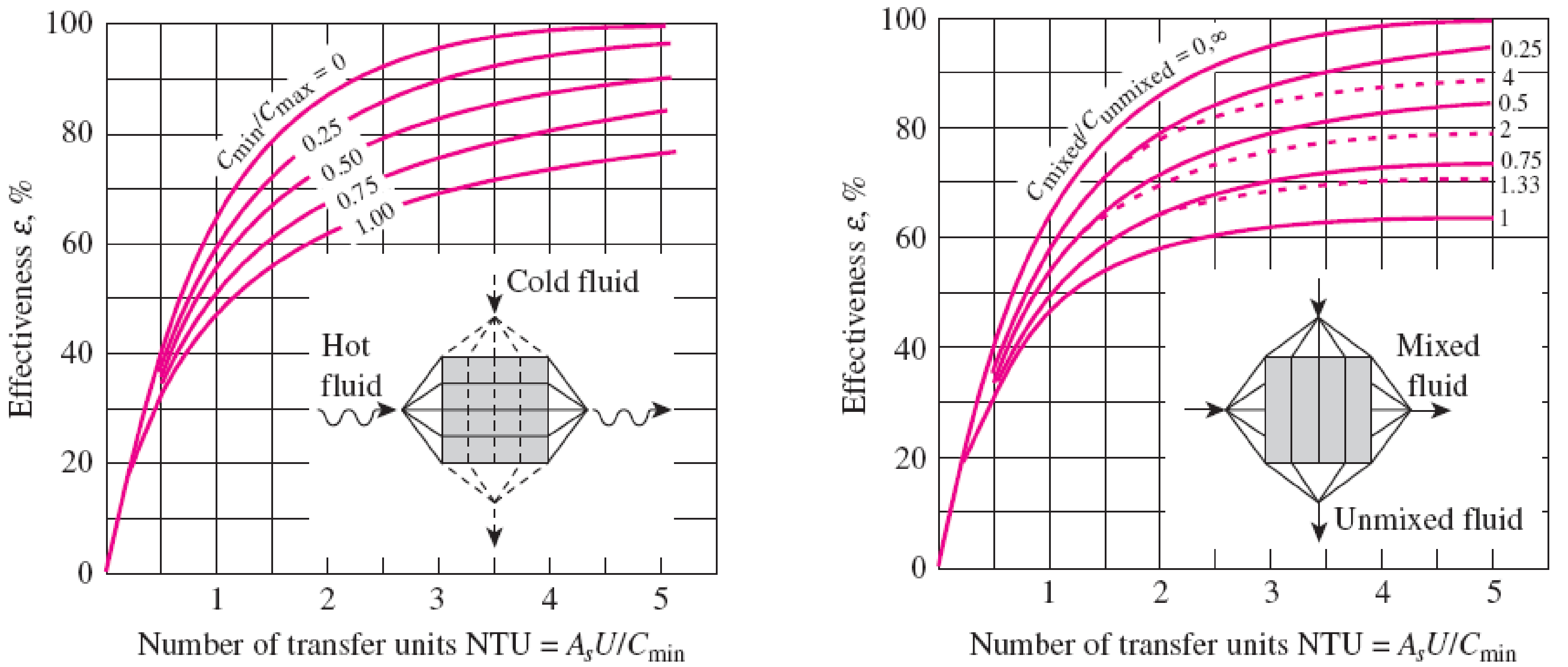

(*e*) Cross-flow with both fluids unmixed

(*f*) Cross-flow with one fluid mixed and the other unmixed

FIGURE 11–26

Effectiveness for heat exchangers.

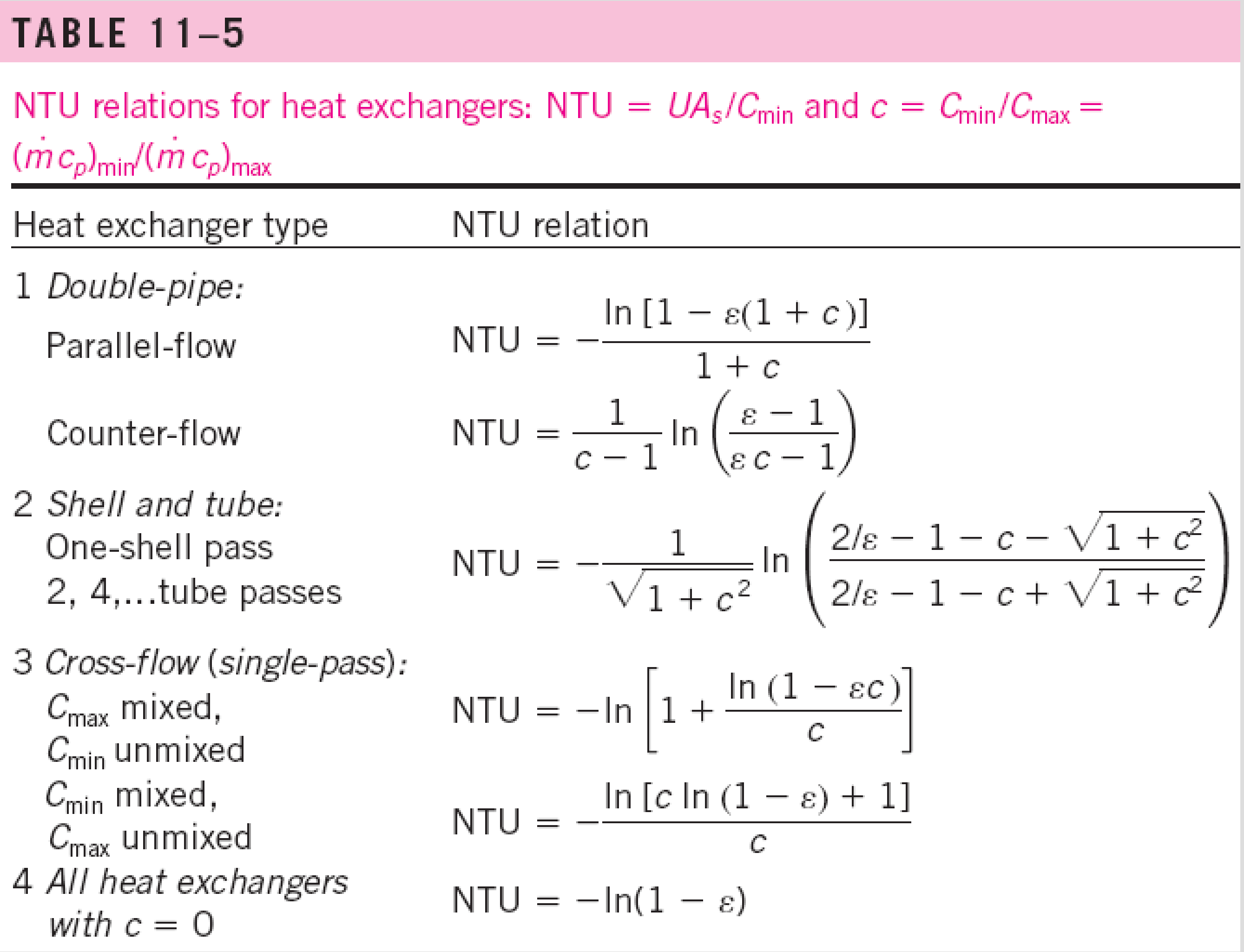

TABLE 11–5

NTU relations for heat exchangers: $\text{NTU} = UA_s/C_{\min}$ and $c = C_{\min}/C_{\max} = (\dot{m}c_p)_{\min}/(\dot{m}c_p)_{\max}$

Heat exchanger type	NTU relation
1 *Double-pipe:*	
Parallel-flow	$\text{NTU} = -\frac{\ln[1-\varepsilon(1+c)]}{1+c}$
Counter-flow	$\text{NTU} = \frac{1}{c-1}\ln\left(\frac{\varepsilon-1}{\varepsilon c-1}\right)$
2 *Shell and tube:* One-shell pass 2, 4,…tube passes	$\text{NTU} = -\frac{1}{\sqrt{1+c^2}}\ln\left(\frac{2/\varepsilon-1-c-\sqrt{1+c^2}}{2/\varepsilon-1-c+\sqrt{1+c^2}}\right)$
3 *Cross-flow (single-pass):*	
$C_{\max}$ mixed, $C_{\min}$ unmixed	$\text{NTU} = -\ln\left[1+\frac{\ln(1-\varepsilon c)}{c}\right]$
$C_{\min}$ mixed, $C_{\max}$ unmixed	$\text{NTU} = -\frac{\ln[c\ln(1-\varepsilon)+1]}{c}$
4 *All heat exchangers with $c = 0$*	$\text{NTU} = -\ln(1-\varepsilon)$

When all the inlet and outlet temperatures are specified, the *size* of the heat exchanger can easily be determined using the LMTD method. Alternatively, it can be determined from the effectiveness–NTU method by first evaluating the effectiveness from its definition and then the NTU from the appropriate NTU relation.

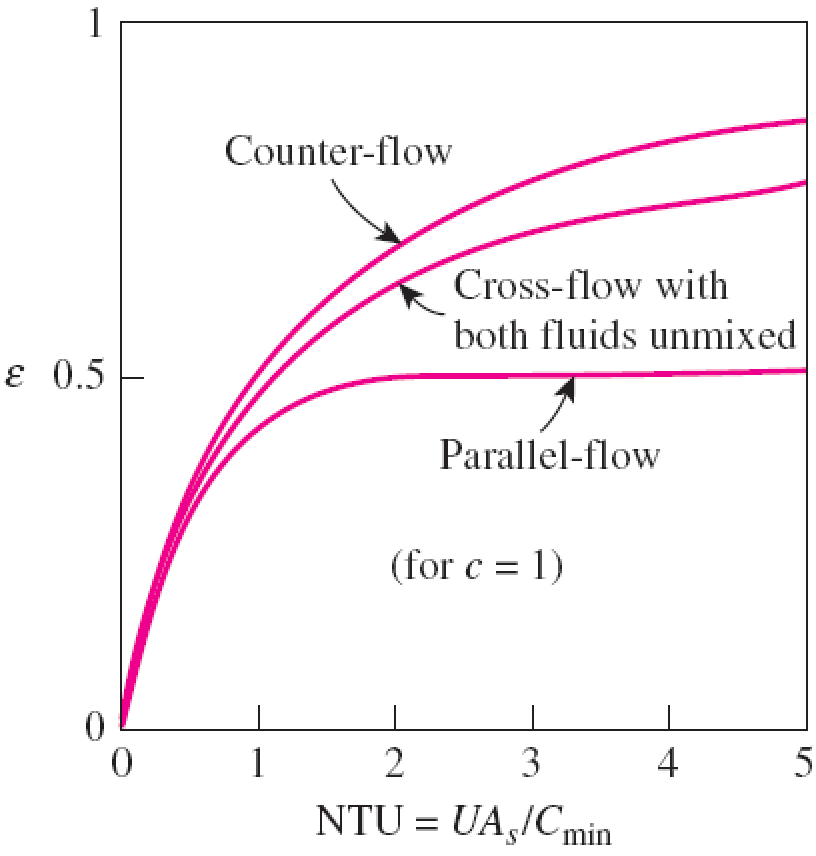

FIGURE 11–27
For a specified NTU and capacity ratio c, the counter-flow heat exchanger has the highest effectiveness and the parallel-flow the lowest.

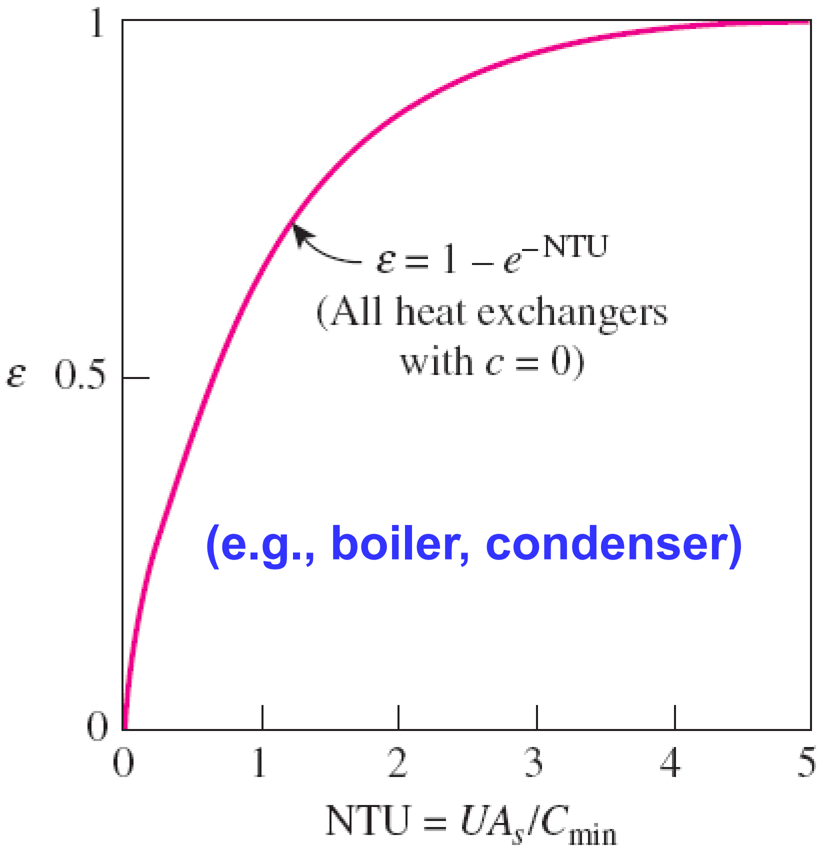

(e.g., boiler, condenser)

FIGURE 11–28
The effectiveness relation reduces to $\varepsilon = \varepsilon_{\max} = 1 - \exp(-\mathrm{NTU})$ for all heat exchangers when the capacity ratio $c = 0$.

Observations from the effectiveness relations and charts

- The value of the effectiveness ranges from 0 to 1. It increases rapidly with NTU for small values (up to about NTU = 1.5) but rather slowly for larger values. Therefore, the use of a heat exchanger with a large NTU (usually larger than 3) and thus a large size cannot be justified economically, since a large increase in NTU in this case corresponds to a small increase in effectiveness.
- For a given NTU and capacity ratio $c = C_{min} / C_{max}$, the *counter-flow* heat exchanger has the *highest* effectiveness, followed closely by the cross-flow heat exchangers with both fluids unmixed. The lowest effectiveness values are encountered in parallel-flow heat exchangers.
- The effectiveness of a heat exchanger is independent of the capacity ratio *c* for NTU values of less than about 0.3.
- The value of the capacity ratio *c* ranges between 0 and 1. For a given NTU, the effectiveness becomes a *maximum* for $c = 0$ (e.g., boiler, condenser) and a *minimum* for $c = 1$ (when the heat capacity rates of the two fluids are equal).

SELECTION OF HEAT EXCHANGERS

The uncertainty in the predicted value of *U* can exceed 30 percent. Thus, it is natural to tend to overdesign the heat exchangers.

Heat transfer enhancement in heat exchangers is usually accompanied by *increased pressure drop*, and thus *higher pumping power.*

Therefore, any gain from the enhancement in heat transfer should be weighed against the cost of the accompanying pressure drop.

Usually, the *more viscous fluid is more suitable for the shell side* (larger passage area and thus lower pressure drop) and *the fluid with the higher pressure for the tube side.*

The proper selection of a heat exchanger depends on several factors:

- **Heat Transfer Rate**
- **Cost**
- **Pumping Power**
- **Size and Weight**
- **Type**
- **Materials**

The *rate of heat transfer* in the prospective heat exchanger

$$\dot{Q} = \dot{m}c_p(T_{\text{in}} - T_{\text{out}})$$

The annual cost of electricity associated with the operation of the pumps and fans

$$\begin{aligned}\text{Operating cost} = {} & (\text{Pumping power, kW}) \times (\text{Hours of operation, h}) \\ & \times (\text{Unit cost of electricity, \$/kWh})\end{aligned}$$

Summary

- Types of Heat Exchangers
- The Overall Heat Transfer Coefficient
    - ✓ Fouling factor
- Analysis of Heat Exchangers
- The Log Mean Temperature Difference Method
    - ✓ Counter-Flow Heat Exchangers
    - ✓ Multipass and Cross-Flow Heat Exchangers: Use of a Correction Factor
- The Effectiveness–NTU Method
- Selection of Heat Exchangers

Heat Transfer Lectures
Fundamentals & Applications

UNIVERSITY OF TECHNOLOGY

Mechanical Engineering department

3rd power plant division

RADIATION HEAT TRANSFER

Dr. Sattar Aljabair

Objectives

- Define view factor, and understand its importance in radiation heat transfer calculations
- Develop view factor relations, and calculate the unknown view factors in an enclosure by using these relations
- Calculate radiation heat transfer between black surfaces
- Determine radiation heat transfer between diffuse and gray surfaces in an enclosure using the concept of radiosity
- Obtain relations for net rate of radiation heat transfer between the surfaces of a two-zone enclosure, including two large parallel plates, two long concentric cylinders, and two concentric spheres
- Quantify the effect of radiation shields on the reduction of radiation heat transfer between two surfaces, and become aware of the importance of radiation effect in temperature measurements

THE VIEW FACTOR

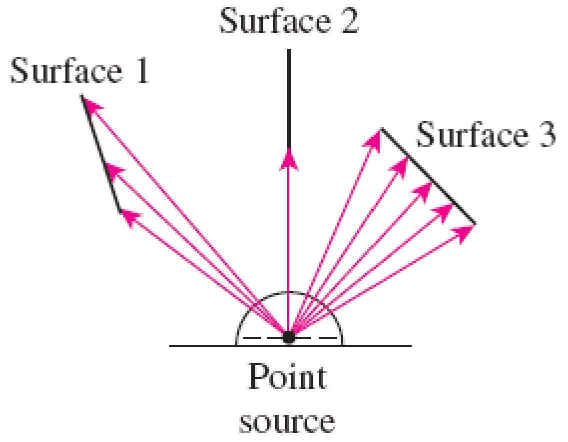

FIGURE 13–1
Radiation heat exchange between surfaces depends on the *orientation* of the surfaces relative to each other, and this dependence on orientation is accounted for by the *view factor*.

View factor is a purely geometric quantity and is independent of the surface properties and temperature.

It is also called the *shape factor*, *configuration factor*, and *angle factor*.

The view factor based on the assumption that the surfaces are diffuse emitters and diffuse reflectors is called the *diffuse view factor*, and the view factor based on the assumption that the surfaces are diffuse emitters but specular reflectors is called the *specular view factor*.

F$_{ij}$ *the fraction of the radiation leaving surface i that strikes surface j directly*

The view factor ranges between 0 and 1.

To develop a general expression for the view factor, consider two differential surfaces dA_1 and dA_2 on two arbitrarily oriented surfaces A_1 and A_2, respectively, as shown in Fig. 13–2. The distance between dA_1 and dA_2 is r; and the angles between the normals of the surfaces and the line that connects dA_1 and dA_2 are θ_1 and θ_2, respectively. Surface 1 emits and reflects radiation diffusely in all directions with a constant intensity of I_1, and the solid angle subtended by dA_2 when viewed by dA_1 is $d\omega_{21}$.

The rate at which radiation leaves dA_1 in the direction of θ_1 is $I_1 \cos \theta_1 dA_1$. Noting that $d\omega_{21} = dA_2 \cos \theta_2 / r^2$, the portion of this radiation that strikes dA_2 is

$$\dot{Q}_{dA_1 \to dA_2} = I_1 \cos \theta_1 \, dA_1 \, d\omega_{21} = I_1 \cos \theta_1 \, dA_1 \frac{dA_2 \cos \theta_2}{r^2} \tag{13–1}$$

The total rate at which radiation leaves dA_1 (via emission and reflection) in all directions is the radiosity (which is $J_1 = \pi I_1$) times the surface area,

$$\dot{Q}_{dA_1} = J_1 \, dA_1 = \pi I_1 \, dA_1 \tag{13–2}$$

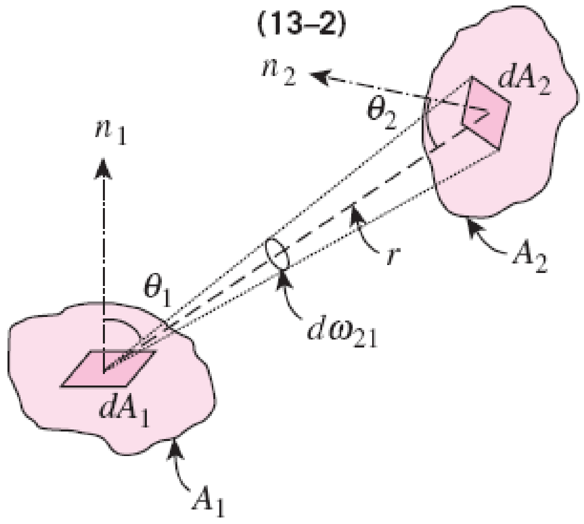

FIGURE 13–2

Geometry for the determination of the view factor between two surfaces.

Then the *differential view factor* $dF_{dA_1 \to d_{A_2}}$, which is the fraction of radiation leaving dA_1 that strikes dA_2 directly, becomes

$$dF_{dA_1 \to dA_2} = \frac{\dot{Q}_{dA_1 \to dA_2}}{\dot{Q}_{dA_1}} = \frac{\cos\theta_1 \cos\theta_2}{\pi r^2}\, dA_2 \qquad \textbf{(13–3)}$$

The differential view factor $dF_{dA_2 \to dA_1}$ can be determined from Eq. 13–3 by interchanging the subscripts 1 and 2.

The view factor from a differential area dA_1 to a finite area A_2 can be determined from the fact that the fraction of radiation leaving dA_1 that strikes A_2 is the sum of the fractions of radiation striking the differential areas dA_2. Therefore, the view factor $F_{dA_1 \to A_2}$ is determined by integrating $dF_{dA_1 \to dA_2}$ over A_2,

$$F_{dA_1 \to A_2} = \int_{A_2} \frac{\cos\theta_1 \cos\theta_2}{\pi r^2}\, dA_2 \qquad \textbf{(13–4)}$$

The total rate at which radiation leaves the entire A_1 (via emission and reflection) in all directions is

$$\dot{Q}_{A_1} = J_1 A_1 = \pi I_1 A_1 \qquad \textbf{(13–5)}$$

The portion of this radiation that strikes dA_2 is determined by considering the radiation that leaves dA_1 and strikes dA_2 (given by Eq. 13–1), and integrating it over A_1,

$$\dot{Q}_{A_1 \to dA_2} = \int_{A_1} \dot{Q}_{dA_1 \to dA_2} = \int_{A_1} \frac{I_1 \cos\theta_1 \cos\theta_2\, dA_2}{r^2}\, dA_1 \qquad \textbf{(13–6)}$$

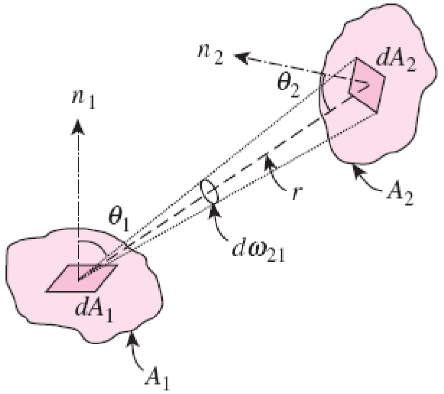

FIGURE 13–2
Geometry for the determination of the view factor between two surfaces.

Integration of this relation over A_2 gives the radiation that strikes the entire A_2,

$$\dot{Q}_{A_1 \to A_2} = \int_{A_2} \dot{Q}_{A_1 \to dA_2} = \int_{A_2}\int_{A_1} \frac{I_1 \cos\theta_1 \cos\theta_2}{r^2}\, dA_1\, dA_2 \tag{13–7}$$

Dividing this by the total radiation leaving A_1 (from Eq. 13–5) gives the fraction of radiation leaving A_1 that strikes A_2, which is the view factor $F_{A_1 \to A_2}$ (or F_{12} for short),

$$F_{12} = F_{A_1 \to A_2} = \frac{\dot{Q}_{A_1 \to A_2}}{\dot{Q}_{A_1}} = \frac{1}{A_1}\int_{A_2}\int_{A_1} \frac{\cos\theta_1 \cos\theta_2}{\pi r^2}\, dA_1\, dA_2 \tag{13–8}$$

The view factor $F_{A_2 \to A_1}$ is readily determined from Eq. 13–8 by interchanging the subscripts 1 and 2,

$$F_{21} = F_{A_2 \to A_1} = \frac{\dot{Q}_{A_2 \to A_1}}{\dot{Q}_{A_2}} = \frac{1}{A_2}\int_{A_2}\int_{A_1} \frac{\cos\theta_1 \cos\theta_2}{\pi r^2}\, dA_1\, dA_2 \tag{13–9}$$

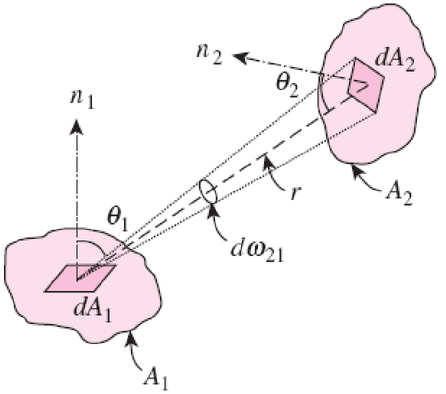

FIGURE 13–2
Geometry for the determination of the view factor between two surfaces.

Note that I_1 is constant but r, θ_1, and θ_2 are variables. Also, integrations can be performed in any order since the integration limits are constants. These relations confirm that the view factor between two surfaces depends on their relative orientation and the distance between them.

Combining Eqs. 13–8 and 13–9 after multiplying the former by A_1 and the latter by A_2 gives

$$A_1 F_{12} = A_2 F_{21} \tag{13–10}$$

which is known as the **reciprocity relation** for view factors. It allows the calculation of a view factor from a knowledge of the other.

$F_{i \to i}$ = the fraction of radiation leaving surface i that strikes itself directly

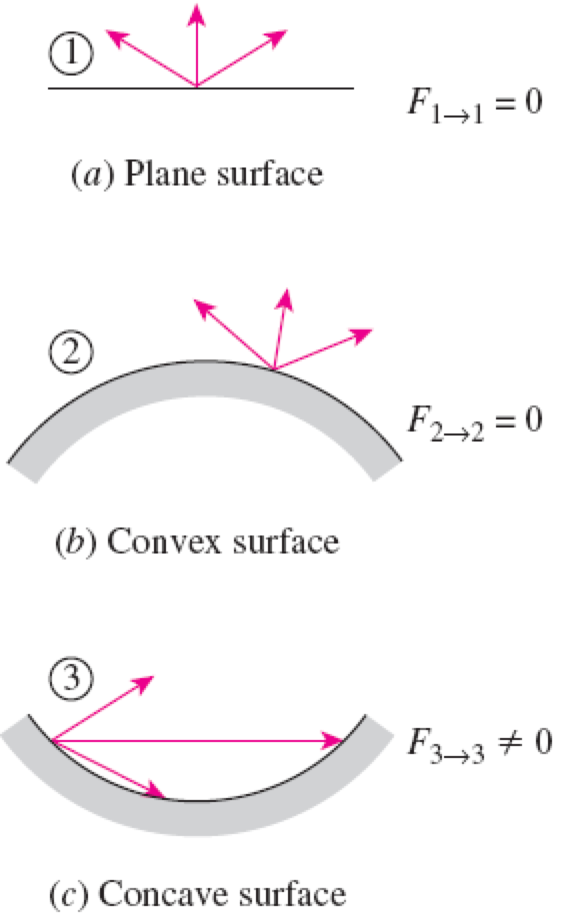

FIGURE 13–3

The view factor from a surface to itself is *zero* for *plane* or *convex* surfaces and *nonzero* for *concave* surfaces.

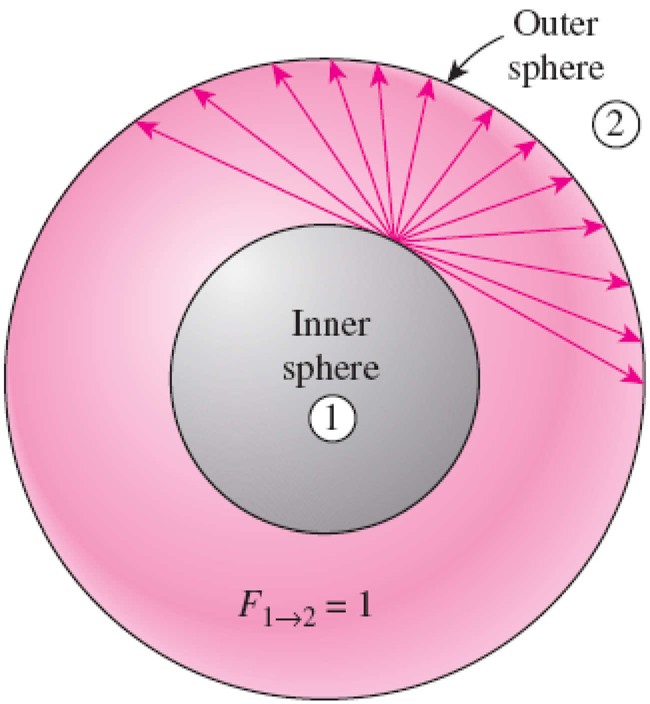

FIGURE 13–4

In a geometry that consists of two concentric spheres, the view factor $F_{1\to 2} = 1$ since the entire radiation leaving the surface of the smaller sphere is intercepted by the larger sphere.

The view factor has proven to be very useful in radiation analysis because it allows us to express the *fraction of radiation* leaving a surface that strikes another surface in terms of the orientation of these two surfaces relative to each other.

The underlying assumption in this process is that the radiation a surface receives from a source is directly proportional to the angle the surface subtends when viewed from the source.

This would be the case only if the radiation coming off the source is *uniform* in all directions throughout its surface and the medium between the surfaces does not *absorb*, *emit*, or *scatter* radiation.

That is, it is the case when the surfaces are *isothermal* and *diffuse* emitters and reflectors and the surfaces are separated by a *nonparticipating* medium such as a vacuum or air.

View factors for hundreds of common geometries are evaluated and the results are given in analytical, graphical, and tabular form.

TABLE 13–1

View factor expressions for some common geometries of finite size (3-D)

Geometry	Relation
Aligned parallel rectangles 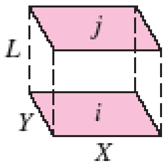	$\overline{X} = X/L$ and $\overline{Y} = Y/L$ $F_{i \to j} = \frac{2}{\pi \overline{X}\,\overline{Y}} \left\{ \ln \left[\frac{(1+\overline{X}^2)(1+\overline{Y}^2)}{1+\overline{X}^2+\overline{Y}^2} \right]^{1/2} + \overline{X}(1+\overline{Y}^2)^{1/2} \tan^{-1} \frac{\overline{X}}{(1+\overline{Y}^2)^{1/2}} \right.$ $\left. + \overline{Y}(1+\overline{X}^2)^{1/2} \tan^{-1} \frac{\overline{Y}}{(1+\overline{X}^2)^{1/2}} - \overline{X} \tan^{-1} \overline{X} - \overline{Y} \tan^{-1} \overline{Y} \right\}$
Coaxial parallel disks 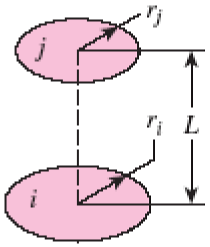	$R_i = r_i/L$ and $R_j = r_j/L$ $S = 1 + \frac{1+R_j^2}{R_i^2}$ $F_{i \to j} = \frac{1}{2} \left\{ S - \left[S^2 - 4\left(\frac{r_j}{r_i}\right)^2 \right]^{1/2} \right\}$ For $r_i = r_j = r$ and $R = r/L$: $F_{i \to j} = F_{j \to i} = 1 + \frac{1 - \sqrt{4R^2+1}}{2R^2}$
Perpendicular rectangles with a common edge 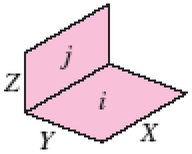	$H = Z/X$ and $W = Y/X$ $F_{i \to j} = \frac{1}{\pi W} \left(W \tan^{-1} \frac{1}{W} + H \tan^{-1} \frac{1}{H} - (H^2+W^2)^{1/2} \tan^{-1} \frac{1}{(H^2+W^2)^{1/2}} \right.$ $+ \frac{1}{4} \ln \left\{ \frac{(1+W^2)(1+H^2)}{1+W^2+H^2} \left[\frac{W^2(1+W^2+H^2)}{(1+W^2)(W^2+H^2)} \right]^{W^2} \right.$ $\left. \left. \times \left[\frac{H^2(1+H^2+W^2)}{(1+H^2)(H^2+W^2)} \right]^{H^2} \right\} \right)$

TABLE 13–2

View factor expressions for some infinitely long (2-D) geometries

Geometry	**Relation**
Parallel plates with midlines connected by perpendicular line 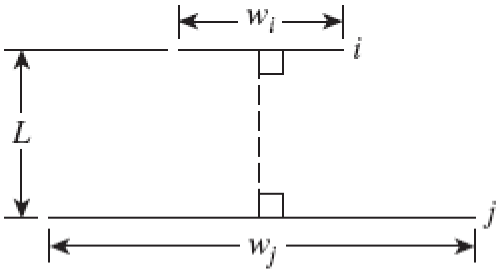 	$W_i = w_i/L$ and $W_j = w_j/L$ $F_{i\to j} = \dfrac{[(W_i + W_j)^2 + 4]^{1/2} - (W_j - W_i)^2 + 4]^{1/2}}{2W_i}$
Inclined plates of equal width and with a common edge 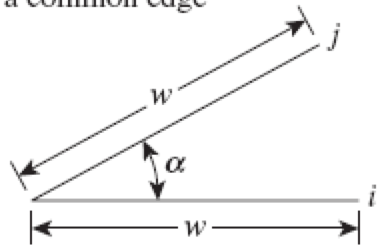 	$F_{i\to j} = 1 - \sin\frac{1}{2}\alpha$
Perpendicular plates with a common edge 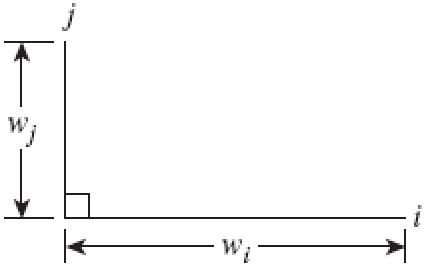 	$F_{i\to j} = \frac{1}{2}\left\{1 + \frac{w_j}{w_i} - \left[1 + \left(\frac{w_j}{w_i}\right)^2\right]^{1/2}\right\}$

TABLE 13–2

View factor expressions for some infinitely long (2-D) geometries

Three-sided enclosure 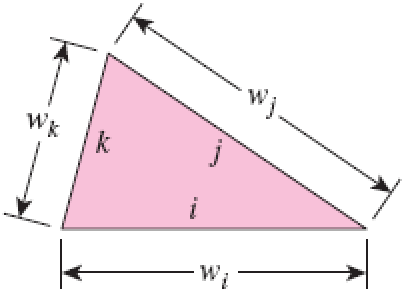 	$F_{i \to j} = \dfrac{w_i + w_j - w_k}{2w_i}$
Infinite plane and row of cylinders 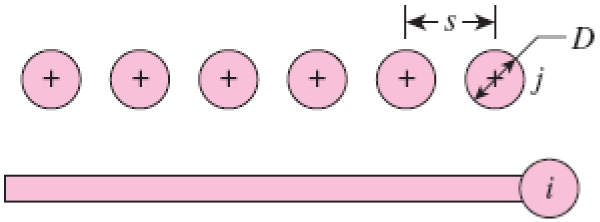 	$F_{i \to j} = 1 - \left[1 - \left(\dfrac{D}{s}\right)^2\right]^{1/2} + \dfrac{D}{s}\tan^{-1}\left(\dfrac{s^2 - D^2}{D^2}\right)^{1/2}$

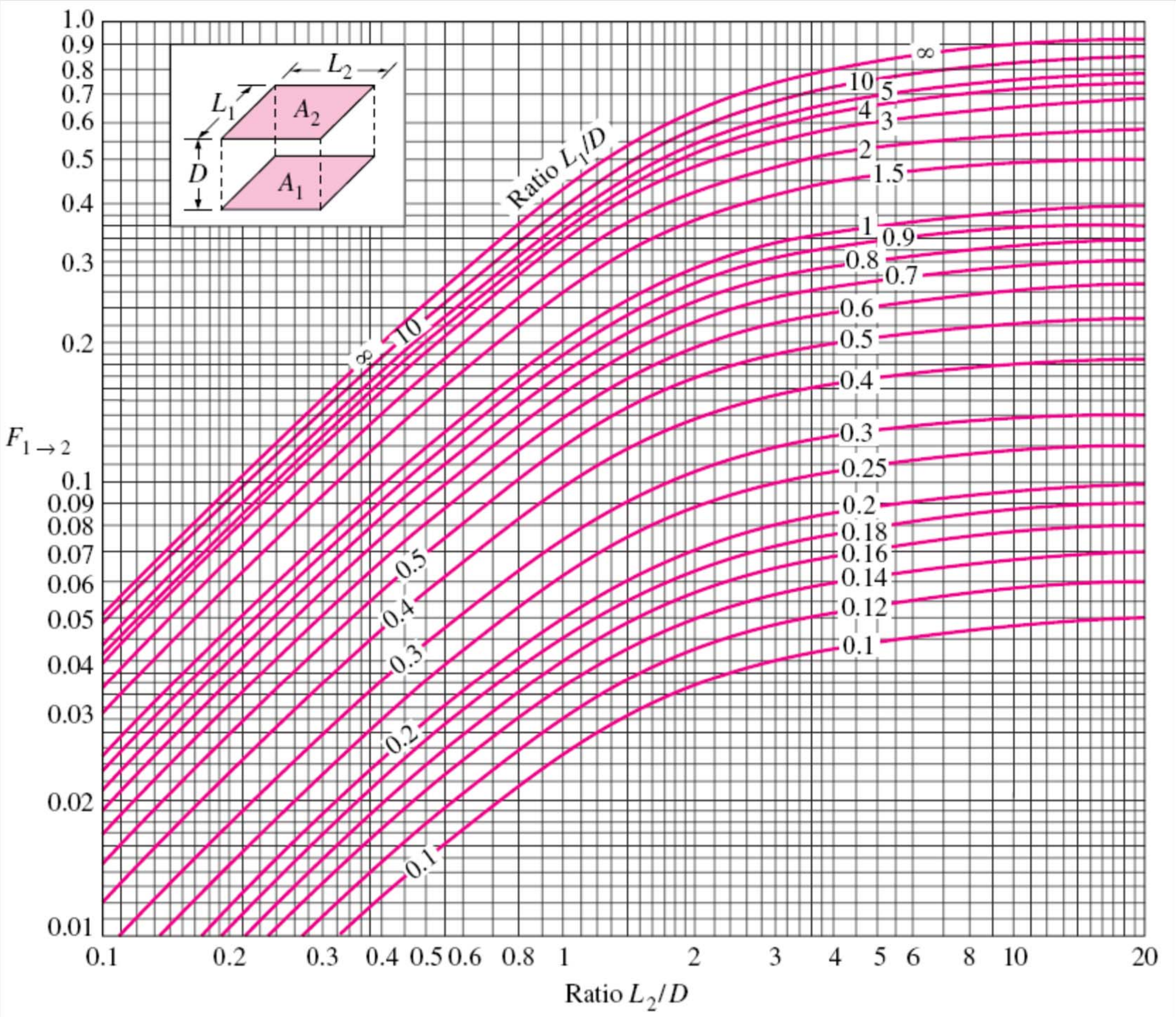

View factor between two aligned parallel rectangles of equal size.

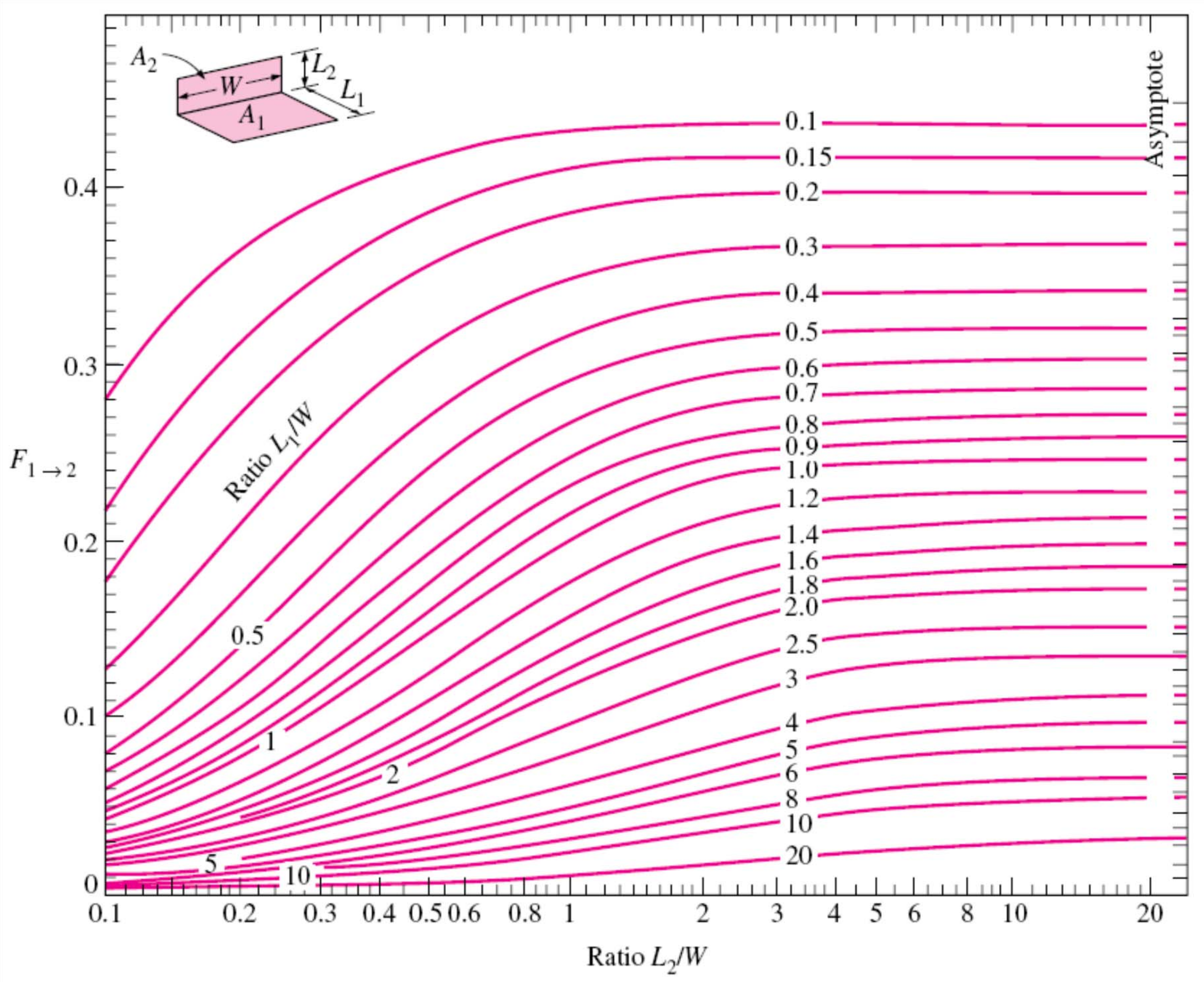

View factor between two perpendicular rectangles with a common edge.

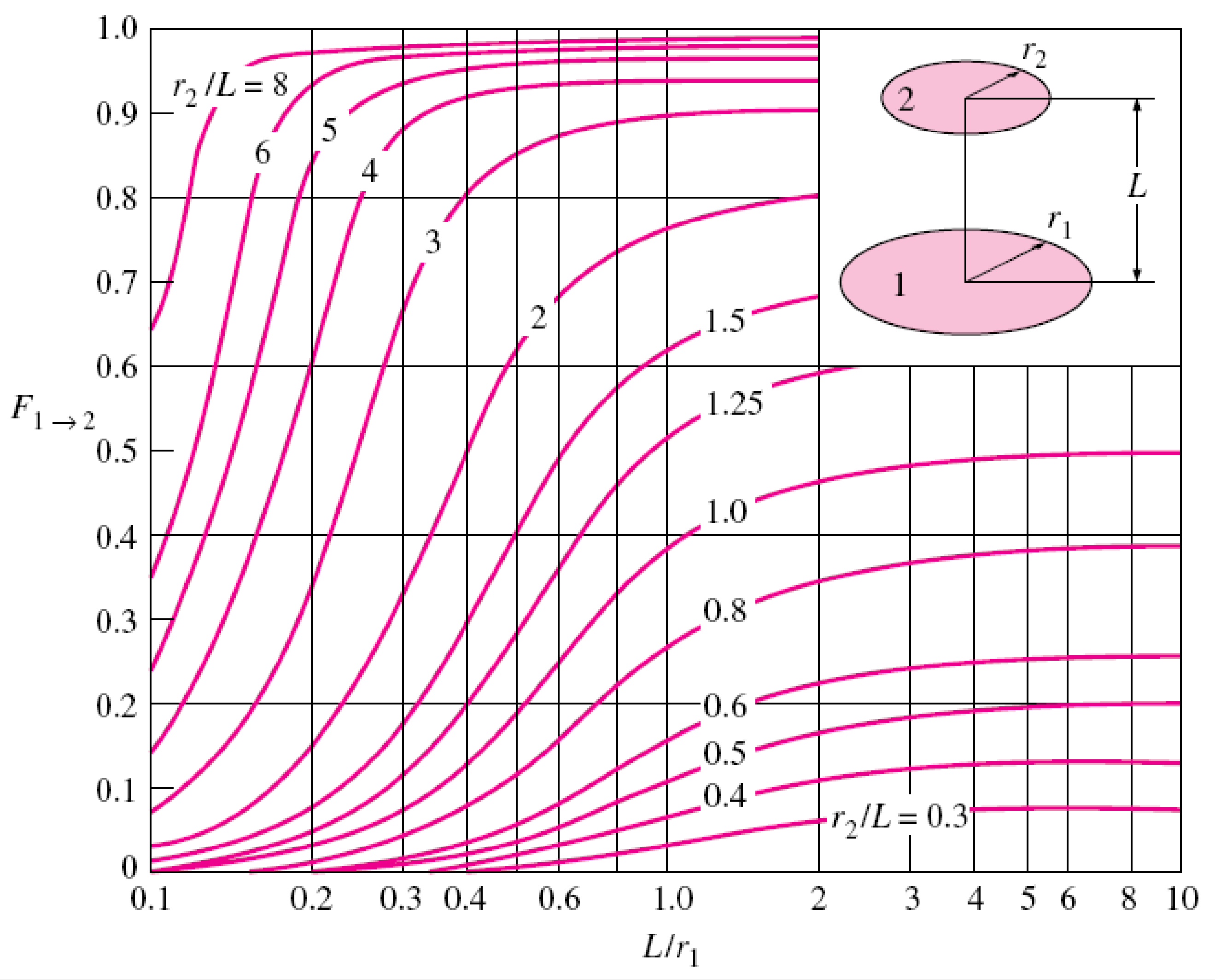

View factor between two coaxial parallel disks.

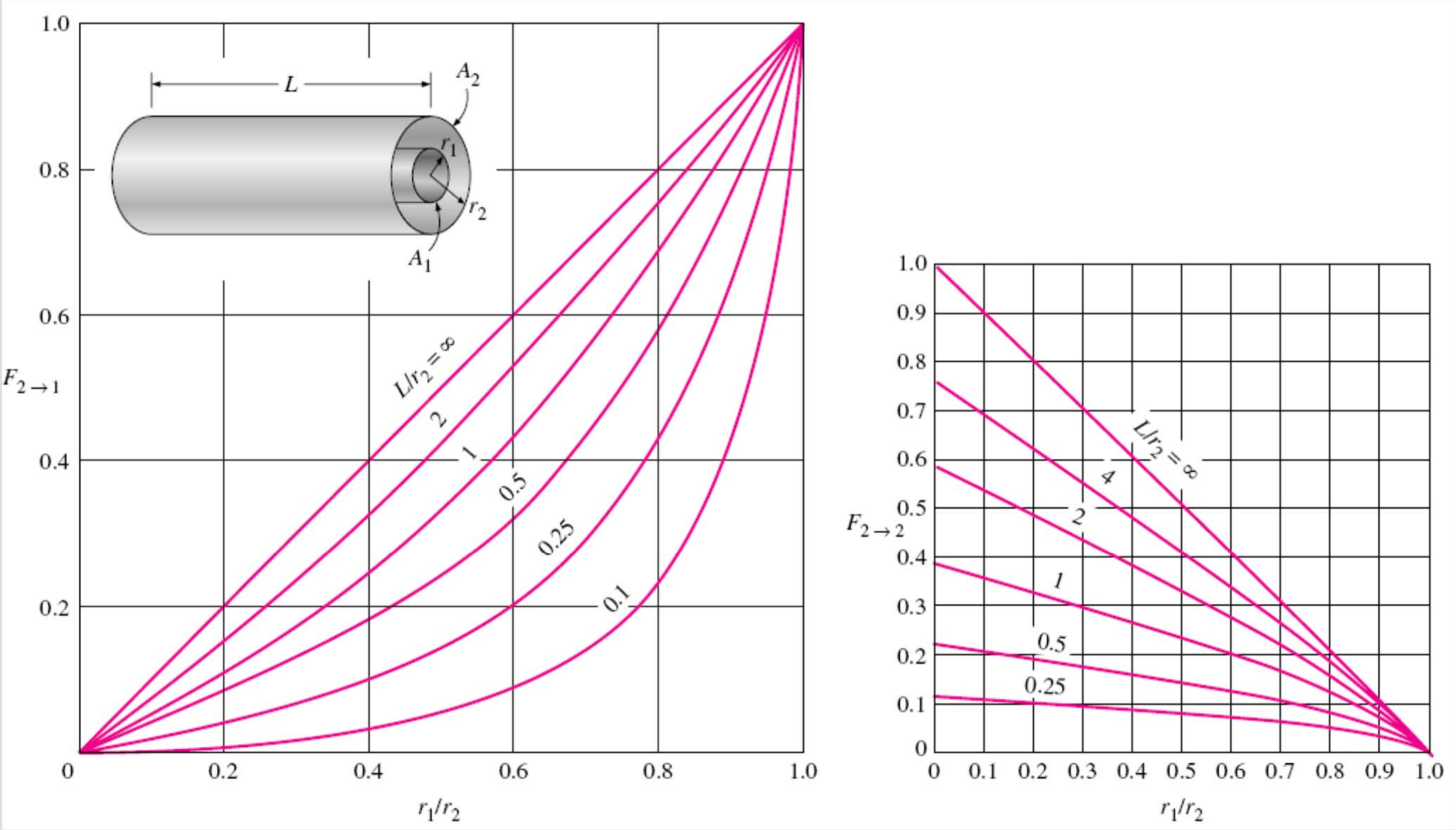

View factors for two concentric cylinders of finite length: (*a*) outer cylinder to inner cylinder; (*b*) outer cylinder to itself.

View Factor Relations

Radiation analysis on an enclosure consisting of *N* surfaces requires the evaluation of N^2 view factors.

Once a sufficient number of view factors are available, the rest of them can be determined by utilizing some fundamental relations for view factors.

1 The Reciprocity Relation

$$\begin{aligned} F_{j\to i} &= F_{i\to j} \quad &\text{when} \quad A_i &= A_j \\ F_{j\to i} &\neq F_{i\to j} \quad &\text{when} \quad A_i &\neq A_j \end{aligned}$$

$$A_iF_{i\to j} = A_jF_{j\to i}$$

reciprocity relation (rule)

2 The Summation Rule

The sum of the view factors from surface i of an enclosure to all surfaces of the enclosure, including to itself, must equal unity.

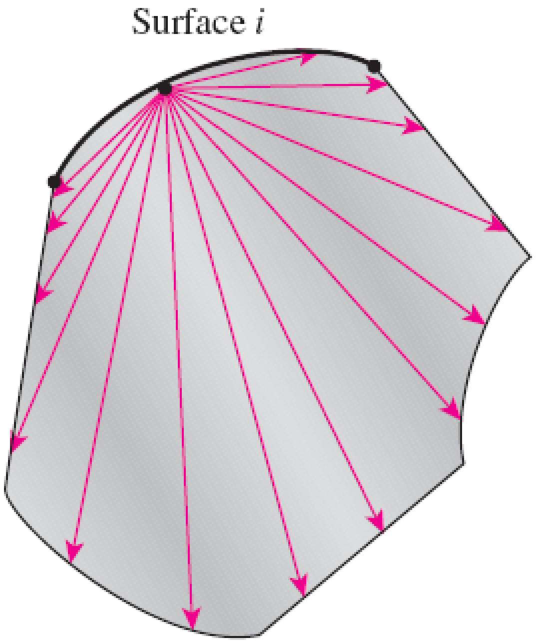

FIGURE 13–9

Radiation leaving any surface i of an enclosure must be intercepted completely by the surfaces of the enclosure. Therefore, the sum of the view factors from surface i to each one of the surfaces of the enclosure must be unity.

$$\sum_{j=1}^{N} F_{i \to j} = 1$$

$$\sum_{j=1}^{3} F_{1 \to j} = F_{1 \to 1} + F_{1 \to 2} + F_{1 \to 3} = 1$$

The total number of view factors that need to be evaluated directly for an *N*-surface enclosure is

$$N^2 - [N + \tfrac{1}{2}N(N-1)] = \tfrac{1}{2}N(N-1)$$

The remaining view factors can be determined from the equations that are obtained by applying the reciprocity and the summation rules.

4 The Symmetry Rule

Two (or more) surfaces that possess symmetry about a third surface will have identical view factors from that surface.

If the surfaces *j* and *k* are symmetric about the surface i then

$F_{i \to j} = F_{i \to k}$ and $F_{j \to i} = F_{k \to i}$

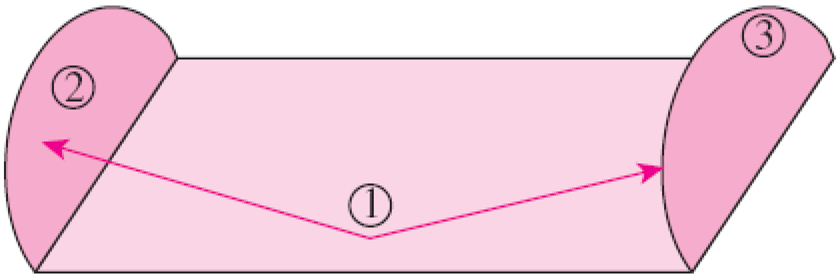

$F_{1\to2} = F_{1\to3}$
(Also, $F_{2\to1} = F_{3\to1}$)

FIGURE 13–13
Two surfaces that are symmetric about a third surface will have the same view factor from the third surface.

RADIATION HEAT TRANSFER: BLACK SURFACES

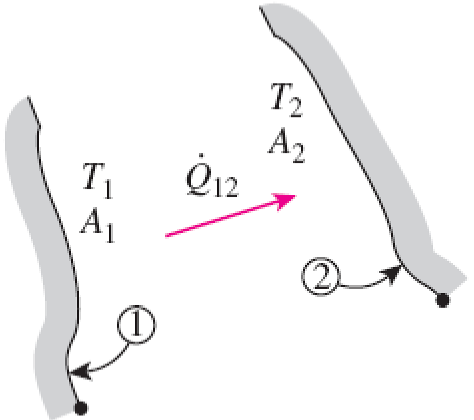

FIGURE 13–18
Two general black surfaces maintained at uniform temperatures T_1 and T_2.

When the surfaces involved can be approximated as blackbodies because of the absence of reflection, the *net* rate of radiation heat transfer from surface 1 to surface 2 is

$$\dot{Q}_{1\to 2} = \begin{pmatrix}\text{Radiation leaving}\\ \text{the entire surface 1}\\ \text{that strikes surface 2}\end{pmatrix} - \begin{pmatrix}\text{Radiation leaving}\\ \text{the entire surface 2}\\ \text{that strikes surface 1}\end{pmatrix}$$

$$= A_1 E_{b1} F_{1\to 2} - A_2 E_{b2} F_{2\to 1} \qquad \text{(W)}$$

$$A_1 F_{1\to 2} = A_2 F_{2\to 1}$$

reciprocity relation

$$E_b = \sigma T^4$$

emissive power

$$\dot{Q}_{1\to 2} = A_1 F_{1\to 2}\,\sigma(T_1^4 - T_2^4) \qquad \text{(W)}$$

A negative value for $Q_{1\to 2}$ indicates that net radiation heat transfer is from surface 2 to surface 1.

The *net* radiation heat transfer *from* any surface *i* of an *N* surface enclosure is

$$\dot{Q}_i = \sum_{j=1}^{N} \dot{Q}_{i\to j} = \sum_{j=1}^{N} A_i F_{i\to j}\,\sigma(T_i^4 - T_j^4) \qquad \text{(W)}$$

RADIATION HEAT TRANSFER: DIFFUSE, GRAY SURFACES

- Most enclosures encountered in practice involve nonblack surfaces, which allow multiple reflections to occur.
- Radiation analysis of such enclosures becomes very complicated unless some simplifying assumptions are made.
- It is common to assume the surfaces of an enclosure to be *opaque*, *diffuse*, and *gray*.
- Also, each surface of the enclosure is *isothermal*, and both the incoming and outgoing radiation are *uniform* over each surface.

Radiosity

For a surface *i* that is *gray* and *opaque* (ε_i = ⍰$_i$ and ⍰$_i$ + ρ_i = 1)

Radiosity *J*: The *total radiation energy leaving a surface per unit time and per unit area.*

$$J_i = \begin{pmatrix}\text{Radiation emitted}\\ \text{by surface } i\end{pmatrix} + \begin{pmatrix}\text{Radiation reflected}\\ \text{by surface } i\end{pmatrix}$$

$$= \varepsilon_i E_{bi} + \rho_i G_i$$

$$= \varepsilon_i E_{bi} + (1 - \varepsilon_i) G_i \qquad (\mathrm{W/m^2})$$

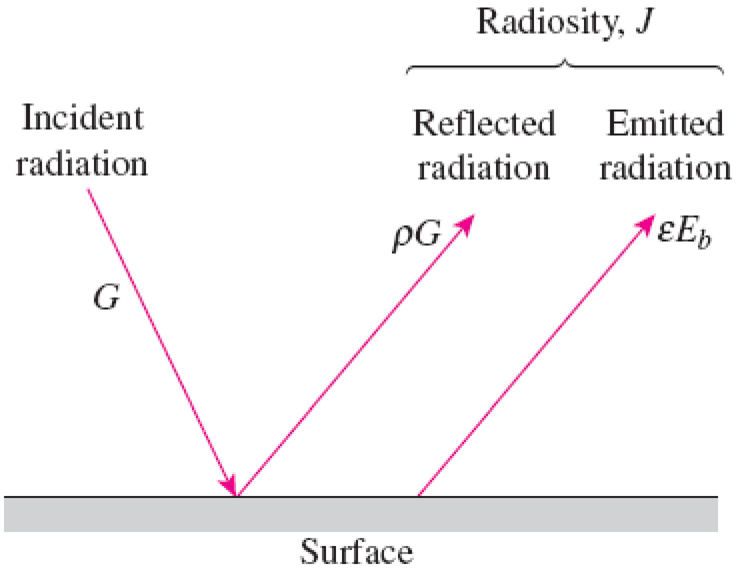

FIGURE 13–20

Radiosity represents the sum of the radiation energy emitted and reflected by a surface.

For a blackbody ε = 1

$$J_i = E_{bi} = \sigma T_i^4 \qquad \text{(blackbody)}$$

The radiosity of a blackbody is equal to its emissive power since radiation coming from a blackbody is due to emission only.

Net Radiation Heat Transfer to or from a Surface

$$\dot{Q}_i = \begin{pmatrix}\text{Radiation leaving} \\ \text{entire surface } i\end{pmatrix} - \begin{pmatrix}\text{Radiation incident} \\ \text{on entire surface } i\end{pmatrix}$$
$$= A_i(J_i - G_i) \qquad \text{(W)}$$

The *net* rate of radiation heat transfer from a surface *i*

$$\dot{Q}_i = A_i\left(J_i - \frac{J_i - \varepsilon_i E_{bi}}{1 - \varepsilon_i}\right) = \frac{A_i \varepsilon_i}{1 - \varepsilon_i}(E_{bi} - J_i) \qquad \text{(W)}$$

$$\dot{Q}_i = \frac{E_{bi} - J_i}{R_i} \qquad \text{(W)}$$

$$R_i = \frac{1 - \varepsilon_i}{A_i \varepsilon_i}$$

surface resistance to radiation.

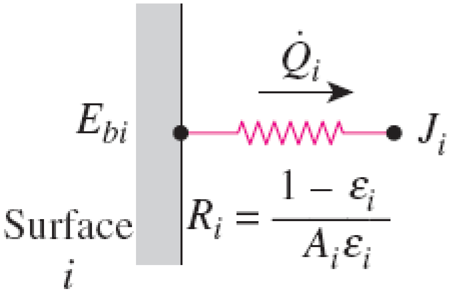

FIGURE 13–21
Electrical analogy of surface resistance to radiation.

The surface resistance to radiation for a *blackbody* is *zero* since $\varepsilon_i = 1$ and $J_i = E_{bi}$.

Reradiating surface: Some surfaces are modeled as being *adiabatic* since their back sides are well insulated and the net heat transfer through them is zero.

$$J_i = E_{bi} = \sigma T_i^4 \qquad \text{(W/m}^2\text{)}$$

Net Radiation Heat Transfer between Any Two Surfaces

The *net* rate of radiation heat transfer from surface *i* to surface *j* is

$$\dot{Q}_{i\to j} = \begin{pmatrix}\text{Radiation leaving}\\ \text{the entire surface } i\\ \text{that strikes surface } j\end{pmatrix} - \begin{pmatrix}\text{Radiation leaving}\\ \text{the entire surface } j\\ \text{that strikes surface } i\end{pmatrix}$$

$$= A_i J_i F_{i\to j} - A_j J_j F_{j\to i} \qquad \text{(W)}$$

$$A_i F_{i\to j} = A_j F_{j\to i}$$

Apply the reciprocity relation

$$\dot{Q}_{i\to j} = A_i F_{i\to j} (J_i - J_j) \qquad \text{(W)}$$

$$\dot{Q}_{i\to j} = \frac{J_i - J_j}{R_{i\to j}} \qquad \text{(W)}$$

$$R_{i\to j} = \frac{1}{A_i F_{i\to j}}$$

space resistance to radiation

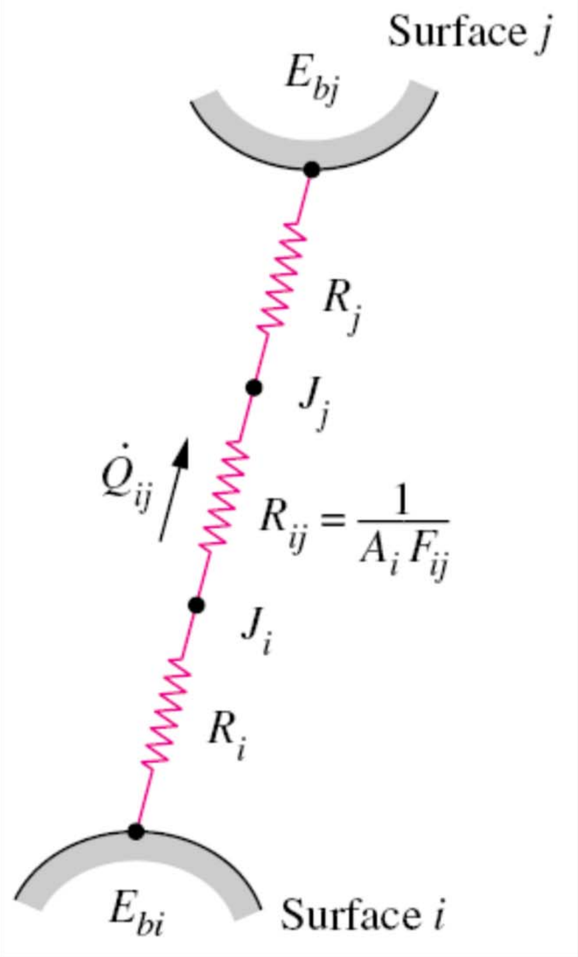

FIGURE 13–22

Electrical analogy of space resistance to radiation.

In an *N*-surface enclosure, the conservation of energy principle requires that the net heat transfer from surface *i* be equal to the sum of the net heat transfers from surface *i* to each of the *N* surfaces of the enclosure.

$$\dot{Q}_i = \sum_{j=1}^{N} \dot{Q}_{i\to j} = \sum_{j=1}^{N} A_i F_{i\to j}(J_i - J_j) = \sum_{j=1}^{N} \frac{J_i - J_j}{R_{i\to j}} \qquad \text{(W)}$$

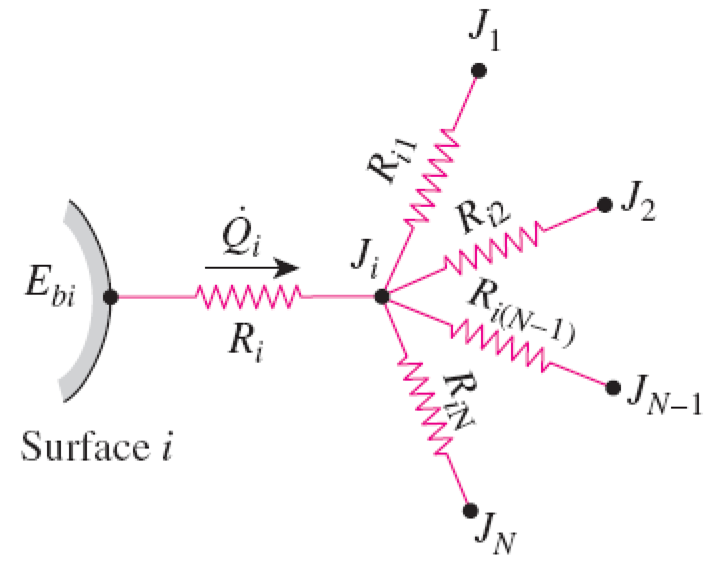

FIGURE 13–23

Network representation of net radiation heat transfer from surface *i* to the remaining surfaces of an *N*-surface enclosure.

$$\frac{E_{bi} - J_i}{R_i} = \sum_{j=1}^{N} \frac{J_i - J_j}{R_{i\to j}}$$

The net radiation flow from a surface through its surface resistance is equal to the sum of the radiation flows from that surface to all other surfaces through the corresponding space resistances.

Methods of Solving Radiation Problems

In the radiation analysis of an enclosure, either the temperature or the net rate of heat transfer must be given for each of the surfaces to obtain a unique solution for the unknown surface temperatures and heat transfer rates.

Surfaces with specified net heat transfer rate $\dot{Q}$

$$\dot{Q}_i = A_i \sum_{j=1}^{N} F_{i \to j}(J_i - J_j)$$

Surfaces with specified temperature T_i

$$\sigma T_i^4 = J_i + \frac{1-\varepsilon_i}{\varepsilon_i} \sum_{j=1}^{N} F_{i \to j}(J_i - J_j)$$

The equations above give N linear algebraic equations for the determination of the N unknown radiosities for an N-surface enclosure. Once the radiosities $J_1, J_2, \ldots, J_N$ are available, the unknown heat transfer rates and the unknown surface temperatures can be determined from the above equations.

Direct method: Based on using the above procedure. This method is suitable when there are a large number of surfaces.

Network method: Based on the electrical network analogy. Draw a surface resistance associated with each surface of an enclosure and connect them with space resistances. Then solve the radiation problem by treating it as an electrical network problem. The network method is not practical for enclosures with more than three or four surfaces.

Radiation Heat Transfer in Two-Surface Enclosures

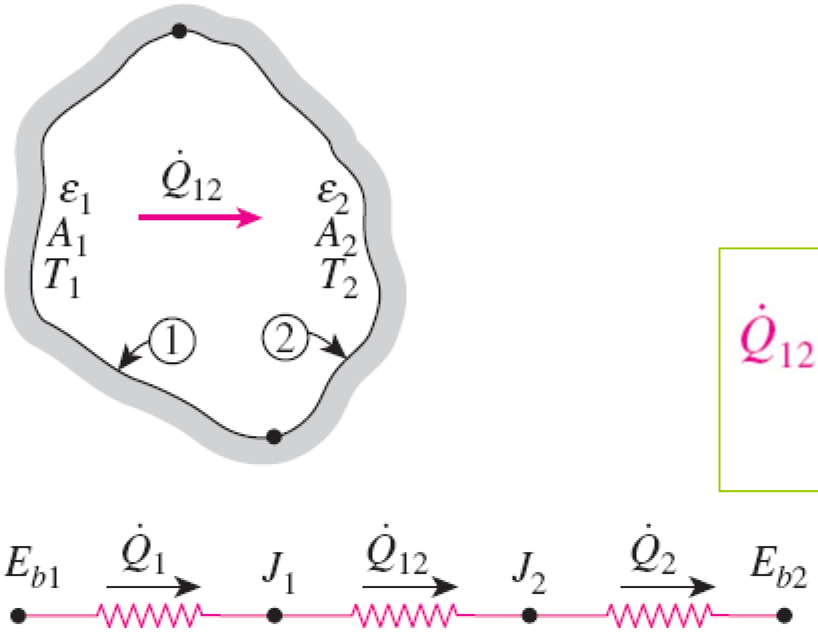

$$R_1 = \frac{1-\varepsilon_1}{A_1\varepsilon_1} \qquad R_{12} = \frac{1}{A_1F_{12}} \qquad R_2 = \frac{1-\varepsilon_2}{A_2\varepsilon_2}$$

FIGURE 13–24

Schematic of a two-surface enclosure and the radiation network associated with it.

$$\dot{Q}_{12} = \dot{Q}_1 = -\dot{Q}_2$$

$$\dot{Q}_{12} = \frac{E_{b1} - E_{b2}}{R_1 + R_{12} + R_2} = \dot{Q}_1 = -\dot{Q}_2$$

$$\dot{Q}_{12} = \frac{\sigma(T_1^4 - T_2^4)}{\dfrac{1-\varepsilon_1}{A_1\varepsilon_1} + \dfrac{1}{A_1F_{12}} + \dfrac{1-\varepsilon_2}{A_2\varepsilon_2}} \qquad \text{(W)}$$

This important result is applicable to any two gray, diffuse, and opaque surfaces that form an enclosure.

TABLE 13–3

Radiation heat transfer relations for some familiar two-surface arrangments.

Small object in a large cavity 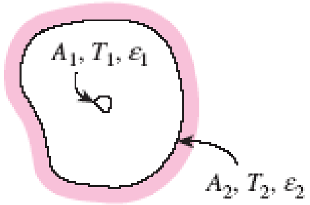 	$\frac{A_1}{A_2} \approx 0$ $F_{12} = 1$	$\dot{Q}_{12} = A_1\sigma\varepsilon_1(T_1^4 - T_2^4)$	(13–37)
Infinitely large parallel plates 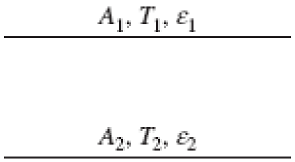 	$A_1 = A_2 = A$ $F_{12} = 1$	$\dot{Q}_{12} = \frac{A\sigma(T_1^4 - T_2^4)}{\frac{1}{\varepsilon_1} + \frac{1}{\varepsilon_2} - 1}$	(13–38)
Infinitely long concentric cylinders 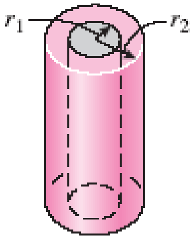 	$\frac{A_1}{A_2} = \frac{r_1}{r_2}$ $F_{12} = 1$	$\dot{Q}_{12} = \frac{A_1\sigma(T_1^4 - T_2^4)}{\frac{1}{\varepsilon_1} + \frac{1 - \varepsilon_2}{\varepsilon_2}\left(\frac{r_1}{r_2}\right)}$	(13–39)
Concentric spheres 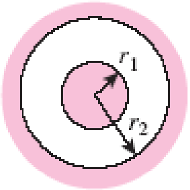 	$\frac{A_1}{A_2} = \left(\frac{r_1}{r_2}\right)^2$ $F_{12} = 1$	$\dot{Q}_{12} = \frac{A_1\sigma(T_1^4 - T_2^4)}{\frac{1}{\varepsilon_2} + \frac{1 - \varepsilon_2}{\varepsilon_2}\left(\frac{r_1}{r_2}\right)^2}$	(13–40)

Radiation Heat Transfer in Three-Surface Enclosures

When Q_i is specified at surface i instead of the temperature, the term $(E_{bi} - J_i)/R_i$ should be replaced by the specified Q_i.

The algebraic sum of the currents (net radiation heat transfer) at each node must equal zero.

$$\frac{E_{b1} - J_1}{R_1} + \frac{J_2 - J_1}{R_{12}} + \frac{J_3 - J_1}{R_{13}} = 0$$

$$\frac{J_1 - J_2}{R_{12}} + \frac{E_{b2} - J_2}{R_2} + \frac{J_3 - J_2}{R_{23}} = 0$$

$$\frac{J_1 - J_3}{R_{13}} + \frac{J_2 - J_3}{R_{23}} + \frac{E_{b3} - J_3}{R_3} = 0$$

These equations are to be solved for J_1, J_2, and J_3.

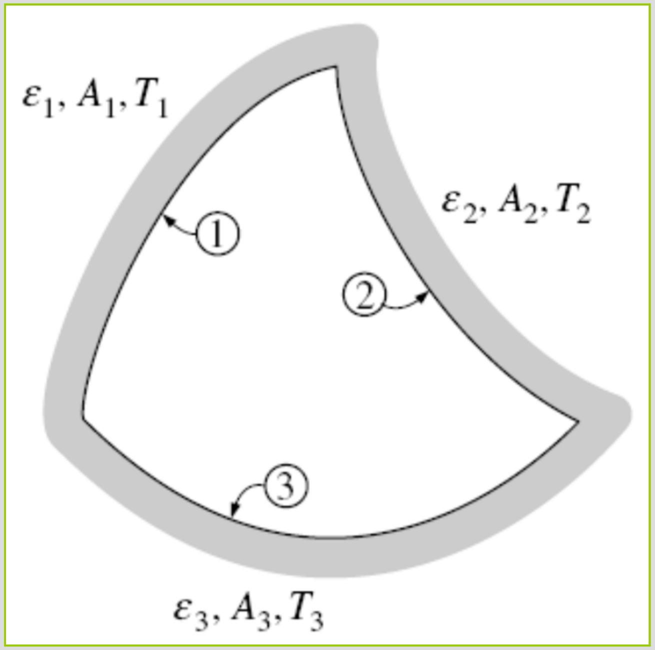

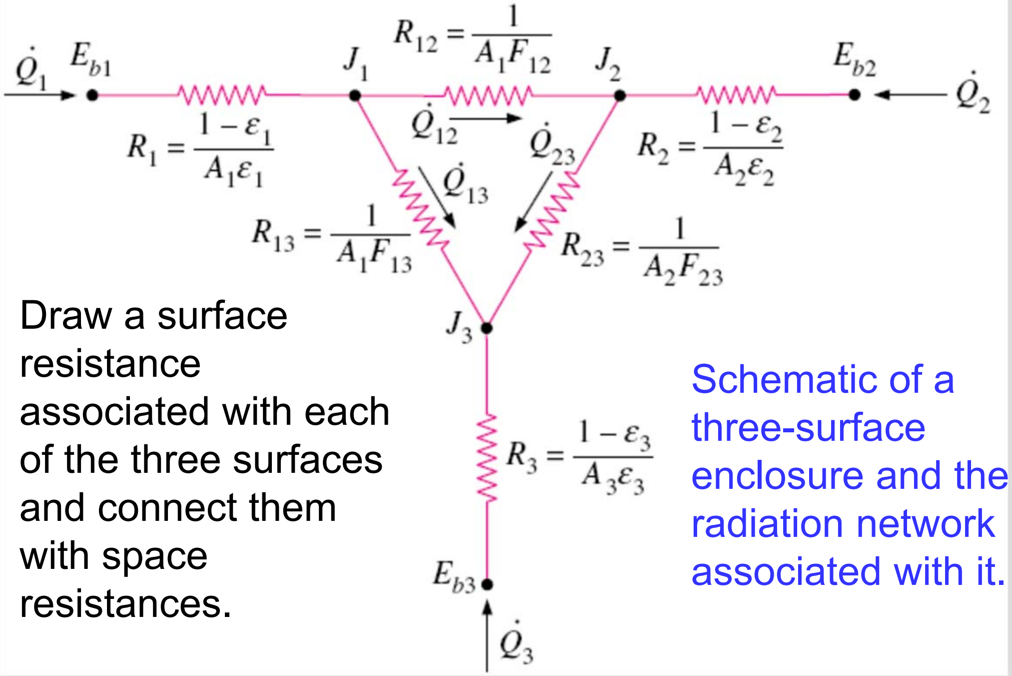

Draw a surface resistance associated with each of the three surfaces and connect them with space resistances.

Schematic of a three-surface enclosure and the radiation network associated with it.

RADIATION SHIELDS AND THE RADIATION EFFECTS

Radiation heat transfer between two surfaces can be reduced greatly by inserting a thin, high-reflectivity (low-emissivity) sheet of material between the two surfaces.

Such highly reflective thin plates or shells are called **radiation shields**.

Multilayer radiation shields constructed of about 20 sheets per cm thickness separated by evacuated space are commonly used in cryogenic and space applications.

Radiation shields are also used in temperature measurements of fluids to reduce the error caused by the radiation effect when the temperature sensor is exposed to surfaces that are much hotter or colder than the fluid itself.

The role of the radiation shield is to reduce the rate of radiation heat transfer by placing additional resistances in the path of radiation heat flow.

The lower the emissivity of the shield, the higher the resistance.

$$\dot{Q}_{12,\text{ no shield}} = \frac{A\sigma(T_1^4 - T_2^4)}{\dfrac{1}{\varepsilon_1} + \dfrac{1}{\varepsilon_2} - 1}$$

Radiation heat transfer between two large parallel plates

Radiation heat transfer between two large parallel plates with one shield

$$\dot{Q}_{12,\text{ one shield}} = \frac{E_{b1} - E_{b2}}{\dfrac{1-\varepsilon_1}{A_1\,\varepsilon_1} + \dfrac{1}{A_1\,F_{13}} + \dfrac{1-\varepsilon_{3,1}}{A_3\,\varepsilon_{3,1}} + \dfrac{1-\varepsilon_{3,2}}{A_3\,\varepsilon_{3,2}} + \dfrac{1}{A_3\,F_{32}} + \dfrac{1-\varepsilon_2}{A_2\,\varepsilon_2}}$$

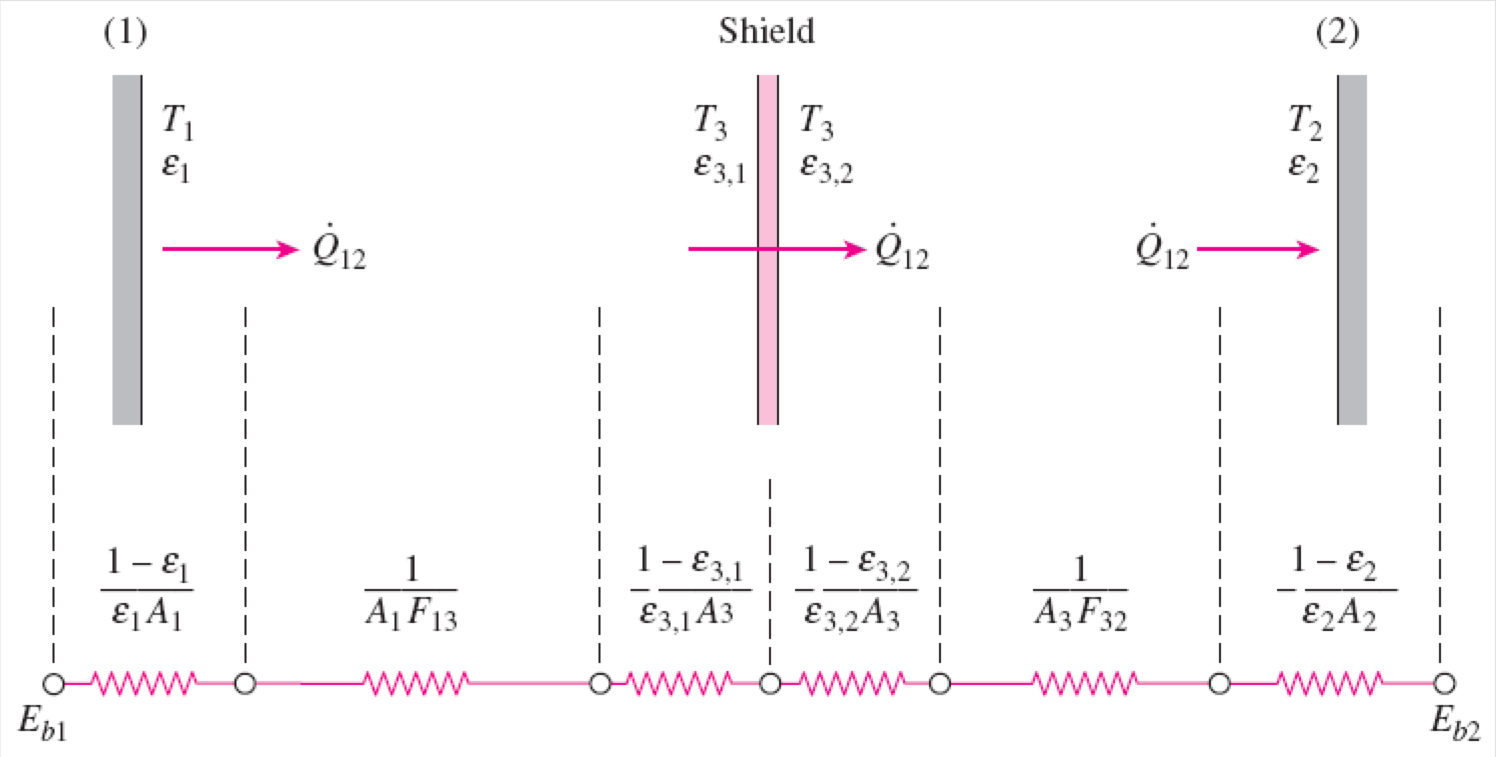

The radiation shield placed between two parallel plates and the radiation network associated with it.

$$\dot{Q}_{12,\text{ one shield}} = \frac{A\sigma(T_1^4 - T_2^4)}{\left(\frac{1}{\varepsilon_1} + \frac{1}{\varepsilon_2} - 1\right) + \left(\frac{1}{\varepsilon_{3,1}} + \frac{1}{\varepsilon_{3,2}} - 1\right)}$$

$$\dot{Q}_{12,\,N\text{ shields}} = \frac{A\sigma(T_1^4 - T_2^4)}{\left(\frac{1}{\varepsilon_1} + \frac{1}{\varepsilon_2} - 1\right) + \left(\frac{1}{\varepsilon_{3,1}} + \frac{1}{\varepsilon_{3,2}} - 1\right) + \cdots + \left(\frac{1}{\varepsilon_{N,1}} + \frac{1}{\varepsilon_{N,2}} - 1\right)}$$

$$\dot{Q}_{12,\,N\text{ shields}} = \frac{A\sigma(T_1^4 - T_2^4)}{(N+1)\left(\frac{1}{\varepsilon} + \frac{1}{\varepsilon} - 1\right)} = \frac{1}{N+1}\dot{Q}_{12,\text{ no shield}}$$

If the emissivities of all surfaces are equal

Radiation Effect on Temperature Measurements

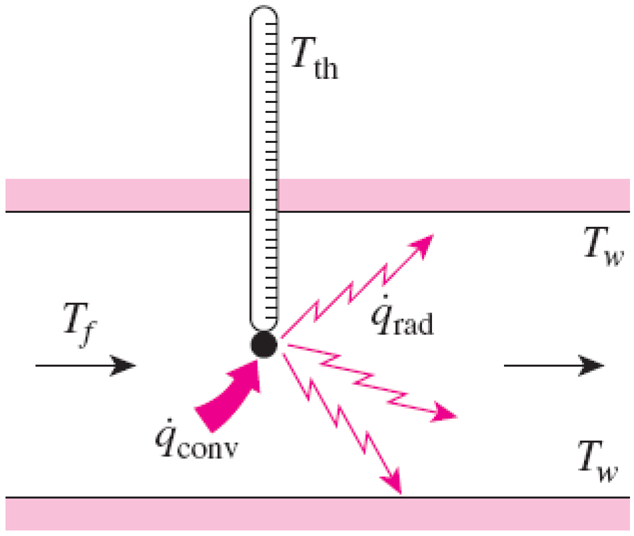

FIGURE 13–31

A thermometer used to measure the temperature of a fluid in a channel.

$$\dot{q}_{\text{conv, to sensor}} = \dot{q}_{\text{rad, from sensor}}$$

$$h(T_f - T_{\rm th}) = \varepsilon\sigma(T_{\rm th}^4 - T_w^4)$$

$$T_f = T_{\rm th} + \frac{\varepsilon\sigma(T_{\rm th}^4 - T_w^4)}{h} \qquad \text{(K)}$$

T_f = actual temperature of the fluid, K
$T_{\rm th}$ = temperature value measured by the thermometer, K
T_w = temperature of the surrounding surfaces, K
h = convection heat transfer coefficient, W/m^2·K
ε = emissivity of the sensor of the thermometer

The last term in the equation is due to the *radiation effect* and represents the *radiation correction.*

The radiation correction term is most significant when the convection heat transfer coefficient is small and the emissivity of the surface of the sensor is large.

Therefore, the sensor should be coated with a material of high reflectivity (low emissivity) to reduce the radiation effect.

Summary

- The View Factor
- View Factor Relations
- Radiation Heat Transfer: Black Surfaces
- Radiation Heat Transfer: Diffuse, Gray Surfaces
  - ✓ Radiosity
  - ✓ Net Radiation Heat Transfer to or from a Surface
  - ✓ Net Radiation Heat Transfer between Any Two Surfaces
  - ✓ Methods of Solving Radiation Problems
  - ✓ Radiation Heat Transfer in Two-Surface Enclosures
  - ✓ Radiation Heat Transfer in Three-Surface Enclosures
- Radiation Shields and The Radiation Effects
  - ✓ Radiation Effect on Temperature Measurements